A NOVEL ROLE FOR SCLEROSTIN IN AORTIC VALVE STENOSIS

By

Jeffery Ethan Joll II

Dissertation

Submitted to the Faculty of the

Graduate School of Vanderbilt University

in partial fulfillment of the requirements

for the degree of

DOCTOR OF PHILOSOPHY

in

Biomedical Engineering

March 31, 2022

Nashville, Tennessee

Approved:

W. David Merryman, PhD

Antonis K. Hatzopoulos, PhD

Brian R. Lindman, MD, MSCI

Jeffry S. Nyman, PhD

Cynthia Reinhart-King, PhD

Dedicated to my grandparents.

ACKNOWLEDGEMENTS

Kami Walters, Stephanie Joll, Jeff Joll, Sophie Joll, Judy Joll, Jim Fassinger, Bill Joll, Donald Midkiff, Karen Midkiff, Chris Midkiff-Brandt, Aimee Walters, Brent Walters, Michael Raddatz, Natalie Noll, Tessa Huffstater, Caleb Snider, Mark Vander Roest, Cami Johnson, Meghan Bowler, Nathan Bloodworth, Alison Vander Roest, Matt Bersi, Cyndi Clark, Erin Booton, Lance Riley, Mike Valentine, Olu Ogungbesan, Dave Armstrong, Dave Merryman, Cyndi Reinhart-King, Jeff Nyman, Brian Lindman, Antonis Hatzopoulous, Lin Zhong, Todd Giorgio, Heather Fedesco, Cynthia Brame, Leah Roberts, Evan Glass, Nick Goodell, Kelly Swope, Derek Price, Max Hamilton, Mike Miga, Brandi Gilbert, Jason Organ, Sungsoo Na, Rowdy, Buster, Vanderbilt Graduate Workers United, the Vandy Pickup Soccer Facebook group, Squad, Salt, Bernie Sanders, Three Brothers Coffee, Kay Bob's, 51st Street Deli, the Nashville Public Library, the Belcourt Theater, and Montgomery Bell State Park.

Thank you.

TABLE OF CONTENTS

Page

LIST OF TABLES

Table **Page**

LIST OF FIGURES

Figure **Page**

GLOSSARY OF TERMS AND ABBREVIATIONS

Abbreviation	Term
ARCH	Study to Determine the Efficacy and Safety of Romosozumab in the Treatment of Postmenopausal Women with Osteoporosis
ARS	Alizarin Red S
aSMA	alpha smooth muscle actin
AVIC	aortic valve interstitial cell
AV	aortic valve
AVEC	aortic valve endothelial cell
AVS	aortic valve stenosis
BMP	bone morphogenetic protein
BMD	bone mineral density
CDH11	cadherin-11
CAVD	calcific aortic valve disease
CV	cardiovascular
DXA	dual-energy x-ray absorptiometry
EF	ejection fraction
EndMT	endothelial-to-mesenchymal transition
ECM	extracellular matrix
FRAME	Fracture Study in Postmenopausal Women with Osteoporosis
HF	heart failure
HOX	homeobox
IF	immunofluorescence
IACUC	Institutional Animal Care and Use Committee
IRB	Institutional Review Board
LV	left ventricle
LRP	low density lipoprotein receptor related protein
MTC	Masson’s Trichrome
MG	mean pressure gradient

mAb	monoclonal antibody
OCT	optimal cutting temperature
OVX	ovariectomy
PV	peak velocity
PSR	Picrosirius Red
PMO	post-menopausal osteoporosis
qPCR	quantitative real-time polymerase chain reaction
RANKL	receptor activator of nuclear factor kappa-B ligand
RNA	ribonucleic acid
STRUCTURE	Study Evaluating Effects of Romosozumab Compared with Teriparatide in Postmenopausal Women with Osteoporosis at High Risk for Fracture Previously Treated with Bisphosphonate Therapy
TAVR	transcatheter aortic valve replacement
TGF-β	transforming growth factor beta
VCPC	Vanderbilt Cardiovascular Physiology Core
VANTAGE	Vanderbilt Technologies for Advanced Genomics
WT	wild-type

CHAPTER 1

Dissertation Overview

There are many shared mechanisms of osteogenesis and bone growth and the ectopic development of calcific lesions often found in cardiovascular (CV) diseases, including aortic valve stenosis (AVS) [1]. Research performed as an undergraduate focused on diseases of the musculoskeletal system, including osteoporosis [2–6]. This work was related to research that discovered the fundamental role of sclerostin in the bone remodeling axis. Closely following the clinical trial results of sclerostin neutralizing antibodies in the treatment of skeletal disease led to interesting questions in the field cardiovascular pathophysiology. Specifically, an outcome of a Phase III clinical trial evaluating the sclerostin neutralizing antibody romosozumab was of great interest. Unexpected CV side-effects of the drug were discovered when compared to current treatments [7]. This provided a fruitful area to study the linkages between skeletal signaling and CV ectopic calcification, thus fusing previous research experience with a new area of focus on which to base the graduate studies found within this document. The first aim of this dissertation is focused on understanding the role of sclerostin on AVS development and how targeting this protein in osteoporosis may inadvertently affect the CV system.

Technical questions arising from this first aim lead to the discovery of the extent of understudy of female CV disease in pre-clinical studies. Only 10% of studies focus on female-only populations compared to 60% in that of men [8]. It is necessary to address this understudy problem head-on in order to accurately study the links between osteoporosis and valve disease. Therefore, the second aim of this dissertation is studying how AVS progresses in a common pre-clinical model of post-menopausal osteoporosis (PMO) – bilateral ovariectomy (OVX). The goal for this aim is to determine if a commonly used female-specific model for pre-clinical PMO can double as a pre-clinical model of female-centric CV disease in order to better understand the relation between bone and CV disease as well as to provide a tool to address understudy of

female CV disease. This topic is closely related to the first in that sclerostin neutralizing antibodies have become a first-in-class drug therapy for treating PMO but questions remain about the off-target side effects [9]. Developing a strong pre-clinical model to study the PMO patient population will be very valuable in understanding the potential CV side effects.

The final arm this dissertation steps out of the laboratory and evaluates biomedical engineering classroom instruction. Approximately 40% of the work in this document was completed during the COVID-19 pandemic. Performing research in a hybrid style led to fundamental questions about the culture of knowledge production and transmission in the biomedical engineering field. In order to systematically evaluate this question, a study was performed to understand how the undergraduate learning experience is affected by a hybrid approach. In an introductory biomechanics course, the effect of hybrid and traditional classrooms was assessed and compared. This study is crucial for evaluating how the biomedical engineering education field develops post-COVID19. While many are eager to return to pre-pandemic teaching habits, there may be something to be learned the necessary shift to virtual and hybrid classrooms.

In summary, this dissertation is organized as follows: first, the foundation of the field of AVS pathophysiology is detailed in how the system works and what can potentially go wrong. Next, the linkages between diseases of the skeleton and aortic valve (AV) are explained. Then, novel evidence of the role of sclerostin in AVS is presented. Next, the sex differences of AVS diagnosis, disease progression, and treatment are introduced. Then, evidence of a potential new pre-clinical model for the evaluation of AV and left ventricle (LV) disease in PMO is described. Finally, evaluation of how a biomedical engineering classroom can be reformatted into a hybrid style and improve student confidence and performance is detailed. The dissertation is concluded

with a look at the impact of the novel research as well as a discussion on the potential future paths new research could follow.

It is the hope of the author that the work contained in this document will allow for new avenues of evaluation of AVS, understanding female specific AVS, and optimal methods of teaching biomedical engineering content in the modern college classroom.

CHAPTER 2

Aortic Valve Disease

Aortic valve development

The heart is the first functional organ in the developing fetus. The heart tissue arises from the mesoderm germ layer 18 to 19 days after fertilization and the primitive AV region begins to form a few days later from a substance known as cardiac jelly. This substance acts as an extracellular matrix (ECM) and lies between the inner and outer tubes of the myocardial heart consisting of collagens, glycoproteins and polysaccharides [10]. The region of the jelly at the outflow tract lying in the atrioventricular canal develops into a region called the endocardial cushions. Endocardial cells begin to undergo an important process called endothelial-to-mesenchymal transition (EndMT) whereby endothelial cells take on a mesenchymal phenotype akin to a fibroblast or smooth muscle cell [11,12]. This transition process is crucial to CV development and disease.

The signaling cytokine Transforming Growth Factor Beta (TGF-β) and protein Bone Morphogenetic Protein (BMP) from the myocardium and Notch signaling from the endothelium work together to spur EndMT and ECM maturation in the cardiac jelly [11]. Sox9 transcription factor is involved in maturation and proliferation of the new mesenchymal stem cells which use integrin receptor signaling and secretion of metalloproteinases to infiltrate and reconfigure the ECM tissue [13,14]. These mesenchymal cells begin to form the stratification of the AV leaflets, maintaining the inner region of the structure with endothelial cells forming the outer barrier.

Mechanical forces are crucial in developing the structure to allow unidirectional blood flow in the valves. Endothelium cells physically rearrange their cytoskeletons to align parallel to blood flow [15]. In 2017, a major component of the mechanobiological mechanism of EndMT was discovered. A shear responsive transcription factor called KLF2 induces WNT9B paracrine signaling which spurs EndMT. Without these elements, the AV does not develop properly [16].

Aortic valve functional anatomy

The AV is one of four heart valves. It is a tri-leaflet structure situated between the LV and aorta. The three leaflets meet along a ridged area known as the commissures. Each leaflet has a cusp which joins the aorta and myocardium at a transitional area known as the annulus. Endothelial cells cover the outer blood contacting regions of the leaflets. In healthy humans, each leaflet has a trilayer interior with distinct regions determined by their primary ECM composition. The region nearest the aorta (the outflow surface) is termed the fibrosa and contains densely packed collagen (particularly type I, III, and V fiber types) to provide support and provide continuous structure with surrounding tissues [17,18]. The area nearest the ventricle (inflow) is termed the ventricularis and is rich in elastin and is thought to maintain collagen configuration and provide structure in relaxed states [19]. Central to these regions is an area termed the spongiosa which is rich in glycosaminoglycans and allows structure flexibility and rearrangement of structural elements due to the mechanically strenuous heart cycle [17].

The AV experiences the highest mean pressure gradient (MG) and peak velocity (PV) magnitude and the largest amount of volumetric flow [20]. In diastole, the ventricle fills with blood and the AV is responsible for preventing regurgitant flow. During systole, the ventricle contracts and blood is expelled from the heart into systemic circulation. During this time, the AV must deform readily to allow the easy and unobstructed flow to the body. This cycle occurs over three billion times over the course of a lifetime [21].

In diastole, the AV is tightly closed in order to prevent regurgitation of blood. The anisotropic nature of the valve anatomy allows for different mechanical properties dependent on the direction on which stresses and strains are applied. Radially, the AV leaflets are extremely compliant in that they deform readily with low strains. This allows for a strong coapting under

high pressures which prevents collapse [22]. Collagen provides stress bearing capabilities and the arrangement of collagen fibrils changes in the systolic and diastolic phases. Collagen achieves a flat and ordered shape during diastole but undergoes a crimping action in order to contract and decrease surface area in response to blood being expelled through the outflow area. With the return of diastole, the collagen resumes its ordered formation to maintain the mechanical barrier between aorta and ventricle. Elastin fibers contract during systole, further reducing the area of the valve [20,21].

During disease, the ordered conformation of the valve subregions can become disorganized, disturbing the hemodynamics found in the healthy valve. Understanding the complex form-function relationship presented here makes clear why disturbances in valve microarchitecture can have drastic effects on the flow characteristics of the region.

Aortic valve cell biology

There are two primary resident cell populations of the AV: valve endothelial cells (AVEC) and valve interstitial cells (AVICs) [23]. The AVECs form an external barrier to the valve, regulating the infiltration of various factors and cells as well as sensing the fluid flow dynamics. AVECs interact with the blood and are thus the first line of interaction of the valve with circulating factors. Indeed, AVECs are involved in response to thrombotic stimuli, inflammation, and are engaged in cross-talk with AVICs in order to regulate valvular physiology [24]. AVECs are unique in that they maintain the ability to naturally undergo EndMT. This drastic phenotypic shift is an important stage of embryological development of the valve and also may be a method by which AVECs can replenish the AVIC population during adulthood [25].

This mechanism therefore is being investigated in its role in calcific aortic valve disease (CAVD) pathophysiology [26].

AVICs are present in all three layers of the AV [27,28]. These quiescent cells have relatively low basal activity but can be activated in response to injury, mechanical perturbation, disease/infection, and other biomolecular stimulations [21]. The activated form of AVICs is generally termed “myofibrobolast” and is characterized by the cells ability to synthesize fibrous matrix and contract its local environment as part of the natural repair process [23,29]. Only a small portion of AVICs are activated in the healthy heart, providing further evidence of their predominantly quiescent state with chronic activation only occurring during disease [21,30,31]. Evidence shows that AVICs re-gain their quiescent phenotype after return to equilibrium [32].

AVIC phenotype is relatively fluid with a number of phenotypes represented in explanted cells. AVICs are also sensitive to their microenvironment, local stiffness, and mechanical strain imposed during the cardiac cycle. These all contribute to AVIC homeostasis, and changes in these factors are seen in many disease states, including CAVD[23,27]. AVIC biology is associated with age-related changes in valve morphology where AVIC numbers drastically decrease with age with a concurrent reduction in the dynamism of the collagen architecture. This leads to a less compliant valve with increasing age [33–35].

Aortic valve disease

CV disease is the most common cause of death in the United States. Much of the focus of societal and research focuses on the more prevalent and acute CV diseases such as coronary artery disease (the most common CV disease) and myocardial infarction (carrying the highest

mortality rate). As a result, heart valve disease is often overlooked. In particular, AVS is the third most common CV disease, responsible for around 16,000 deaths per year [36].

AS is defined as the narrowing of the LV outflow area in such a way that valve hemodynamic properties are drastically altered. The AV acts as a one-way valve controlling the flow of oxygen-rich blood from the LV (where it has arrived from the lungs) into systemic circulation. The delivery of vital oxygen and nutrients to the many tissues of the body requires regular and unobstructed flow between the LV and the rest of the body. Therefore, stenosis of the AV results in less efficient pumping between these two bodies. This is predominantly caused by a congenital defect called bicuspid AV where patients have two AV leaflets instead of three. AS is also seen in older individuals that have anatomically normal AVs that have accrued ectopic calcification over time, altering the structure-function relationship of the healthy valve anatomy [37].

Calcified nodules build up on the outflow surfaces of the valve via dystrophic (cell-death mediated) or osteogenic processes. Dystrophic calcification has found to be more prevalent in explanted valves [38]. *In vitro* studies have shown that AVICs are capable of undergoing both dystrophic and osteogenic mechanisms of calcification and are a likely source of calcification from either mechanism [23]. Numerous cell interactions and biological stimuli can augment or prevent the calcific potential of AVICs *in vitro*. These lesions cause a material stiffening (causing more than a doubling in young's modulus of leaflet stiffness) and the once pliable leaflets no longer fully open and close to their full capacity, resulting in lower efficiency of oxygenated blood delivery [39]. In response to the increased resistance of the diseased valve, the LV will enlarge itself with muscle to try and overcome the resistance. This feedback loop can

lead to congestive heart failure (HF) which results in a decrease in quality of life and potentially death if left untreated.

AS is generally preceded by a thickening of the valve without disturbed hemodynamics – termed sclerosis [40]. The gradual fibrosis and accumulation of calcific nodules within the valve structure decreases the compliance and reduces the outflow area, producing extremely high exit velocities and pressure gradients between the aorta and the LV during systole [21,37]. This leads to progressive cardiac hypertrophy which can lead to congestive HF. Patients generally do not present until severe CAVD symptoms occur such as angina (chest pain) or syncope (loss of consciousness). These patients require immediate surgical replacement of the valve to remove the obstruction [41]. There are currently no treatments beside surgical intervention which is problematic due to around half of patients being ineligible for surgery due to high risk factors such as obesity, hypertension, and kidney disease [21].

The past decade has marked a shift in the core understanding of CAVD pathophysiology. The disease was originally postulated to be degenerative and passive accumulation of calcification and wear on the valve structure, through which local cells may respond in a way that furthered the disease phenotype. Instead, recent work has shown the disease is actively regulated and cell driven with AVIC disease activation, phenotypic shifts, mineralization, inflammation, matrix dysregulation, and other cellular functional mechanisms [42]. Further, many of these pathological mechanisms seemed to be regulated by AVICs [21,23].

Dystrophic calcification is dependent on programmed cell death, cell membrane damage, oxidative stress, inflammation, osteogenic phenotype switch, and lipid infiltration, among others [42]. Transforming growth factor, fibroblast growth factor, bone-morphogenetic protein, lipoprotein, and Wnt signaling have shown to be major molecular drivers of CAVD disease

phenotype in cell and animal models [23,43–45]. AVIC phenotype shift to osteogenic and chondrogenic lineage has also shown to be associated with CAVD [46]. Major lineage regulators of Runx2, Sox9, Msx, among others also have varying roles in the prevention or causation of CAVD symptoms in various pre-clinical studies. Osteogenic, dystrophic, chondrogenic, and atherosclerotic regions have all been identified in explants of disease human valves [45,47–49]. The role of inflammatory cell infiltration is a rapidly growing area of CAVD research but results are by no means definitive. The most likely immune cell contributor to CAVD progress are cells of the macrophage/monocyte lineage which are able to interact with AVECs and enter the interior of the valve where release of pro-inflammatory cytokines can contribute to chronic activation of AVICs in disease [21,50].

AVICs activated to become myofibroblasts dysregulate the AV architecture by dysregulated production of ECM factors such as collagen and fibronectin [51]. Activated AVICs also disturb the valvular structure through expression of matrix remodeling factors. AVIC activation is shown to be regulated by TGF-β, FGF, nitric oxide, Wnt signaling, and mechanical strains [21,23]. Hypercontractile AVICs become enriched in cell junctional proteins such as cadherin-11 which allow for tight attachment leading to damaging of neighboring cell membranes where cell materials become the nucleation point for dystrophic calcifications [52–55]. Chronic activation of these cellular processes can lead to CAVD symptoms. The cell biology and molecular pathophysiology of the AV is summarized in **Fig 2.1.**

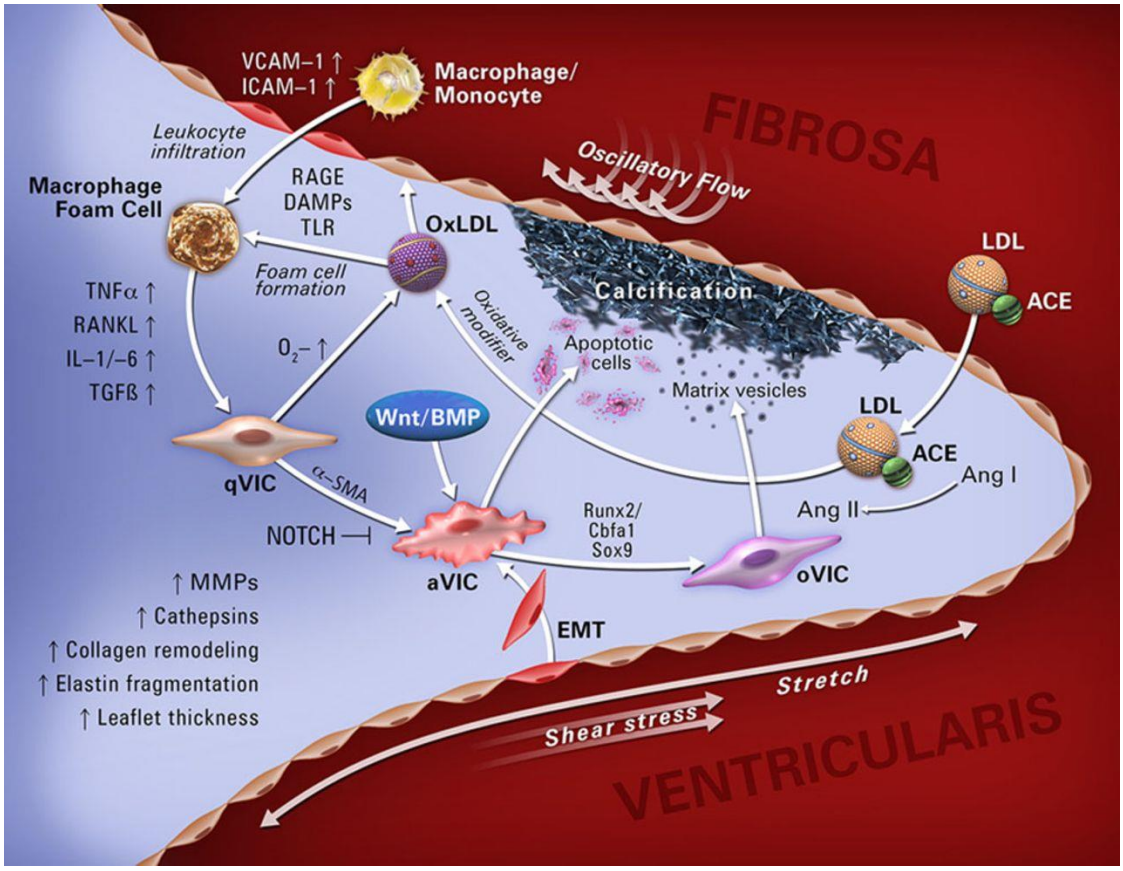

Figure 2.1. Overview of AV cellular and molecular pathophysiology. The aortic valve controls blood flow from the left ventricle into systemic circulation. AVIC and AVEC cells populate the tissue. Quiescent AVICs can become activate through a number of different factors leading to dystrophic or osteogenic calcification. This figure summarizes many of the primary factors in the disease progression of the AV. Reprinted with permission from © 2014 Yutzey et. al. Originally printed in ATVB [56].

Aortic valve disease burden and treatment

CV disease is an increasing public health concern in our aging population. Furthermore, poor diet and sedentary lifestyle contribute to poor overall CV health leading to a myriad of diseases [57]. Valvular diseases contribute to approximately 25,000 deaths per year, of which most are associated with AS and mitral regurgitation [58]. 25% of patients over the age of 65 present with aortic sclerosis – thickening of the AV. While this does not always progress to more advanced AS or CAVD, the risk of CV event increases by 50% in sclerotic patients. Further, this correlates to an 80% chance of HF, necessity of surgical valve replacement, or death over the next 5 years of life [59].

AS affects 3% of individuals over the age of 75, around 1.5 million patients in total, and accounts for 17,000 deaths per year in the United States. The number of individuals perishing from this disease is expected to double over the next 25 years [21]. Valvular stenosis lead to global changes in heart and peripheral blood vessels, and other organ systems in the body. Death by this disease usually occurs from cardiac hypertrophy and failure stemming from LV overload [37]. There are, in fact, no drug treatments known to slow, stop, or reverse the damage that eventually leads to AVS. Currently the only effective treatment for CAVD is surgical replacement of the diseased valve with a synthetic replacement. This is because most clinical presentations of the disease are already in the severe, symptomatic stages, which require immediate relief. However, only about half of severe CAVD patients are candidates for surgical replacement due to high surgical risk [21,41]. This is problematic for several reasons. AVS primarily affects the extremely elderly, and complications due to age can disqualify the elderly from complete valve replacements (**Fig. 2.2**). Further, AVS is associated with a few other risk factors that make the potential patient population extremely vulnerable to surgery.

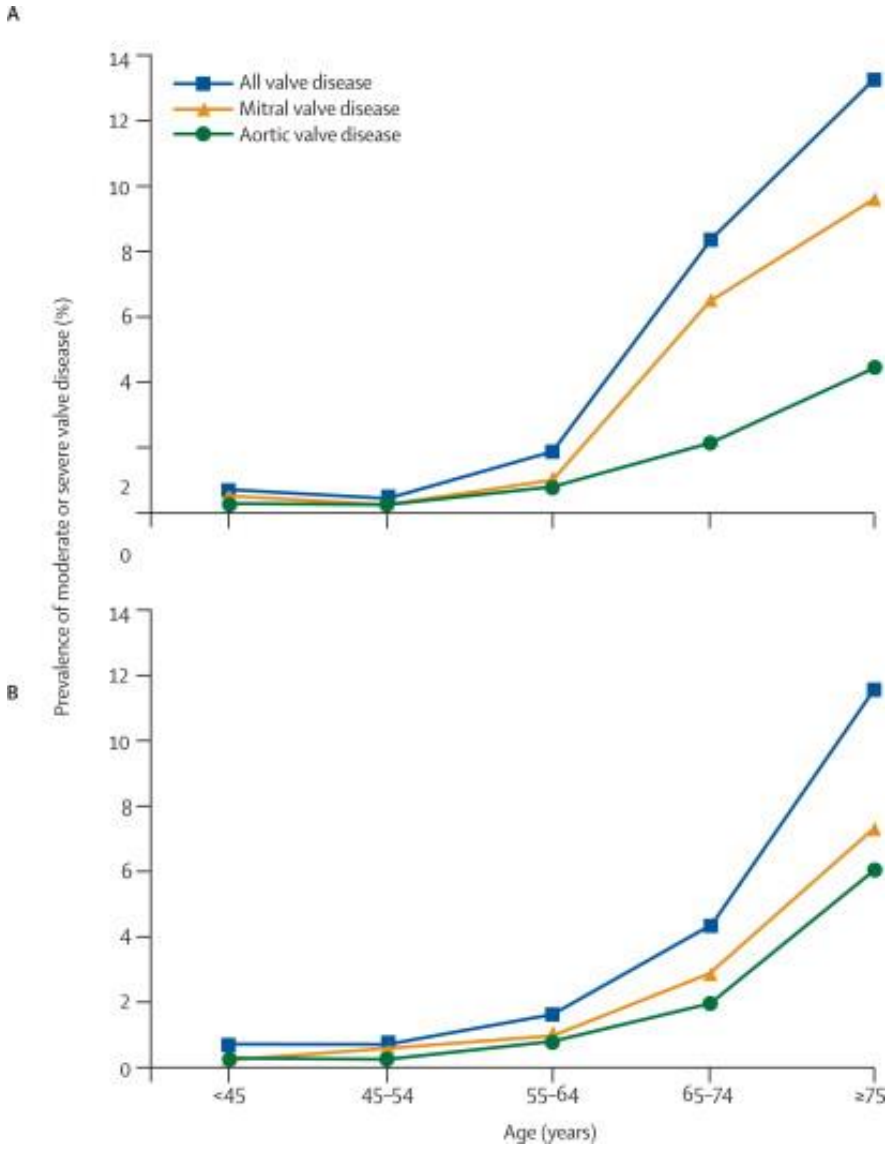

Figure 2.2. Valve disease prevalence increases exponentially with age. Results from two clinical trials indicating the prevalence of all valve disease (as well as mitral and aortic valve specific) prevalence. The rate of disease increases drastically as patients age past 55-64, demonstrating how the disease primarily afflicts the elderly presenting treatment challenges. Reprinted with permission from © 2006 Nkomo et. al. Originally printed in The Lancet [60].

Open-heart surgical replacement of the valve was long the standard for treatment. For appropriate patients, it can greatly improve quality of life and life expectancy. However, there are many potential operative and post-operative complications. The transcatheter aortic valve replacement (TAVR) technique has recently presented a percutaneous solution to this problem – avoiding the risks of open surgery. TAVR, which involves threading a catheter through the vasculature and remotely deploying a prosthetic with no need for heart resection, may be as effective at reducing symptoms and restoring healthy blood flow. Additionally, TAVR is safer for those patients at highest risk for open surgery. Early results show that TAVR is an effective treatment for people with CAVD at high surgical risk [61]. However, the TAVR placed prosthetic is notorious for earlier failure and may necessitate multiple replacement surgeries which can be costly and time-consuming. Additionally, there are still no treatments that target the disease non-surgically. This is due to an unclear understanding of the mechanism of disease combined with an unclear effective therapeutic window due to the long-time course of disease progression.

AV disease is also not responsive to drugs which are effective in treating related pathologies. Lipid lower drugs, such as statins, were evaluated in clinical trials of AVS but were shown to have no effect on the progression of severe AV disease [62]. Anti-hypertensive drugs have shown confounding results from exploratory studies [63]. Drugs which affect the osteoclastogenesis pathways such as receptor activator of nuclear factor kappa-B ligand (RANKL) inhibitors have also shown inconclusive results [64]. It is therefore necessary to attempt to better understand the pathobiological mechanisms of AV disease so that new pharmaceuticals can be developed to avoid the necessity for costly and risky AV replacement.

Clinical trials investigating the use of statins were conducted as the pathology of CAVD shares some similar aspects with that of atherosclerosis. However this trial failed to affect the progression of CAVD [65]. This is likely due to the differences in disease mechanism as well as the stage at which the intervention occurred [66]. Thus, there is theorized to be a point of irreversibility where pharmacological targeting can no longer halt or reverse the progression of CAVD [67].

Currently, trials for RANKL inhibitors in slowing CAVD are in progression. This drug is used to slow bone resorption in osteoporosis by targeting the activation and activity of osteoclasts [68]. Interestingly, RANKL has shown to be a pro-disease factor in CAVD and it is currently undergoing studies to see if RANKL targeting may have the dual effect of reducing CV calcium burden while improving skeletal BMD parameters [69,70]. While RANKL contributes to osteoclastogenesis in the bone, it is involved with myofibroblast activation and calcification in AVICs [71]. Our lab has produced robust pre-clinical justification for CDH11 blocking monoclonal antibody (mAb) as a potential therapeutic option for treating CAVD. This mAb reduces dystrophic calcification and upregulates protective Sox9 signaling in a Notch1 haploinsufficiency model of CAVD [72]. Further research needs to be performed in this area but could represent an exciting new avenue for CAVD treatment.

Therapeutic options for treating CAVD are severely lacking and there is great potential benefit in elucidating the molecular mechanism of disease and factors that may be targeted to prevent, slow, or even reverse disease progression. This will improve outcomes for patients who may experience early stages of disease but would not be candidates for surgical replacement later down the road. Identification and early intervention with a pharmacological strategy could prevent the high mortality rates associated with CAVD.

CHAPTER 3

Sclerostin

Aortic valve disease and osteoporosis

A link between CAVD and osteoporosis has been proposed since the late 1990's [73]. Recent studies using molecular imaging techniques have identified there is concomitant valvular calcium burden inversely correlated with BMD in osteoporosis [67,74]. Clinical studies have shown osteoporosis is independently associated with CV mortality and CV calcification is associated with increased incidence of fracture due to low BMD [75]. High-fat diet induced CV disease can also cause obesity-induced osteoporosis in small animals [76].

The paradoxical nature between CV calcification and low-bone mass has raised interesting possibilities in treatment of these diseases. Factors that have disparate effects on bone and CV cells may prove fruitful areas of multi-scale treatment. The most common example is RANKL. In bone, RANKL activates osteoclasts and upregulates resorption which leads to osteoporosis [77]. The mAb denosumab targets this factor to slow the breakdown of bone tissue. RANKL also acts on AVICs to drive inflammatory signaling in the AV, leading to CAVD. It stands to reason that targeting this protein may have the dual effect of decreasing bone resorption as well as calcific deposition on the AV. Unfortunately, clinical trials for denosumab in the treatment of AVS have shown little effect [78].

Sclerostin in cardiovascular disease

Sclerostin activity was originally thought to be confined to the skeletal system. However recent work shows expression in the protein of a number of organ systems and in various physiological and disease processes. Sclerostin has shown to be present in the CV system, which is of great interest due to the apparent CV effects observed when targeting the protein in osteoporosis patients.

Wnt signaling itself is known to play a role in a number of CV systems and diseases. The pathway is involved in cardiac and vascular development. It is particularly important in atherosclerosis and CAVD [79]. Canonical Wnt signaling is a driver of CAVD in hypercholesteremia models and is involved in the osteogenic shift of AVICs in a substrate stiffness dependent manner [47,80–82]. Low density lipoprotein receptor related protein (LRP) 5 is a major contributor to CAVD [80]. LRP6 genetic mutations result in coronary artery disease, osteoporosis, and hypertension indicating a dual role in low bone mass disease and CV disease in a paradoxical nature [83,84]. Warfarin induces vascular calcification by up-regulation of Wnt signaling in vascular smooth muscle cells [85].

While the role of Wnt signaling is fairly well characterized in CV development and disease, the role of sclerostin is relatively unclear and very few studies investigate the molecule specifically. As previously described, the specific CV status of patients with genetic disease of sclerostin is unclear. Many sclerosteosis patients perish due to brain herniation at a relatively young age when CV disease is quite uncommon. Elderly patients with sclerosteosis and van Buchem disease do not appear to have a propensity to CV disease but these patients come from relatively homogenous groups and may not be indicative of the effects sclerostin deficiency on the population overall [86]. Small animal models of this disease have not been thoroughly investigated for CV phenotype.

Sclerostin has recently been shown to be associated with calcific nodules on diseased AVs at the ribonucleic acid (RNA) and protein level [87,88]. Upregulation has also shown to be present in atherosclerotic lesions [89]. *In vitro* experiments focusing on vascular smooth muscle cell lines show that these cells upregulate sclerostin expression in osteogenic conditions which is recapitulated at the *in vivo* level [90]. Further, sclerostin has shown to be present in the

extracellular proteome of the aorta [91]. Sclerostin was shown to be associated with vascular calcifications at the *in vivo* level as well. The most thorough investigation of the sclerostin mutant phenotype in CV disease showed that sclerostin overexpression and excess protein treatment was able to ameliorate atherosclerosis and aortic aneurysm in an angiotensin-II mouse infusion model. This was associated with decreased immune factor circulation and macrophage infiltration. These effects were associated with downregulation of the Wnt signaling pathway [92]. This study paints a potentially protective role for sclerostin in the vascular disease and may begin to explain the negative effects on stroke and heart attack in clinical trials targeting the factor.

Many studies have been performed investigating circulating levels of sclerostin and association with CV disease progression and mortality. Results have been heterogeneous: circulating sclerostin has shown positive associations with CAVD and arterial calcification in postmenopausal women [87,88,93]. There was no association between sclerostin and coronary artery calcification [94]. In African-American patient cohorts, a negative association between serum sclerostin and vascular calcification [95]. Studies also show that sclerostin and aortic calcification are inversely proportional in CKD patients [96]. Meta-analysis of these disparate findings asserts there is no overall association with serum sclerostin and CV mortality [97]. These complex and sometimes contradictory results do little to resolve the specific mechanism of action of sclerostin in the CV system. Signs point to a complex and potentially multifactorial role across a number of different CV tissues and diseases. Further investigation of these effects is crucial to better understand the off-target effects of targeting this protein in the treatment of osteoporosis.

Molecular biology of sclerostin signaling

Sclerostin is a secreted glycoprotein comprised of 190 amino acids. While originally described as an antagonist of BMP signaling, it was found to primarily be an antagonist of Wnt signaling through direct inhibitory effectors on the LRP family (**Fig 3.1**) [98,99]. LRP5 and 6 are the primary receptors of canonical Wnt signaling and sclerostin has been found to interact directly with their extracellular signaling regions.

Normal Wnt signaling is activated via the binding of Wnt ligands to the LRP5/6 co-receptors and the interaction with the Frizzled co-receptors. The activation of this unit sequesters a multi-protein destruction complex to the cell membrane allowing for the stabilization of cytoplasmic β-catenin. B-catenin is then translocated to the nucleus where it activates Wnt gene transcription in concert with the TCF/LEF transcription factor family [100]. Additionally, sclerostin has also shown to interact with LRP4 which helps facilitate its negative effect on the Wnt signaling

pathway [101–103].

Wnt signaling is involved in a number of important biological processes in development and homeostasis as well as diseases such as CV calcification disorders, cancer, and many others [104]. Sclerostin is one of the most well studied Wnt signaling antagonists and is particularly active in regulating bone remodeling in the skeletal system. Sclerostin is secreted by osteocytes under varying stimuli. It travels through the canalicular network to the surface of bone where it interacts with the first or second EGF propeller domain of the LRP proteins [98]. Sclerostin blocks the binding of canonical Wnt signaling proteins to these sites and blocks the activation of this protein [105]. Through this mechanism, sclerostin is involved in the osteocyte-controlled inhibition of Wnt signaling driven bone formation.

Mechanical strain is a well characterized factor in increased bone formation. Increases in activity induce mechanical strains on the bone matrix which are sensed by embedded osteocytes [106,107]. These strains translate to downstream activation of pathways which cause the deposition of new matrix in an effort to better resist these mechanical forces. This phenomenon is known as Wolff's Law [108]. Experiments show that sclerostin is a major regulator of this mechanodependent bone remodeling. Specifically, expression is enhanced during unloading and downregulated under loading exercise by osteocytes [109]. Abundant sclerostin production in the absence of mechanical strain in the hindlimbs of mice inhibits Wnt-dependent bone deposition by osteoblasts and also contributes to the production of RANKL which acts to cause the differentiation and activation of osteoclast cells to begin resorption [110,111]. Sclerostin mutant mice do not experience disuses osteopenia whereas sclerostin overexpression mice are resistant to loading induced bone formation [112,113]. In this way, sclerostin is a unique regulator that affects new bone deposition and resorption of existing matrix.

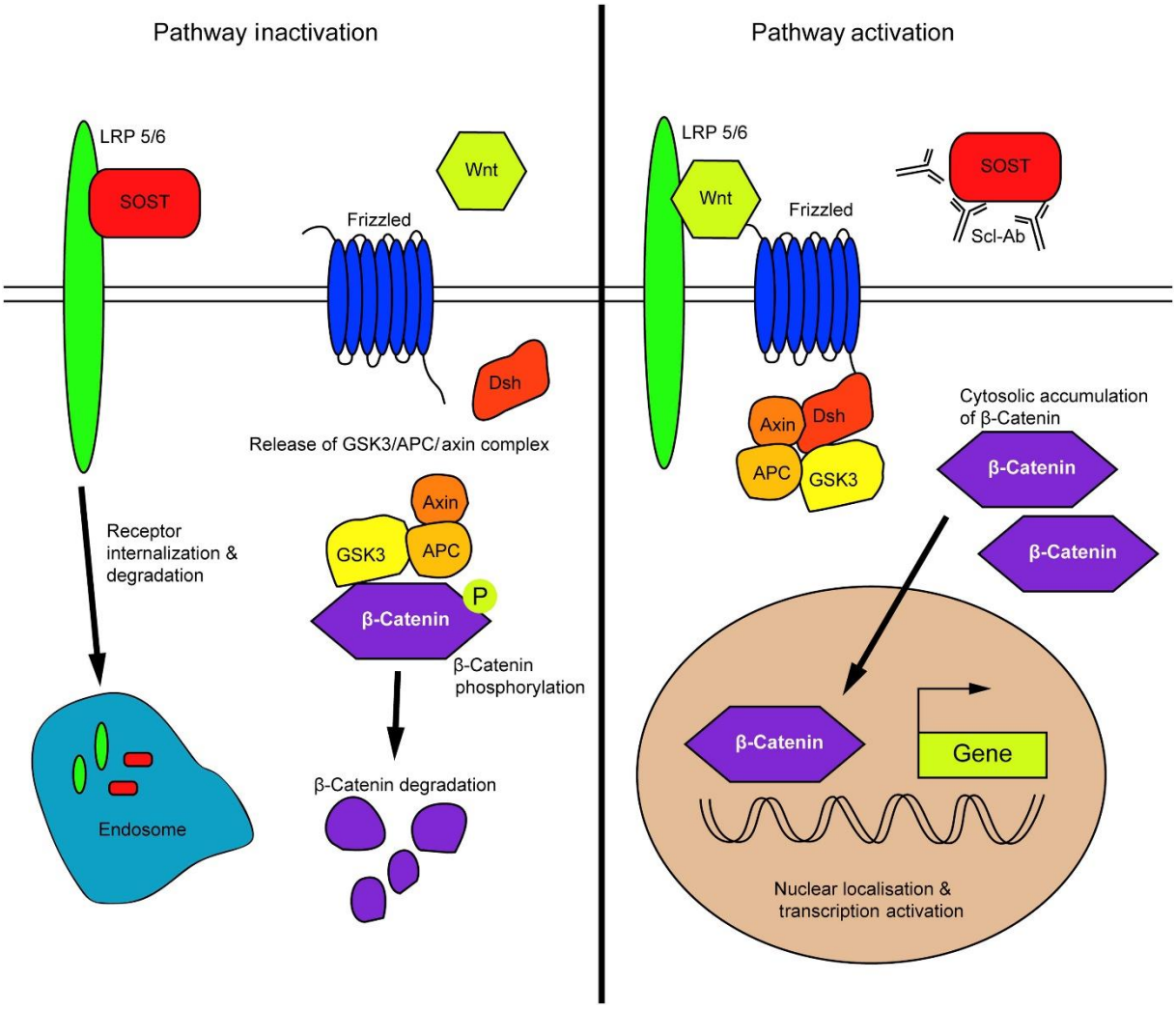

Figure 3.1. Sclerostin is a potent Wnt-signaling inhibitor whose activity is blocked by romosozumab. The Sclerostin protein primarily binds to the canonical surface receptor LRP5 and LRP6 to inhibit Wnt signaling (left). This results in sequestration, phosophorylation, and degradation of the β-catenin protein. Romosozumab inactivates the sclerostin protein (right). This allows the Wnt ligand to facilitate formation of a dimer between LRP and Frizzled surface receptors. This prevents degradation of β-catenin which translocates to the nucleus and affects downstream gene activation. Reprinted under the Creative Commons license © 2016 Suen and Qin. Originally printed in the Journal of Orthopaedic Translation [114].

Sclerostin associated genetic diseases

Sclerosteosis is a genetic disorder first characterized in the 1950's which predominantly affects the Afrikaner population of South Africa [115]. There were approximately 100 identified cases in the 20th century [116]. The hallmark of the disease is progressive skeletal overgrowth and a number of symptoms stem from this phenomenon. Bone overgrowth affects both the axial and appendicular skeleton. Patients are highly resistant to fracture with the only case arising from a vertebral fracture due to increased weight of the skull [116]. Sclerosteosis patients are generally well above average height and weight [86]. Facial overgrowth results in deformity characterized by prominent jaw due to overgrown mandible and enlarged and protruding forehead [116,117]. Facial overgrowth results in loss of function of nerves involved in hearing and vision, which commonly result in impairment [86,118]. The first symptom most commonly observed is syndactyly and deformities of the digits such as fusion or webbing [86,116]. Skull overgrowth leads to compression of the intracranial space resulting in high pressure leading to persistent headaches, nausea, and dizziness which often requires surgical intervention [119,120]. Most patients die in early adulthood (~30 years) from brain herniation due to increased pressure or complications from the craniotomy procedure [116]. Notably, patients who survive into adulthood generally experience stabilization of symptoms [86,117,121]. While two patients to date have died due to heart disease, elderly patients with sclerosteosis do not show signs of impaired cardiac or vascular function or disease [116].

Van Buchem disease is another rare disorder affecting residents of a genetically isolated northern Netherlands community [122]. There were about 30 cases identified in the 20th century [116]. First described in 1955, it presents with symptoms similar to sclerosteosis – skeletal overgrowth, facial deformity, deafness, facial palsy, and increased intracranial pressure. The

phenotype of van Buchem patients is milder than sclerosteosis and only one case required craniotomy and carries a normal life expectancy [116,123,124]. Further, patients are of normal height, do not display digital deformities, and have only mildly impaired hearing. Fractures are infrequent in this population but occur at a higher rate than in sclerosteosis patients [123]. Clinical presentation of these diseases is shown in **Fig. 3.2.**

Similarities between sclerosteosis and van Buchem disease were identified in the 1980's and genetic analysis revealed mutations throughout chromosome location 17q12-q21 [119,125,126]. Patients with sclerosteosis shared a number of mutations in the coding region of the gene *SOST* while van Buchem patients shared a deletion in the spacer region between *SOST* and neighbor *MEOX1* [127–130]. Later studies revealed *SOST* regulatory elements within this spacer region. This reduced (but not eliminated) sclerostin expression is thought to explain the intermediate disease phenotype found in van Buchem patients [131]. Patients heterozygous for sclerostin coding deletion found in sclerosteosis also exhibit an intermediate phenotype with a high BMD and lower sclerostin expression but are free of the severe symptoms found in homozygous deletion [121].

In order to better understand the various mechanisms through which sclerostin acts on the skeletal system, numerous small animal models were generated to study the phenotype in more detail. Germ-line knockouts of sclerostin mimicking the sclerosteosis phenotype exhibit a very high bone mass phenotype as well as increased bone formation rates and mechanical strength. This model does not recapitulate the digital or facial deformations commonly found in human patients and does not carry a decreased life expectancy compared to wild-type (WT) controls. However osteoblast activity appears to be upregulated and circulating markers of bone formation are increased with deletion of the sclerostin gene [132]. Conversely, mice overexpressing human

sclerostin showed opposite effects and displayed an osteopetrotic phenotype with decreased mineralization in the axial and appendicular skeleton. Deposited bone was less organized and strength testing displayed higher fragility and susceptibility to fracture. There was also a corresponding decrease in metrics of osteoblast activity [131].

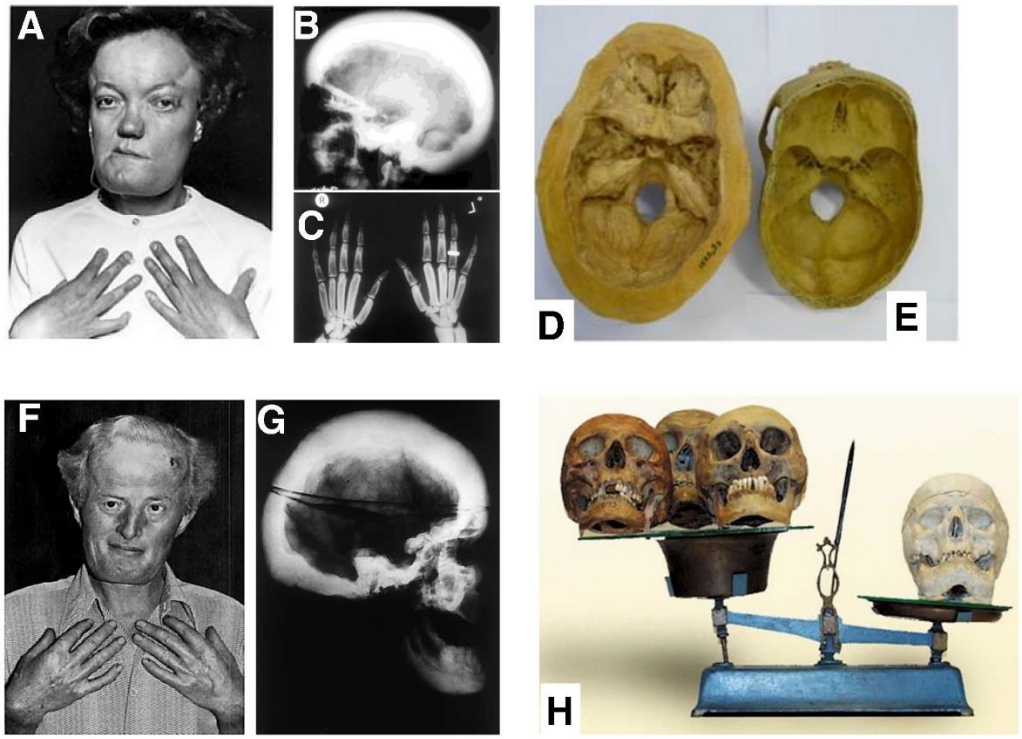

Figure 3.2. Genetic mutation of the sclerostin gene and regulating elements causes a severe bone overgrowth phenotype. A patient (A) with a full frame deletion of the *SOST* gene exhibits skeletal overgrowth in the skull (B, D, E) and digits (C). A patient (F) with a mutation in a *SOST* enhancing regulation region also displays skull overgrowth (G) but at a lower severity. These diseases are called Sclerosteosis (full *SOST*) deletion and Van Buchem Disease (enhancer element deletion). Reprinted under the Creative Commons license © 2018 Sebastian and Loots. Originally printed in Metabolism [133].

Preclinical studies for sclerostin in osteoporosis treatment

Sclerostin's effects were long thought to be isolated to the skeleton. Due to its negative effect on bone formation and positive effect on resorption, its pharmacological targeting seemed to be a promising strategy for diseases of low bone mass such as osteoporosis, disuses osteopenia, and osteogenesis imperfecta. A mAb was developed and tested in a number of pre-clinical animal models with the expectation that blocking the protein would increase bone mass and reduce fracture incidence with minimal off-target effects.

Sclerostin mAb was shown to be effective in a rat model of disuse osteopenia. Rats were normally mobilized or subject to underloading of the hindlimb bones. Vehicle and sclerostin mAb were administered and the trabecular and cortical anatomy of the tibial metaphysis and shaft were analyzed. Immobilized rats with vehicle treatment had increased bone resorption and decrease of bone formation. In normally loaded and unloaded mice, sclerostin neutralizing mAb increased bone mass and decreased resorption [134,135]. This study showed potential efficacy for sclerostin mAb treatment in patients with disuse osteopenia such as those confined to bed rest.

Osteoporosis affects a large number of women in post-menopause due to the loss of the protective effect of estrogen [136]. Sclerostin neutralizing mAb was potentially thought to be a mechanism of reducing loss of bone mass in these patients. To test the hypothesis, the OVX procedure was performed in rats. This model induces rapid development of PMO symptoms included signatures of osteoporosis. One year after OVX, rats were treated with sclerostin neutralizing mAb. The PMO phenotype was reversed and OVX rats actually displayed greater metrics of bone formation, mass, and strength when compared to non-OVX control mice [137]. This study was a strong endorsement for sclerostin mAb treatment in management of PMO.

Decrease in bone mass and incidence of osteoporosis is prevalent in aging. Reducing bone mass, mineral content, and susceptibility to fracture are major factors associated with increasing age and neutralization of sclerostin is thought to be a potential mechanism of reducing these negative events [138,139]. Pre-clinical studies in aged rats show improvements in bone mineral density (BMD) in vertebrae and long bones and improved bone structure in vehicle controls. This correlated with bone strength and increased metrics of bone formation [140]. Simultaneously, aged female rats were examined in a similar fashion at 10 months of age. One month of sclerostin mAb treatment resulted in improved bone formation metrics and trabecular volume. Bone resorption was also decreased [141]. Sclerostin mAb seems promising for treatment of age-related low-bone mass in both men and women.

In addition to efficacy in common low bone mass disease, sclerostin mAb treatment has also shown to be effective in fracture healing in numerous studies in rats as well as improvement of healing after surgical osteotomy in a non-human primate study [142–145].

To prove efficacy in a non-human primate model, sclerostin neutralizing mAb was administered to female cynomolgus monkeys with no alteration of hormonal state. Only two treatments displayed dose-dependent increases in bone anabolism in all studied compartments. This was also seen in bone mineral studies and bone strength and structure in comparison to vehicle controls [146]. This study greatly improved the rationale for study of sclerostin neutralization in humans suffering from low-bone mass disorders.

Clinical trials for sclerostin in osteoporosis treatment

Long theorized to be a potential target in treating low bone mass disease in humans, positive results from pre-clinical animal studies justified beginning clinical trials in a number of patient populations.

Phase I trials were first published in 2010. 72 individuals comprised of healthy men and postmenopausal women were administered sclerostin blocking mAb or placebo in ascending dosage via subcutaneous or intravenous injection. After three months of treatment there were minimal adverse effects with only one case of hepatitis and zero deaths or treatment discontinuations. Markers of bone formation increased in a dose-dependent fashion and BMD improved in treated patients compared to placebo in the spine and hip [147]. A follow up phase I trial was then performed and published in 2014 focusing on men and women who presented with low bone mass phenotype. 48 patients received ascending dosage of sclerostin mAb or placebo and bone formation metrics were assayed along with BMD assessed by imaging. Markers of bone formation increased drastically with blocking of sclerostin with a concurrent increase in BMD. Adverse effects were once again minimal and balanced between groups [148].

Following the promise of phase I trials, phase II trials were published in 2014 and were focused on comparing the efficacy of sclerostin mAb treatment in comparison to current standards of treatment – bisphosphonates. These drugs take advantage of the affinity of the bisphosphonate structure to bind to hydroxyapatite – a primary component in actively remodeled bone. When osteoclasts encounter bone matrix with embedded bisphosphonate molecules they cease resorption and undergo apoptosis – thus slowing bone loss [149]. These drugs therefore slow bone loss but do little to encourage new bone formation. Over 400 postmenopausal women with low bone mass phenotype received sclerostin neutralizing mAb, vehicle, or a

bisphosphonate. Treatment occurred for one year and BMD and markers of bone remodeling were assessed. Adverse effects were balanced amongst groups and sclerostin blocking improved metrics of bone formation compared to bisphosphonate treatment, indicating potential for a new gold standard in osteoporosis care [150].

Large-scale phase III trials were conducted to assess long-term effects of sclerostin neutralization treatment and effects on fracture reduction and improved bone metrics. Results from the Fracture Study in Postmenopausal Women with Osteoporosis (FRAME) trial were published in 2016. Patients were treated for one year with sclerostin mAb or placebo followed by treatment with denosumab. This drug is a RANKL inhibitor acting to downregulate activation of osteoclasts and reduce new bone resorption. Patients treated with sclerostin mAb had a 0.27 risk ratio of vertebral fracture when compared to placebo with no significant decrease in nonvertebral fractures. After denosumab treatment there was a 0.25 risk ratio of vertebral fracture in sclerostin mAb treated individuals and 0.75 hazard ratio for non-vertebral fractures however this effect had a non-significant adjusted p-value [151].

The Active Controlled Fracture Study in Postmenopausal Women with Osteoporosis at High Risk (ARCH) trial was published in 2017 and included over 4000 patients (**Fig. 3.3**). Patients were given sclerostin blocking or bisphosphonate treatment for one year followed by one year of further bisphosphonate treatment in each group. Patients with initial treatment of sclerostin blocking were half as likely to experience vertebral fracture as patients only treated with bisphosphonates. Overall fracture risk reduced by 27% when patients were treated with combination therapy as opposed to bisphosphonates alone [7].

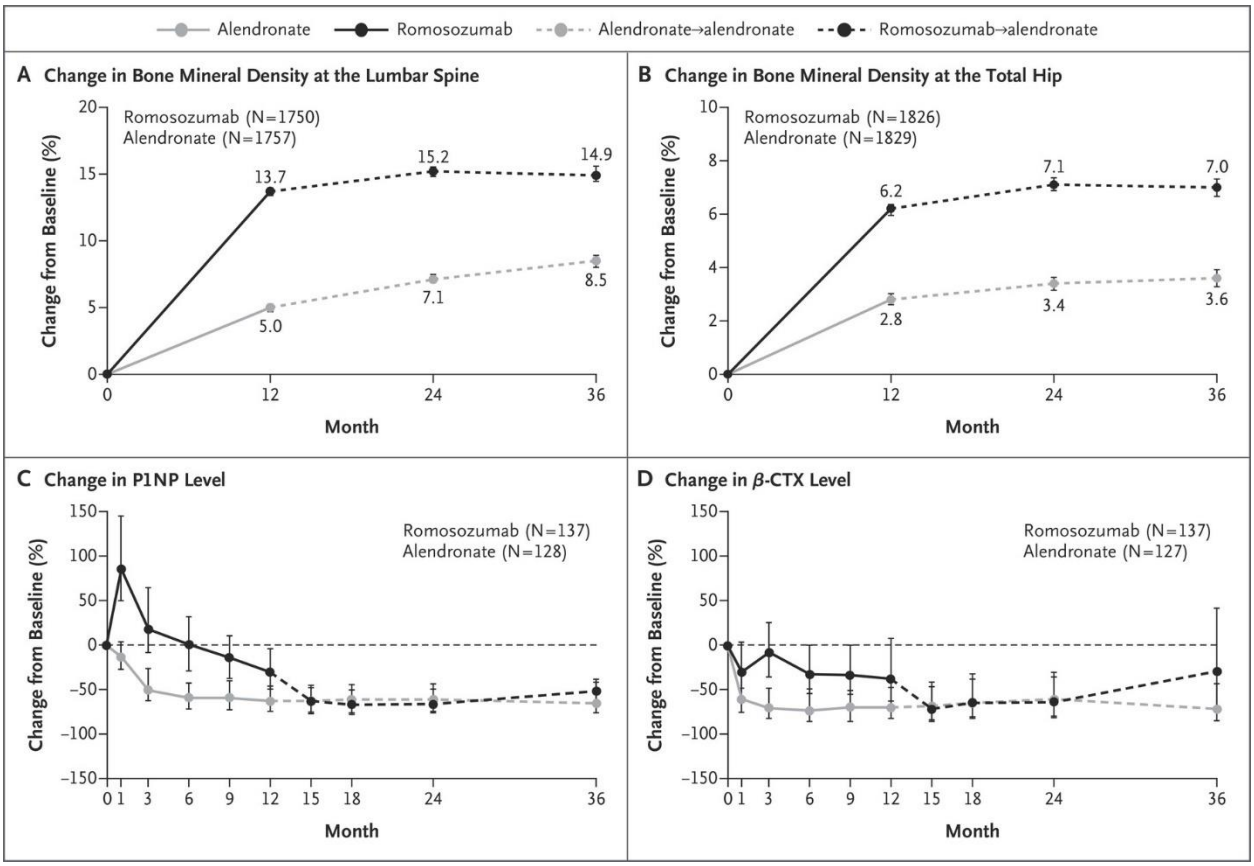

Figure 3.3. Romosozumab is a more effective post-menopausal osteoporosis treatment than alendronate. Results from the ARCH trial were acquired based on BMD and bone remodeling agent levels. BMD at the spine (A) was nearly tripled compared to alendronate after one year. BMD approximately doubled at the hip (B). P1NP (C) and β-CTX (D) circulating levels were similarly diminished between the two drugs. Reproduced with permission from 2017 Saag et. al. © Massachusetts Medical Society. Originally printed in NEJM [7].

Finally, the Study Evaluating Effects of Romosozumab Compared with Teriparatide in Postmenopausal Women with Osteoporosis at High Risk for Fracture Previously Treated with Bisphosphonate Therapy (STRUCTURE) trial analyzed over 400 women who had been treated for over three years with bisphosphonate therapy. Half of patients were continued on bisphosphonate therapy while the others were transitioned to a sclerostin blocking therapy and analyzed after one year. Results showed a 2.6% increase in BMD in sclerostin mAb patients compared a 0.6% decrease in bisphosphonates. These changes were consistent in other skeletal sites and indicate an advantage of sclerostin blocking even when bisphosphonates have become ineffective in patients at severely high fracture risk [152].

While the skeletal effects of sclerostin neutralization are extremely positive in treating patients with a number of low bone mass afflictions, results of the ARCH trial indicated troubling CV side effects (**Table 3.1**). Specifically, serious CV events were more frequent in patients treated with sclerostin blocking mAb than bisphosphonates. Digging into the reported differences, cardiac ischemic and cerebrovascular events were more commonly observed in sclerostin treated individuals with odds ratios of 2.65 and 2.27, respectively. Death after sclerostin treatment was numerically higher than bisphosphonate and became level after groups switched to bisphosphonates alone. Interestingly, incidence of noncoronary revascularization and HF were lower in sclerostin treated groups and remained lower after reverting back to bisphosphonate treatment [7]. These effects resulted in a safety flag by the U.S. Food and Drug Administration and delayed approval for treatment [153].

	Alendronate	Romosozumab
Adjudicated serious cardiovascular event‡	38 (1.9)	50 (2.5)
Cardiac ischemic event	6 (0.3)	16 (0.8)
Cerebrovascular event	7 (0.3)	16 (0.8)
Heart failure	8 (0.4)	4 (0.2)
Death	12 (0.6)	17 (0.8)
Noncoronary revascularization	5 (0.2)	3 (0.1)
Peripheral vascular ischemic event not requiring revascularization	2 (<0.1)	0
Death	21 (1.0)§	30 (1.5)

Table 3.1. Summary of cardiovascular side-effects in ARCH trial. Results of cardiovascular side-effects after one-year of treatment of alendronate or romosozumab. There were significant increases in cardiac ischemic and cerebrovascular events. Adapted with permission from 2017 Saag et. al. © Massachusetts Medical Society. Originally printed in NEJM [7].

Data gathered from robust clinical trials indicates a strong effect of sclerostin blocking therapy in improving the effects of low bone mass in old age and particularly in PMO. However, the myriad of CV side effects is obviously a cause for concern. The safety flags even resulted in postponement of FDA approval of the drug for treatment. However, approval was first gained in Japan and was nearly unanimously approved in the U.S.A. In April of 2019 for postmenopausal women at very high risk of fracture. This took place after pooling of data from multiple trials to try to determine overall CV risk. The drug is marketed under the brand name Evenity, carries a warning label, and is not recommended for patients at high risk for CV diseases or those with a history of CV disease. This obviously limits the clinical utility of the drug, as the patients most likely being treated are elderly and at higher risk for CV disease the general population. Therefore, it is important to develop a thorough understanding of sclerostin in the CV system in order to fully understand the effects of targeting this drug for low bone mass diseases.

CHAPTER 4

Sclerostin Ablation Prevents Aortic Valve Stenosis in Mice

Introduction

Sclerostin (human gene: *SOST*, mouse gene: *Sost*) is a secreted glycoprotein that has shown to be a potent regulator of bone remodeling [154]. It was first discovered to be the causative root of excessive bone overgrowth in Sclerosteosis (full *SOST* deletion) and van Buchem diseases (deletion of a genetic regulator) [125,126,130,155]. Further studies clarified the mechanisms whereby sclerostin regulates ossification, resorption, and mechanotransduction in bone by altering the Wnt and RANKL pathways of the skeletal system [110,111,156,157].

Due to the protein's involvement in bone remodeling and its apparent localization to the skeletal system, sclerostin became a target of great interest for the treatment of low bone mass diseases such as osteoporosis. Clinical trials of a mAb targeting sclerostin - known as romosozumab - substantially improved bone quality metrics and reduced hospitalization in PMO patients [7,151,152,158,159]. However, the stage III ARCH trial noted an imbalance in CV effects compared to the current standard bisphosponate medication, alendronate. The authors specifically noted a significant increase in cardiac and cerebrovascular ischemic events and a numerical decrease in HF [7]. This resulted in the drug receiving a warning of CV side effects which must be weighed when considering prescribing romosozumab to patients who may have, or be at risk for, CV disease.

Discovery of off-target effects in the CV system prompted a review of existing literature as well as new studies directly interrogating the role of sclerostin in various disease models. While the body of literature for sclerostin's role in the AV is quite limited, there are some studies of interest. AVs excised from human patients with AVS showed that sclerostin protein and mRNA are upregulated in diseased tissue near sites of ectopic calcification [88]. A study from the same year found that serum sclerostin levels are associated with valve calcification in

individuals undergoing hemodialysis. This was also confirmed at the tissue level using immunohistochemistry and quantitative real-time polymerase chain reaction (qPCR) [94]. While these studies show correlation between valve disease and sclerostin expression, it is unclear if the increase is a direct contributor to AVS.

The pathways associated with sclerostin signaling in the skeletal system also contribute to the progression of AVS which augment the necessity for direct investigation. Activated Wnt and RANKL signaling have shown to be involved in ectopic calcification of the AV, indicating there may be shared processes sclerostin acts on in the skeletal and CV systems [49,160].

AVS is a complicated and poorly understood disease process and it is unclear whether sclerostin plays a significant role in its progression. To this end, we hypothesized, based on the CV events in the stage III ARCH trial, long-term loss of sclerostin would worsen AVS in a mouse model. Surprisingly, we found *Sost* ablation had a protective effect in the progression of AVS via reduced myofibroblast activation and AVIC contractility potentially due to upregulation of protective *Homeobox (Hox)* gene expression.

Materials and Methods

Animals

All mouse experiments were carried out under appropriate approval and supervision from the Vanderbilt University Institutional Animal Care and Use Committee (IACUC). *Sost* knockout mice (NULL) were provided by Dr. Gabriela Loots and bred as previously described [161]. Littermates homozygous for the WT *Sost* gene were used as controls. Equal amounts of male and female mice were used. At 4 months of age, mice transitioned from standard chow to a 1% cholesterol Western diet (TestDiet 5TJT). Food and water were provided ad libitum. Mice were aged for 8 additional months on the Western diet to 12 months of age, euthanized by carbon dioxide inhalation followed by cervical dislocation, and AV tissue was harvested for processing and analysis (**Fig 4.1A**).

Cells

Mouse AVICs were isolated as described previously [53]. Briefly, WT mice were crossed with the "Immortomouse" line (Charles River, 237 HO, 238 HE) in order to generate cell lines capable of undergoing prolonged growth under specific culture conditions. Mice were euthanized and the heart carefully excised under sterile conditions. Using a dissection microscope, the aortic root was isolated and the individual leaflets removed, soaked in 600 U/mL collagenase II (Worthington Biochemical Corp, Lakewood, NJ) for 30 minutes, and centrifuged. Leaflets were then placed on 0.1% gelatin coated tissue culture dishes in immortalized media (10% fetal bovine serum, 1% penicillin/streptomycin antibiotic, 10 U/mL interferon-Ɣ in Dulbecco's Modified Eagles Medium), with environmental conditions of 33° C and 5% CO_2. AVICs were allowed to adhere to the culture dish, migrate from the leaflet tissue, and expand for about one

week until confluence was reached (**Fig 4.1B**). To verify the isolation of a myofibroblast cell line, cell morphology was confirmed visually and the presence of the contractile protein alpha-smooth muscle actin (aSMA) was confirmed using immunostaining. Prior to all experiments, cells were maintained for 24 hours at 37° C and 5% CO_2,in complete media without interferon-Ɣ (10% FBS, 1% pen/strep antibiotic in DMEM) to inactivate the immortalization element.

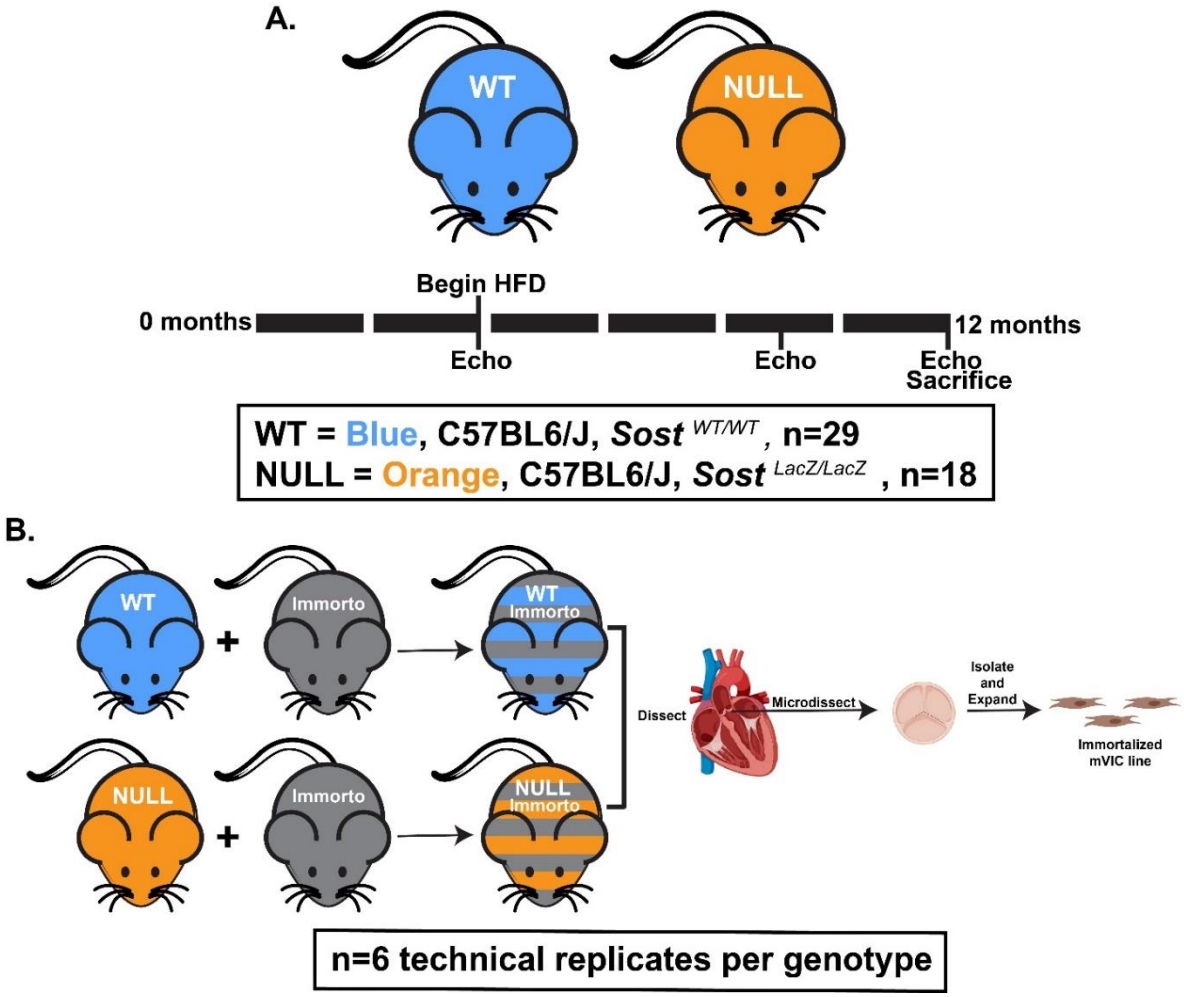

Figure 4.1. The effects of genetic ablation of the *Sost* gene, aging, and high-cholesterol diet were assessed using *in vivo* and *in vitro* models. A. Mice were given high-cholesterol diet beginning at 4 months and aged to 12 months. The development of AVS was tracked using echocardiography at 4, 9, and 12 months of age. Black bar = 2 months. **B.** In parallel, immortalized mouse lines were generated for WT and NULL groups. Aortic valve interstitial cells were isolated and expanded for *in vitro* analysis. Image partially created with Biorender.com.

Echocardiography

Echocardiographic assessment was performed at 4, 9, and 12 months of age to identify changes in cardiac structure and function. All imaging was performed by skilled technicians in the Vanderbilt Cardiovascular Physiology Core (VCPC) using the Vevo 2100 small animal imaging system. Mice were lightly anesthetized (mean: 492 bpm) using isoflurane and laid supine on a heated platform. Transthoracic aortic pulsed wave Doppler imaging was used to generate AV velocity profiles. Parasternal short-axis M-mode imaging was performed to measure LV performance and cardiac function as indicated by changes in strain throughout the cardiac cycle.

For AV-specific measurements, a custom MATLAB script was used to automatically trace pulsed wave Doppler waveforms and determine cardiac-gated hemodynamic metrics such as PV and MG [162]. At each time point, three Doppler measurements were gathered for each mouse resulting in 50 to 100 independent cardiac cycles being averaged to produce representative metrics. LV thickness and motion were manually measured over each cardiac cycle. Three cycles were averaged for each M-Mode image for a total of 9 cycles analyzed per mouse per time point.

Dual Energy X-Ray Absorptiometry

Femur bone metrics were measured using the Hologic UltraFocus Dual Energy X-Ray Absorptiometry and associated software. Samples were placed on the stage at 2X magnification and images were acquired in a series of 4 captures at 40 kV followed by 4 captures at 80 kV captures. Using a custom Region of Interest analysis in the system software (Version 3.1), the bone mineral content, BMD, and femur length were measured.

Histological Staining

Excised aortic roots were embedded in Optimal Cutting Temperature (OCT) compound and flash frozen. Using a -20° C cryostat, aortic root samples were serially sectioned at 10 μm. For all staining analysis, 3 sections per aortic root were analyzed for a representative metric. Picrosirius Red (PSR) (FisherScientific) staining was performed to assess collagen characteristics and morphology of the aortic roots. Alizarin Red S (ARS) (Sigma-Aldrich) staining was performed to assess the extent of valve calcification. For both stains, standard manufacturer protocols were followed without deviation. After staining, slides were dehydrated in progressively concentrated alcohol baths (70%, 90%, 100%), cleared in xylene, mounted in organic mounting media, coverslipped, dried overnight, and sealed prior to imaging. Brightfield images were captured at a 4X magnification objective using a Nikon Eclipse E800 microscope equipped with an Olympus DP74 digital polychromatic camera. Representative images were shown to best illustrate the quantitatively determined phenotype.

Immunohistochemical Staining

Fluorescent immunostaining was used to characterize the prevalence and localization of aSMA (contractile) and Runx2 (osteogenic) proteins - both of which are common markers of AV disease. Slides were washed in PBS prior to fixation/permeabilization for 10 minutes in a 4% paraformaldehyde/0.1% Triton solution in PBS. Sections were then blocked for non-specific binding using 10% bovine serum albumin in PBS for 1 hour at room temperature. Primary antibodies were added to a 10% diluted blocking solution at the following concentrations: 1:100 rabbit polyclonal anti-aSMA (Abcam ab5694), 1:100 rabbit monoclonal anti-Runx2 (Cell Signaling Technology 12556) and incubated overnight at 4° C. The following day, sections were

washed in PBS prior to incubation in 1:1000 goat anti-rabbit IgG Alexa Fluor 647 (ThermoFisher A-21245) for 1 hour at room temperature and covered from light. After secondary staining, slides were once again washed in PBS prior to being mounted in ProLong Gold Antifade with DAPI (Cell Signaling Technology 8961), coverslipped, allowed to dry overnight at room temperature, then sealed. Fluorescent images were captured at 20X magnification objective using an Olympus BX53 microscope and Qimaging Retiga 3000 digital monochromatic camera.

Quantitative Image Analysis

For the analysis of PSR staining, brightfield images of the stained aortic root were acquired and cropped to contain only the AV leaflets. Total leaflet area was calculated from brightfield images and collagen composition within the leaflet area was determined as previously described [163,164]. Expression of contractile (aSMA) and osteogenic (Runx2) proteins of interest in the AV was determined from analysis of immunofluorescence (IF) images, as previously described [165]. Briefly, AV sections fluorescently labeled for either aSMA or Runx2 were stained with DAPI to indicate leaflet nuclei and provide an estimate of leaflet area based on a manually defined boundary. Segmentation of individual nuclei was performed using a modified watershed transform and concave object separation algorithm [163,166]. aSMA area fractions were then computed as the ratio of positive pixels to total pixels within the leaflet boundary. Runx2 positive nuclei were defined based on the ratio of positive pixels to total pixels within the identified nuclear boundary.

RNA Sequencing

Aortic roots from WT and NULL mice were isolated via microdissection and flash frozen in liquid nitrogen prior to storage at -80˚C until RNA isolation. To collect total RNA from each sample, single aortic roots were homogenized in Trizol prior to isolation using the Zymo Direct-zol RNA Microprep kit. RNA integrity was measured with an Agilent Bioanalyzer prior to library preparations. All samples had RIN values greater than 7. Aortic roots were analyzed as isolating adequate quantities of high-quality RNA from individual leaflets has proven technically infeasible.

The Vanderbilt Technologies for Advanced Genomics (VANTAGE) center performed library preparation, sequencing, and read alignment. Briefly, cDNA libraries were generated from total RNA using the NEBNext Ultra II Directional RNA Library Prep Kit then sequenced on an Illumina NovaSeq 6000 to an average depth of 63.5 M reads per sample using 150bp paired-end chemistry. Sequencing quality was assessed using FastQC. Reads were aligned to mouse genome mm10 and gene counts were determined using the Illumina DRAGEN pipeline.

For analysis of RNAseq datasets, differential gene expression and normalization to library size was performed using the R package DEseq2 using Cook's outliers to filter low gene counts and $\alpha = 0.05$. KEGG and GO over-representation analysis was performed using the R package clusterProfiler using the respective enrich function with default parameters. Gene sets were considered over-represented if padj < 0.05. Visualizations were generated using a combination of enrichplot and ggplot2 packages in R.

3-D Cell Contractility Assay

The contractile phenotype of AVICs was assessed using the 3-D Gel Contraction Assay as described previously [55]. A collagen gel solution was mixed (80% PureCol, 10% 10X PBS, 10% 0.1 M NaOH) and stored on ice. AVICs were suspended in complete media supplemented in either 0 or 1 ng/mL of recombinant TGFβ1 (R&D Systems 7666MB005) or 0 or 100 ng/mL of recombinant sclerostin (R&D Systems 1406-ST). Cells were added to the collagen gel solution at a 1:1 ratio to achieve a concentration of 250 cells/ μL collagen:media solution. The combined solution was mixed thoroughly to ensure a uniform distribution of cells across the gels. Sterilized teflon rings (no. 5612-303-62, Seastrom Manufacturing) were placed in non-tissue culture treated dishes and 250 μL of the mixture was evenly pipetted in the rings. The mixture of collagen gel, cells, and media was allowed to solidify for one hour in a 37° C incubator. Solidified gels were covered with complete media supplemented with 0 or 1 ng/mL TGFβ1 and the Teflon rings were carefully removed using sterilized forceps. The gels were allowed to float freely in the media solution. The circular gels were imaged after 24 hours using a Leica M165 FC stereo microscope and the contraction ratio was calculated as the change in gel area relative to the initial area (at time = 0h).

Real-time quantitative polymerase chain reaction

WT and NULL immortalized AVICs were lysed using Trizol Reagent (ThermoFisher Scientific 15596026). The Direct-zol RNA Miniprep Kit (Zymo Research R2050) was used to isolate high-quality mRNA directly from lysed samples. Isolation was performed by following manufacturer protocols without deviation. Samples were analyzed for concentration and purity using a NanoDrop UV Spectrophotometer (ND-ONE-W). A 260/280 wavelength ratio of ~2.0

was considered pure RNA and used for downstream analysis. cDNA was synthesized using SuperScript IV First-Strand Synthesis System (ThermoFisher 18091150). SYBR Green qPCR Master Mix (ThermoFisher 4309155) was used to allow fluorescent detection during amplification. Manufacturer protocols were followed without deviation. CFX96 Real-Time PCR Detection System (Bio-Rad) was used for thermocycling amplification and measurement of fluorescent signal. cDNA was denatured at 95º C for 4 minutes, then the following cycle was carried out 40 times for amplification: 10 sec 95º C, 10 sec 55º C annealing, and then a plate read to determine fluorescent intensity. After amplification, melt curves were generated for each sample using the following protocol: initialize 65º C, plate read, 0.5º C, plate read, until a maximum of 95º C was reached. Only samples with strong single-peak melt curves around ~80º C without evidence of primer-dimer formation were considered in analysis. Bio-Rad CFX Manager 3.1 software was used to quantify amplification by defining detection thresholds and assigning each sample a C_t value. Sample C_t values were normalized to that of a stable housekeeper, *Gapdh*, and statistics were performed on non-transformed ΔC_t values. Primer sequences are defined in **Table A.4.1**.

Validated primers were selected from the Harvard PrimerBank database. Sequences were independently verified using the NCBI Primer-BLAST resource to ensure target specification and no secondary binding potential.

Statistical Analysis

All data are presented as mean +/- error as noted in figure captions. The following statistical tests were used and are noted in each figure caption: Student's t-test for 2 group comparison, one-way analysis of variance (ANOVA) for 3 or more groups, and two-way

ANOVA for time-course echocardiography data to determine the effects of time vs. genotype. For repeated-measures ANOVA tests, mixed-effects analysis was performed with the Geisser-Greenhouse correction and Tukey's multiple comparisons test. For all tests, a p-value of 0.05 was considered statistically significant. Data storage and statistical analysis was performed using Microsoft Excel, MATLAB r2019a, and GraphPad Prism 9.1.1. Analysis was performed by the authors but sample identification was blinded and quantitative analysis was performed using custom programs instead of qualitative or manual measurement to reduce bias.

Results

Deletion of the Sost gene recapitulates the high bone mass phenotype observed clinically

Human patients lacking the *SOST* gene display a bone overgrowth phenotype which can be recapitulated in a mouse model [133,155]. Dual energy x-ray absorptiometry (DXA) scans were used to confirm this phenotype in experimental groups (**Fig 4.2A**). Consistent with prior reports, there was a clear high bone mass phenotype based on a doubling of BMD in NULL mice, relative to WT (51.81+/-1.12 vs. 106.9+/-6.25; $p<0.0001$) without a significant change in femur length (13.21+/-0.13 vs. 13.30+/-0.22; $p=0.71$) (**Fig 4.2A**) [132]. Body mass was also unchanged between the two groups (**Fig A.4.1**).

Deletion of the Sost gene prevents the hemodynamic hallmarks of aortic valve stenosis

Hemodynamic parameters across the AV and structure and functional parameters in the LV were assessed using cardiac echocardiography to track the development of AVS between groups. WT mice developed mild to moderate increases in aortic PV (140.1+/-7.15 vs. 125.9+/-9.32, 160.1+/-10.05 vs. 122.7+/-7.31, 176.2+/-13.82 vs. 130.7+/-6.81; $p=0.72$, $p<0.05$, $p<0.001$; 4, 9, 12 months, respectively) and MG (2.09+/-0.2 vs. 1.66+/-0.95, 2.79+/-0.48 vs. 1.46+/-0.19, 4.10+/-0.85 vs. 1.72+/-0.23; $p=0.92$, $p=0.22$, $p<0.001$; 4, 9, 12 months, respectively) while NULL mice remained largely unchanged between 4 and 12 months of age (**Fig 4.2B**). Both groups experienced similar insignificant levels of hypertrophy in the LV as measured by LV mass (94.49+/-2.85 vs. 96.48+/-3.9, 112+/-3.81 vs. 116.5+/-4.91, 118.3+/-5.73 vs. 113.5+/-5.71; $p=0.99$, $p=0.88$, $p=0.86$; 4, 9, 12 months, respectively) (**Fig 4.2C**). In addition, LV function remained similar over time with little difference between WT and NULL groups LV ejection fraction (EF) during the heart cycle (46.26+/-1.1 vs. 44.14+/-1.19, 50.65+/-1.65 vs. 45+/-2.31,

48.13+/-1.39 vs. 50.66+/-2.85; p=0.78, p=0.07, p=0.68; 4, 9, 12 months, respectively) (**Fig 4.2C**). There was not a significant difference due to sex of the mice. Raw echo data separated by sex is found in **Table A.4.2**. Left ventricular outflow tract diameter was also used to normalize for heart anatomy changes. However, this did not change the results in any way (**Fig A.4.2**).

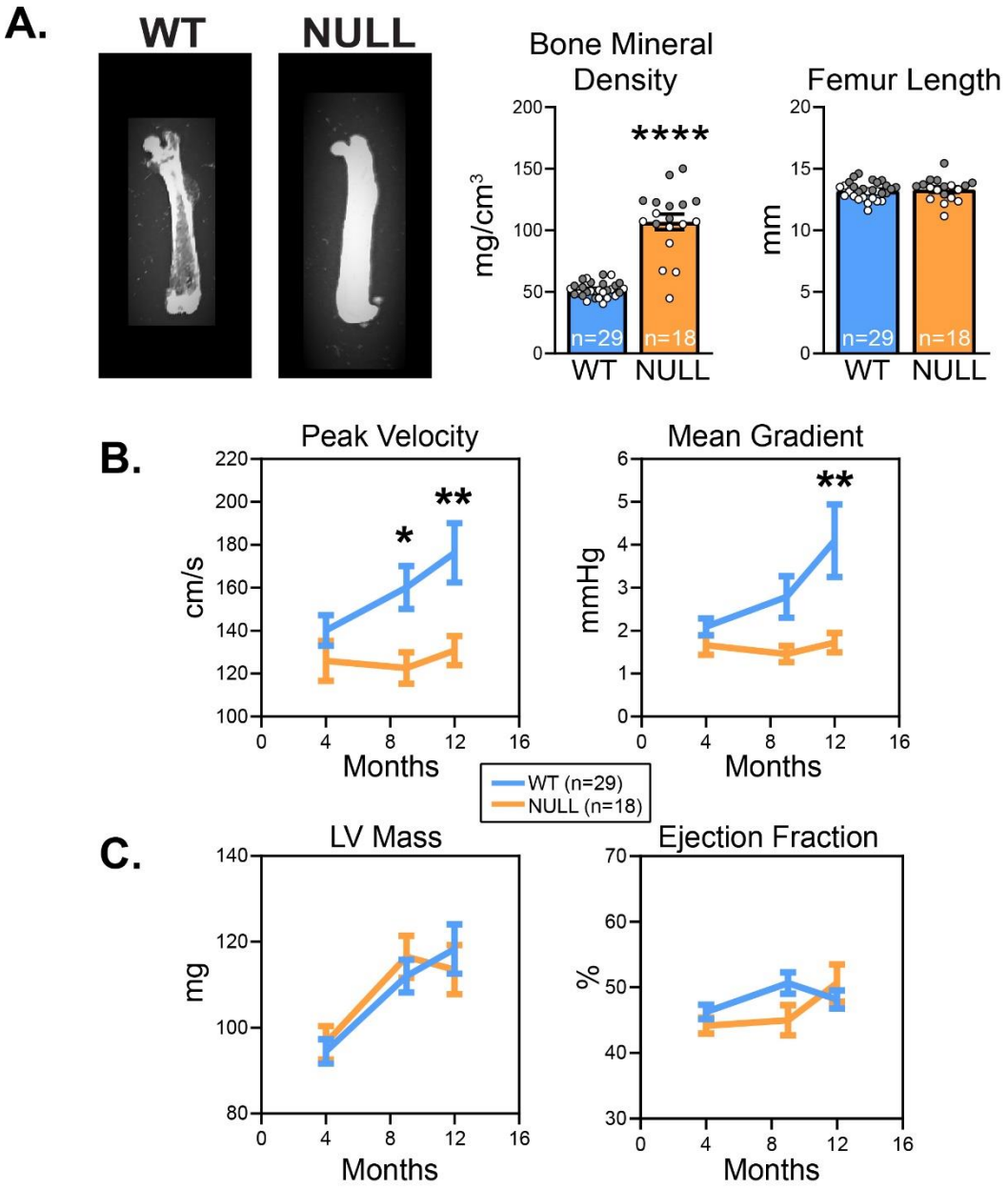

Figure 4.2. Genetic ablation of *Sost* results in a bone overgrowth and prevention of AVS. A. Dual energy x-ray absorptiometry was used to assess femur BMD (middle) and length (right). NULL mice display a sclerotic phenotype with no change in limb length. **B.** Aortic valve hemodynamics were assessed using pulsed doppler imaging tracked over time. Standard markers of AVS (peak velocity and mean gradient) were significantly increased in WT groups while remaining unchanged in NULL. **C.** Left ventricle measurements were taken by m-mode echocardiography. Both groups had similar left ventricular hypertrophy (left) in order to compensate with weight increase. Ejection fraction (right) did not display a clear phenotype with no significant differences. **A.** Mean+/-SEM, Students t-test. Gray dots=female, White dots=male. **B.** Mean+/-SEM, 1-way ANOVA with post-hoc Tukey test. *p<0.05, **p<0.01, ***p<0.001, ****p<0.0001.

Sost knockout mice have thinner leaflets

Leaflet morphology, collagen conformation, and calcification was assessed in AVs from WT and NULL mice using PSR and ARS staining (**Fig 4.3A**). Measurement of the full thickness of the AV leaflets showed WT leaflets were generally 30% thicker than NULL leaflets (16.52+/-1.00 vs. 11.48+/-1.01; $p<0.01$), on average (**Fig 4.3A**). Both groups were highly packed with collagen at similar densities (99.59+/-0.09 vs. 99.53+/-0.13; $p=0.71$) and did not show any clear patterns of calcification on the leaflets (**Fig 4.3A**).

Sost knockout mice have lower prevalence of myofibroblast markers of aortic valve disease

The mechanisms of AVS progression (i.e., dystrophic vs. osteogenic) were assessed using quantitative analysis of aSMA and Runx2 immunostaining (**Fig 4.3B**). NULL leaflets had significantly lower expression of aSMA than WT (69+/-5 vs. 38+/-6; $p<0.01$), a marker of myofibroblast activation and dystrophic calcification associated with early AVS (**Fig 4.3B**). There was no significant difference in Runx2 nuclear expression, a marker of later stage osteogenic calcification (3.6+/-1.2 vs. 2.0+/-1.1; $p=0.42$) (**Fig 4.3B**).

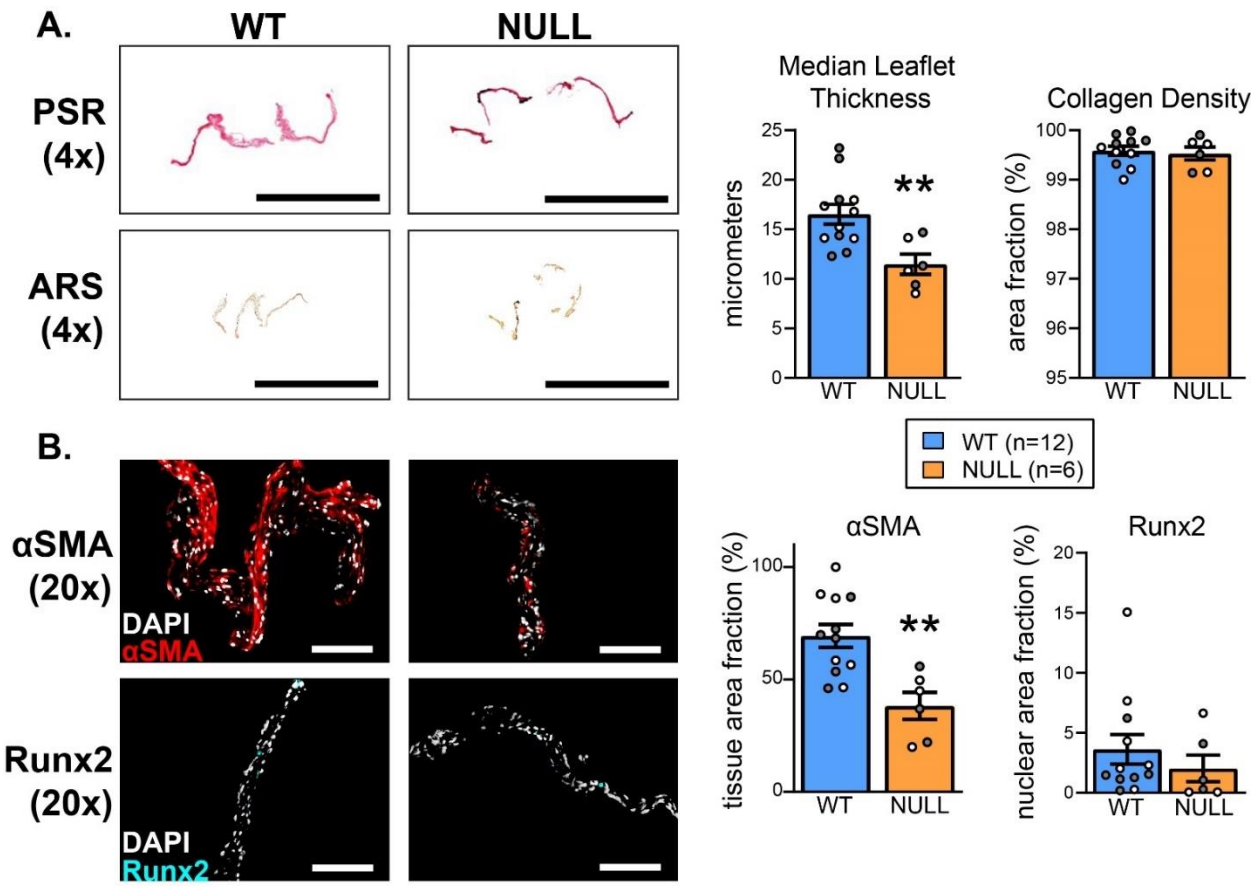

Figure 4.3. *Sost* knockout prevents early myofibroblast related AVS phenotype. A. Picrosirius Red (top row) and Alizarin Red S (bottom row) were used to assess valve collagen and calcification, respectively. While there were no trends regarding calcification or collagen, median leaflet was thicker in WT mice indicating mild hypertrophy. **B.** Immunofluorescent staining was used to determine if myofibroblast (αSMA, top row) or osteogenic (Runx2, bottom row) was driving phenotypic change. αSMA was significantly more prevalent in WT mice while Runx2 was unchanged, indicating a potential myofibroblast AVS phenotype. **A.** Mean+/-SEM, Students T-test. Gray dots=female, white dots=male. **B.** Mean+/-SEM, Students t-test. Gray dots=female, white dots=male. *p<0.05, **p<0.01, ***p<0.001, ****p<0.0001. Scale bar magnitudes: 4x=1mm, 20x=100microns.

RNA sequencing of aortic roots reveals significant change in Hox transcription factors

To determine potential mechanistic explanations for the divergent phenotypes, RNA sequencing was performed on 3 aortic roots from the WT and NULL groups (**Fig 4.4A**). Overrepresentation analysis was performed to identify which genes were interacting with the most GO Biological processes and the top genes are isolated. Biological processes associated with development, regionalization, connective tissue development are highlighted (**Fig 4.4B**). Several of the genes in the *Hox* family of transcription factors were shown to interact with these processes. Upon further investigation, nearly half of all *Hox* genes were upregulated in NULL groups compared to WT. Six of the most highly regulated are highlighted in the volcano plot (**Fig 4.4C**).

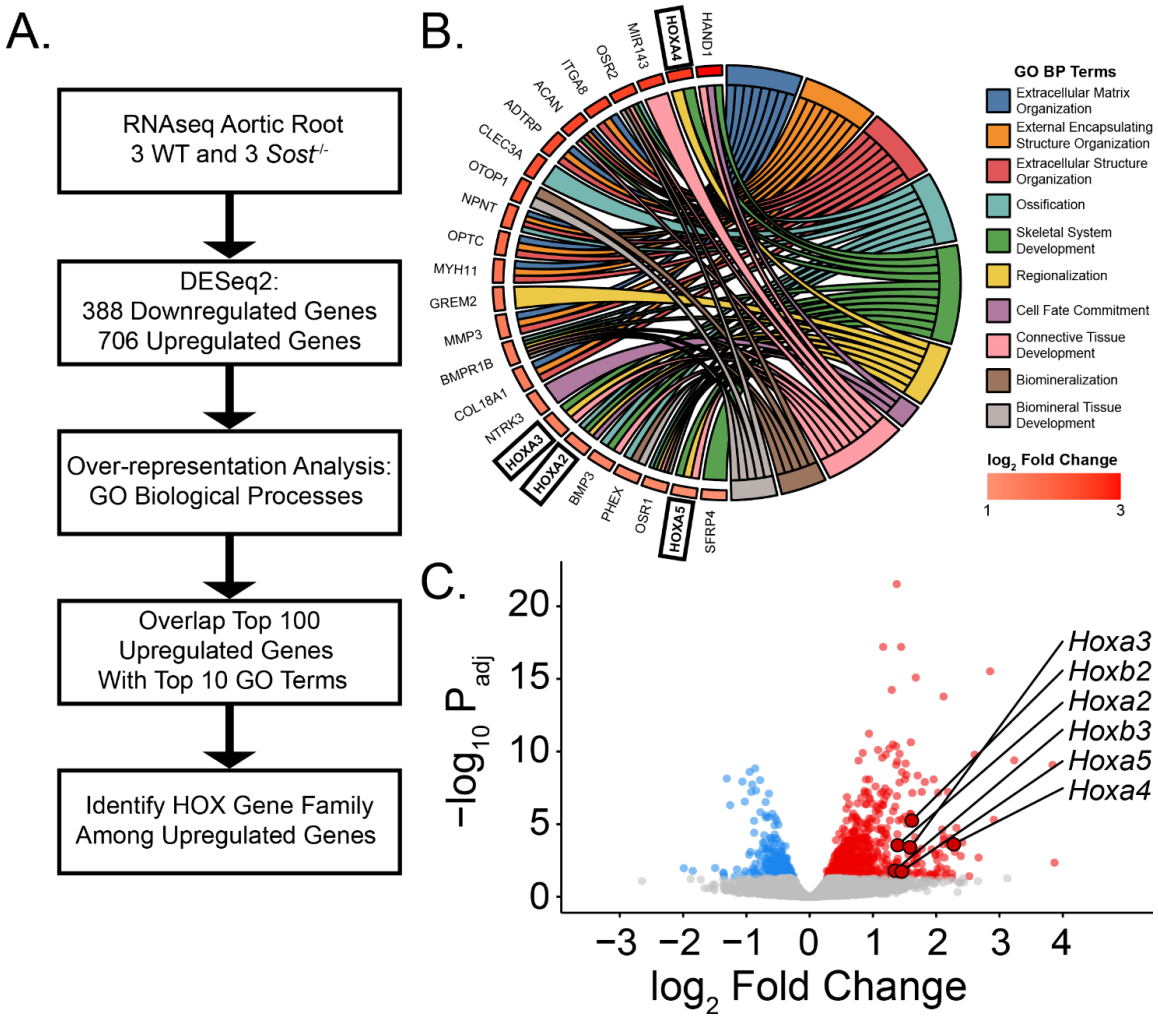

Figure 4.4. RNA sequencing of aortic roots shows over 1000 differentially regulated genes and an increase in pan-*Hox* gene expression in NULL groups. A. Schematic of RNAseq read analysis by differential gene analysis, over-representation analysis, and *Hox* identification. **B.** Top over-represented genes paired with all of the over-represented GO Bioprocess terms associated. **C.** Volcano plot of differentially expressed genes with notation of top expressed *Hox* genes. Blue genes are significantly downregulated in NULL mice (n=388) and red genes are significantly upregulated in NULL mice (n=706).

Several Hox transcription factors are upregulated in isolated aortic valve interstitial cells

AVIC lines were established in order to assess potential mechanisms contributing to the observed valvular phenotype and *Hox* genes of interest were assessed using qPCR. Of the 13 *Hox* genes identified from the RNAseq data, 3 were more highly expressed in NULL AVICs (*Hoxa1, Hoxb2, Hoxd3*) with *Hoxa3* near significance (p=0.17). *Hoxa7* was significantly downregulated in NULL AVICs compared to WT controls (**Fig 4.5A**).

Isolated WT AVICs are more contractile than NULL

In order to verify the *in vivo* data indicating WT valves had a greater level of myofibroblast activation, isolated AVICs from the WT and NULL groups were embedded in collagen gels and treated with 0 or 1 ng/mL of recombinant TGFβ1 (**Fig 4.5B**). WT cells were also embedded and treated with 0 or 100 ng/mL of recombinant sclerostin (**Fig 4.5C**). Neither cell type exhibited contractility without stimuli (-2.40+/-0.95 vs. -1.74+/-1.14). Addition of TGFβ1 in media caused significant contraction in both cell lines (-2.40+/-0.95 vs. -76.33+/-6.54, -1.74+/-1.14 vs. -28.16+/-2.8; $p<0.0001$, $p<0.001$; WT and NULL, respectively). Furthermore, WT cells displayed nearly 3x as much contractile capacity when compared to NULL group (-76.33+/-6.54 vs. -28.16+/-2.8; $p<0.0001$) (**Fig 4.5B**). WT cells treated with recombinant sclerostin protein also exhibited slightly higher contractility than untreated controls (-6.91+/-1.24 vs. -19.43+/-2.25; $p<0.001$) (**Fig 4.5C**).

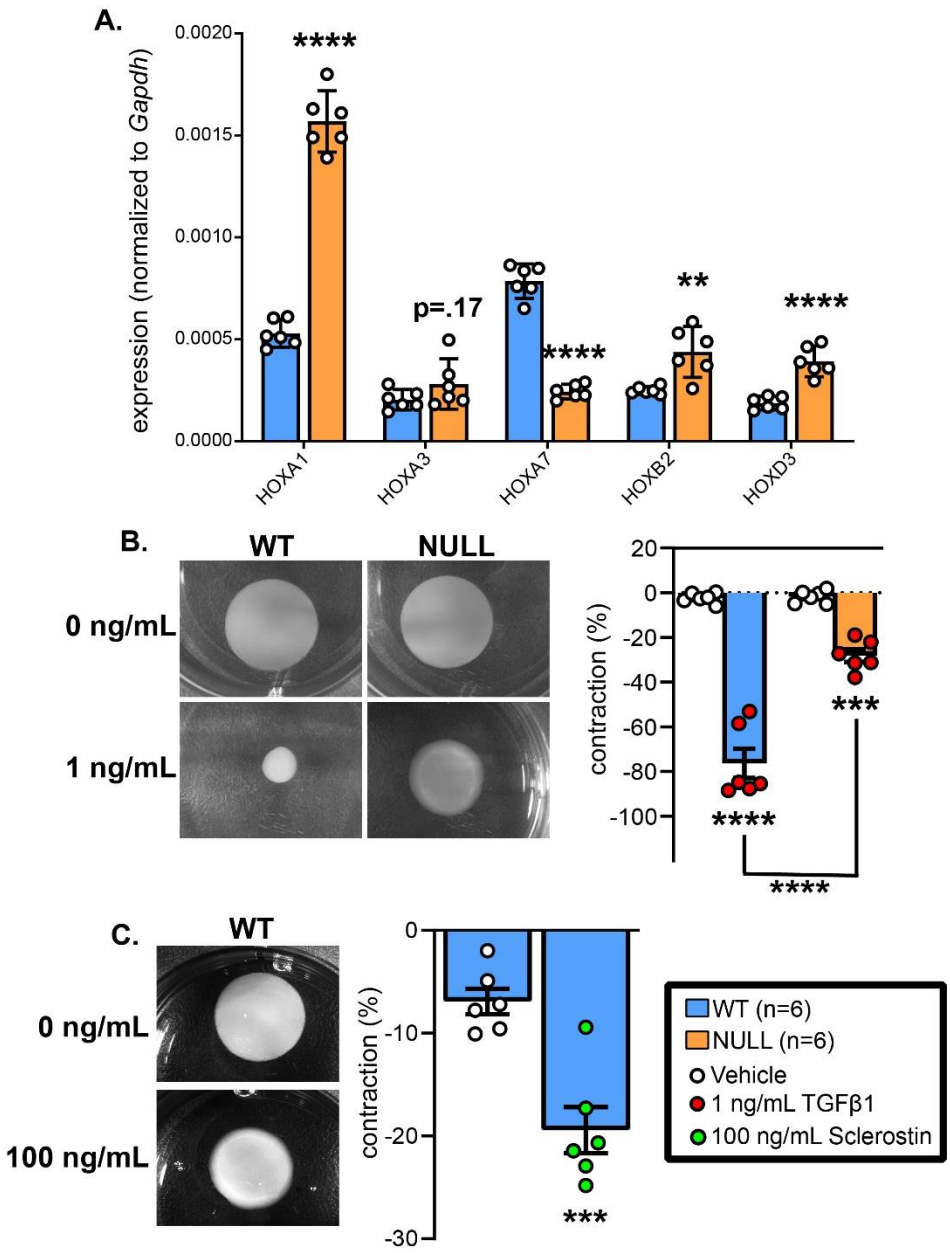

Figure 4.5. *Sost* null AVIC have altered *Hox* genes and decreased contractility. A. qPCR was used to assess *Hox* gene expression in isolated WT and NULL AVICs. *Hoxa1, Hoxb2,* and *Hoxd3* were significantly higher in NULL mice with *Hoxa3* non-significantly increase (p=0.17). *Hoxa7* was decreased in NULL cells. **B.** WT and NULL AVICs were embedded in collagen gels and treated with 0 or 1 ng/mL TGFβ1. Both groups were unaltered at baseline but WT AVICs exhibited much greater contractility under treatment when compared to NULL. **C.** WT AVICs were embedded in collagen gels and treated with 0 or 100 ng/mL Sclerostin. Treatment induced a slight increase in contractility. **A.** Mean+/-SEM, Students t-test. **B.** Mean+/-SEM, 2-way Analysis of Variance with Šídák's multiple comparisons test. White dots=0 ng/mL TGFβ1, Red dots= 1 ng/mL TGFβ1. **C.** Mean+/-SEM, Students t-test. White dots=0 ng/mL Sclerostin, Green dots=100 ng/mL Sclerostin. *p<0.05, **p<0.01, ***p<0.001, ****p<0.0001.

Discussion

AVS and osteoporosis are two common diseases increasingly afflicting ageing populations in the United States and around the world. AVS is the second most common CV disease and studies show that over half of individuals over the age of 65 have some form of mild valve disease with estimates of 6.4% of these individuals displaying moderate to severe disease. Between 1999 and 2009, nearly 150,000 individuals died due to valve disease in the United States alone [36,37]. Currently, the only treatments for AVS are surgical intervention or TAVR and importantly there are no approved efficacious pharmaceutical options [37,167].

Osteoporosis is present in approximately 10% of individuals over the age of 50 in the United States and osteoporosis-related fractures have shown to lead to excess mortality [168,169]. Pharmaceutical treatment options for osteoporosis are better developed than for AVS, with the American College of Physicians historically recommending treatment of osteoporosis with a bisphosphonate-derivative or RANKL inhibitor [170]. Romosozumab, a mAb targeting sclerostin, provided a strong new option in the field of osteoporosis treatment due to indications it can both reduce bone resorption and enhance new bone development. This is a substantial improvement over existing therapies which only target the bone resorption mechanism, preventing the loss of existing bone content [171]. Indeed, the stage III ARCH trial showed romosozumab-bisphosphonate combination therapy can improve BMD and reduce fracture risk compared to bisphosphonate treatment alone. However there was an unexpected imbalance in adverse CV events in patients treated with romosozumab [7]. Romosozumab, however, was approved for the market in 2017 and now carries a CV warning label which must be considered during diagnosis.

Sclerostin inhibition has shown to be a powerful new therapeutic option for the treatment of low bone mass disease and has the potential to improve quality of life for many individuals. Outside of the skeletal system, sclerostin has been known to be expressed by aortic smooth muscle cells and explanted, post-natal vascular smooth muscle cells in calcifying conditions [90,172]. A direct investigation into the role of sclerostin in vascular disease recently showed that mice treated with exogenous recombinant sclerostin protein, or overexpressing the *Sost* gene, are protected from aortic aneurysm and atherosclerosis in an angiotensin II infusion mouse model through local inhibition of the Wnt signaling pathway [92]. This supports the hypothesis that sclerostin may perform a protective role in vascular tissue by performing local Wnt signaling inhibition. But while atherosclerosis shares similar risk factors and disease progression as AVS in early stages, the aorta and AV tissues are distinct in their development, resident cell populations, and mechanical environments, which make separate investigation crucial [173]. This divergence is evident in numerous clinical trials of the statin drug class, which have showed to be an effective treatment for lipid lowering and atherosclerosis but have little to no effect on the progression of AVS [174].

In the current study, we investigated the role of sclerostin in AVS by assessing the effects of *Sost* genetic ablation on the progression of AVS in an aged Western Diet mouse model. To this end, mice lacking *Sost* (replaced with a *LacZ*-neo cassette) were generated and compared to their WT littermates. Mice on a C57BL6/J background have been shown to develop hallmarks of AVS (in as few as four months) when receiving a high-cholesterol Western diet [175]. Herein, mice were aged for eight months on high-cholesterol diet to ensure adequate development of AVS for subsequent analysis (**Fig 4.1**). We have had success with this disease model in previous

studies, and based on the results from the current study, we have shown that eliminating sclerostin signaling is sufficient to slow the progression of AVS [72,165].

In vivo analysis of CV health using echocardiography indicated the development of hemodynamic hallmarks of AVS in WT mice independent of functional changes in the LV (**Fig 4.2**). Increases in PV and MG across the AV are expected as the mice begin to develop AVS. *Sost* ablation caused no significant hemodynamic change from baseline over time indicating attenuated development of AVS in these mice. There was a slight upward trend by twelve months that was not statistically significant. Therefore, it is possible the NULL mice may have been in the earliest stages of AVS development that did not yet manifest at the 12-month time point in the mouse as this age represents ~50 years of human age; valve disease in humans does not typically manifest until advanced old age (70-80 years and over) [176].

Both WT and NULL groups showed consistent increases in LV mass (**Fig 4.2**). This is likely a consequence of the excess cardiac output required as a result of the weight gain experienced by these mice. While weight was not tracked over time, the average weight of approximately 50 grams at 12 months of age is far greater than average age-matched mouse fed standard chow (The Jackson Laboratory). It is possible this increase in LV mass may have contributed to the increase in PV and pressure across the AV in the WT group, however the *Sost* knockout mice did not have altered AV hemodynamics despite having experienced similar levels of cardiac hypertrophy. Taken together, this may indicate a sclerostin-dependent effect that is specific to the AV as opposed to changes in other areas of the heart.

Measurement of leaflet thickness confirmed that WT mice experienced leaflet thickening compared to NULL mice (**Fig 4.3**). Analysis of brightfield PSR staining did not indicate differences in collagen density within the leaflets or differences in collagen conformation based

on polarized light imaging. ARS staining indicated minor sections of focal calcification as well as some instances of annular calcification however there did not appear to be a clear trend across genotypes nor evidence of excess fibrocalcific deposits in any mouse measured. This is not unexpected based on the moderate hemodynamic changes observed indicating the mice may be experiencing early stages of fibrotic AV disease in the absence of substantial calcific lesions.

IF for myofibroblast markers was performed (aSMA) as well as the common osteoblast marker Runx2 (**Fig 4.3**). aSMA was shown to be less prevalent in NULL mice than WT, which indicates that *Sost* ablation limits early development of AVS by interfering with early stage events of AVIC fibroblast to myofibroblast activation. Nuclear Runx2 staining was not different between the two groups, although there was a trend toward reduced activation in the NULL group.

To determine potential molecular mechanisms that would give rise to this differential phenotype in *Sost* ablation in AVS, RNA sequencing was performed on aortic roots from both groups (**Fig 4.4**). Over 1000 genes were differentially expressed, the majority of those being increased in NULL compared to WT. This is likely due to the removal of a Wnt inhibitor which allows for uninhibited Wnt signaling and associated mechanisms to become upregulated. A number of expected bioprocesses were differentially regulated such as biomineralization and ECM organization. Over representation found genes that interacted with a large number of bioprocesses. Some of the most highly involved genes belonged to the *Hox* family of transcription factors. This family of transcription factors contains four subcategories in vertebrates (A, B, C, D) and are involved in body axis patterning [177]. While the family has long known to be involved in development, more recent work has focused on their re-activation in post-natal tissue during CV disease [178]. Of particular interest are the *Hoxa1* and *Hoxa3*

subtypes. *Hoxa1* function loss in humans leads to CV malformations in humans and knockout mice have been shown to have a myriad of cardiac abnormalities, including outflow tract defects due to necessity of expression precursor cardiac neural crest cells [179,180]. *Hoxa3* knockout has been shown to cause stenosis of the AVs as well as several other CV abnormalities [181]. These protective effects of *Hox* genes and concurrent upregulation in NULL animals may lead to the protective affects in AVS found in this study.

qPCR analysis indicated that NULL AVICs had upregulated *Hoxa1* mRNA which lends further evidence toward these factors being involved in the protection NULL mice from AVS (**Fig 4.5**). In addition to *Hoxa1*, *Hoxb2* and *Hoxd3* were also increased, although these factors have less of a literature basis for having a protective effect in the valve. Interestingly, *Hoxa7* was significantly decreased in NULL mice, although there is little evidence that may point to its role in the AV. WT and NULL cell lines were also assessed for the contractility in order to determine if the myofibroblast phenotype transition may partially explain the *in vivo* phenotype. Results indicate that WT cells are far more prone to hypercontractility compared to NULL, which further supports that NULL mice are protected from early development of AVS by a lower propensity toward myofibroblast activation and contraction.

Limitations

Like many small animal studies investigating mechanisms of AV disease, there are a number of caveats which must be considered when interpreting results. Mice were only aged to one-year, which roughly correlates to middle-age in humans, whereas the most striking effects of AV disease generally occur in older individuals at 70 to 80 years of age. Ideally, mice could be aged to 18 months or even two-years of age but this is often not feasible because mouse health

rapidly deteriorates past one year of age when animals are placed on a high-cholesterol Western diet that can lead to premature deaths at unexpected time points. In addition, we wanted to test romosozumab in our model system, but Amgen declined our request to collaborate.

Conclusions

This study presents a novel role for sclerostin in the CV system - specifically in the AV. While sclerostin is an excellent target to diminish the effects of low bone mass diseases such as osteoporosis, the existence of off-target CV effects should better be understood as sclerostin inhibition becomes a more commonly adopted therapy. This study indicates that genetic ablation of the *Sost* gene in mice slows the development of AVS in a high-cholesterol diet model. This is divergent from the effect in aortic diseases such as aortic aneurysm and atherosclerosis. Our findings further indicate that sclerostin has an effect on early markers of AV disease involved in myofibroblast activation of resident cells through *Hox* signaling. Future studies should focus on better understanding the mechanisms through which sclerostin acts in diseases of the AV as well as if this genetic effect can be recapitulated in a pharmacological inhibition study. Additionally, the potentially negative role of lacking sclerostin on slowing late stage osteogenic AVS should be evaluated. More importantly, in contrast to the CV events observed in clinical trials, this study indicates a potentially protective role for sclerostin inhibition, at least in the development of AVS and can further inform clinical decision making as the drug becomes more commonly adopted as a treatment for osteoporosis.

CHAPTER 5

Evaluation of Early Bilateral Ovariectomy in Mice as a Model of Aortic Valve Stenosis or Left Ventricle Hypertrophy

Introduction

Heart disease is the most common cause of death in the United States and AVS is the third most common heart disease and results in approximately 16,000 deaths per year [36,37,182]. This prevalent and deadly disease is becoming more common in aging populations with incidence estimated to triple over the next 40 years [183]. AVS is characterized by the slow narrowing of the aortic outflow tract via progressive fibrocalcification and stiffening of the AV leaflets [37].

Severe AVS without treatment carries an extremely poor prognosis with only 22% survival after 2 years [59]. Historically, the only treatments for severe AVS have been open surgical interventions which carry high risk of complications and mortality, particularly in the very elderly populations which most commonly needs the procedure. Recently, non-invasive interventions such as the TAVR have made the procedure less risky [184]. Trials evaluating drugs that treat related pathologies including anti-calcific treatments and lipid-lowering have largely been negative and development of efficacious drug treatments are sorely needed [185].

AVS afflicts both male and female patients. Historically, female-specific CV disease has been drastically understudied in the literature. Literature meta-analysis suggests only 10% of pre-clinical CV research articles focus exclusively on female animals [8]. There appears to be a fundamental disconnect in the understanding of how AVS presents in female patients and should be treated. Outcome analysis show that female patients tend to have worse outcomes, lower referral, and more common complications following surgical and interventional valve replacement [186]. Female patients appear to present AVS differently which leads to misclassification and suboptimal treatment [187,188]. Indeed, the pathophysiology of AVS appears to differ at the tissue level between male and female patients. Female patients tend to

develop severe AVS at relatively low calcium burdens compared to men and excised tissue samples of diseased valve leaflets indicate a higher prevalence of fibrosis when compared to male valves, which contained higher amounts of calcific deposits [189,190]. Female patients may be slipping through the cracks as diagnosis methods are not optimized.

Methods of studying AVS at the pre-clinical level are limited. C57BL6/J mice develop mild aortic sclerosis but little evidence of hemodynamically significant AVS [175]. Many models also require Western style diets to induce rapid weight gain combined with aging which can be a barrier to performing studies in this area [191]. The *Notch1* heterozygous mice has shown to reliably develop AVS within a reasonable time frame by mimicking the fully penetrant mutation leading to AVS in humans [72,192]. In addition, diseases used to study atherosclerosis such as $Ldlr^{-/-}/ApoB^{100/100}$ mice are also effective [191]. However, there is a need to develop non-genetic models of AVS that are more generalizable to the population at large.

The OVX procedure is commonly used to study the effects of PMO. This model results in rapid loss of bone mineral via estrogen depletion [193]. Women experiencing PMO are at greater risk for CV disease that is proportional to the severity of their disease [194]. Young women receiving bilateral oophorectomy tended to have an increase in CV mortality [195].

The purpose of this study is twofold: determine if the OVX procedure faithfully recreates the CV effects that seem to accompany PMO as well as determine if the OVX can be used as a female-specific model of AVS absent of genetic manipulation. We found that OVX combined with high-cholesterol diet and aging to one year did not induce a strong AVS phenotype but did result in LV hypertrophy absent significant fibrosis. OVX may be useful as a model for LV hypertrophy but genetic insults such as *Notch1* or *Ldlr* ablation may be necessary to excel the phenotype and induce measurable differences in the AVS phenotype.

Materials and Methods

Animals

Mouse experiments were carried out under appropriate supervision and approval by the Vanderbilt University IACUC. 20 female WT mice of the C57BL6/J background were obtained from The Jackson Laboratory. At four months of age, mice were randomly selected for the SHAM or OVX groups (n=10 for each group). Study authors blindly performed the procedure. Briefly, mice were anesthetized using isofluorane induction. The lower back slightly above the hips was shaved and disinfected. A small incision was made and the mouse uterus, fallopian tubes, and ovaries were removed. The ovaries were quickly excised using a cautery pen. Mice in the SHAM group underwent the same procedure, however the ovaries were left intact at the final stage. This procedure was repeated for both ovaries. The uterus was returned to the body cavity and the skin was closed using surgical stables and local anesthetic was applied and mice allowed to recover on a heated pad. One mouse in the SHAM group died of unknown surgical complications resulting in a final sample size of 9 in this group. After one week of recovery, mice were transitioned to a 1% cholesterol Western diet (TestDiet 5TJT). Food and water were provided *ad libitum* at all stages of the study. Mice were aged to 12 months of age, euthanized by carbon dioxide inhalation and cervical dislocation. Tissue was harvested for *ex* vivo analysis at the study endpoint (**Fig 5.1A**).

Echocardiography

Echocardiographic imaging was performed at 4 and 12 months of age to track the hemodynamic development of AVS over time. All measurements were performed by skilled technicians in the VCPC using the Visual Sonics Vevo 2100 small animal imaging system.

Mice were lightly anesthetized using isofluorane and laid supine on a heated platform. Transthoracic AV pulsed wave Doppler imaging was used to record blood velocity profiles. Parasternal short-axis M-mode imaging was used to visualize LV structure and function over the course of the heart cycle.

AV metrics were determined using a custom MATLAB script which automatically traced the Doppler waveforms to determine metrics such as PV and MG across the leaflets [162]. Three independent measurements were made for each mouse at each time point to account for operator variability. In total, between 50 and 100 heart cycles were considered to generate representative values for each sample at each time point. M-mode measurements were performed by hand by the study authors. Three cycles were measured across three repeated images per mouse per time point. 9 cycles were considered for each sample to generate representative metrics including LV mass and EF.

Dual X-Ray Absorptiometry

Bone metrics were assessed by the study authors using a Hologic UltraFocus Dual Energy X-Ray Absorptiometry once per month from 4 to 12 months of age. Mice were anesthetized using isofluorane induction and placed facing down on the capture stage. Images were acquired at 2X magnification in a series of 4 captures at 40 kV then followed by 4 additional captures at 80 kV. Manufacturer software (Version 3.1) was used to determine whole body fat mass content and BMD over time.

Histological Staining

Whole hearts were excised from mice at 12 months and embedded in OCT compound and flash frozen. 12 µm serial sections were cut using a -20º C cryostat and affixed to histology slides. For all staining analysis, three sections across different regions of the heart were analyzed and averaged (in the case of quantitative analysis) to generate representative metrics.

Masson's Trichrome (MTC) stain was used to assess LV and AV morphology as well as collagen density in both regions. Staining was performed by expert histological technicians in the Vanderbilt University Medical Center Translational Pathology Shared Resource. ARS (Sigma-Aldrich) staining was used to study the prevalence of calcification on the valve leaflets. Sections were washed in Phosphate Buffered Saline without calcium or magnesium to remove OCT. Sections were then rinsed in deionized water for 2 minutes at room temperature and then covered in 14 mM ARS solution for 5 minutes at room temperature. The slides were then shaken dry, rinsed with deionized water, cleared, and dehydrated in sequential baths of acetone, 1:1 acetone/xylene mixture, then xylene. Slides were then coverslipped in organic mounting media and dried overnight.

Brightfield images were captured for both stains at 1X (LV) and 4X (AV) using the Nikon Eclipse E800 microscope and an Olympus DP74 digital polychromatic camera. Representative images were chosen to match the trends determined from quantitative analysis.

Immunohistochemical Staining

Immunostaining was performed on AV leaflets in order to determine relative amounts of aSMA and Runx2 which are common markers of dystrophic and osteogenic calcification, respectively. Slides were washed of OCT using PBS. Tissue was then fixed and permeabilized

using a 4% paraformaldehyde/0.1% Triton solution. Sections were then treated with 10% bovine serum albumin for 1 hour at room temperature in order to reduce non-specific antigen binding. Primary antibodies were added to 10% blocking solution at 1:100 dilutions at 4º C overnight: rabbit polyclonal anti-aSMA (Abcam ab5694) and rabbit monoclonal anti-Runx2 (Cell Signaling Technology 12556). Separate slides were used for each target. Sections were then washed in PBS and then incubated in 1:1000 dilution of goat anti-rabbit IgG Alexa Fluor 647 (ThermoFisher A-21245) for 1 hour at room temperature away from light. Slides were then washed in PBS, mounted in ProLong Gold Antifade with DAPI (Cell Signaling Technology 8961), coverslipped, dried overnight at room temperature, and edges sealed. Fluorescent images were taken 20X magnification with an Olympus BX53 microscope equipped with a Qimaging Retiga 3000 digital monochromatic camera. Multiple locations were imaged and combined to build a representative sample of each AV leaflet.

Quantitative Image Analysis

Custom MATLAB scripts were utilized to measure tissue area and collagen composition as previously described [163,165,196]. Images were all captured using identical exposure and background levels in order to accurately compare across samples. Whole heart images obtained at 1X magnification were cropped to only include LV tissue. AV leaflets were similarly removed from 4X images. Colorimetric segmentation was used to determine regions of collagen, stained blue (H=150º-250º, S=0.1-1.0, L=0.1-0.93), and cytoplasm and myocardium, stained red (H=250°-25°, S = 0.1–1.0, L = 0.1–0.93). Whole tissue fraction as well as collagen and cytoplasm/myocardium are fractions were calculated as the ratio of positive pixels to non-background pixels in the specified region of interest.

Quantification of immunohistochemical staining was performed as previously described [165]. Fluorescently labeled stains were co-stained with DAPI to determine location of cells in AV leaflets. Nuclei were segmented using a modified watershed transform and concave object separation algorithm [163,166]. aSMA area fractions were calculated as the ratio of positive pixels to total pixels in the leaflet boundary. Runx2 area fraction was defined as the ratio of positive pixels within the nuclear boundary.

Statistical Analysis

All data are displayed as mean +/- error with raw data overlaid as defined in the figure captions. Percent change between time points was analyzed using the single-sample Students t-test to see if values significantly changed from zero. Direct comparisons between SHAM and OVX data utilized the Students unpaired t-test. Each data set was analyzed for statistical outliers using the ROUT method. Outliers were excluded from statistical calculations but were left on figures and noted in the figure captions. A p-value lower than 0.05 was considered statistically significant for all tests.

Results

Ovariectomy results in diminished bone mineral density and increased fat mass

The OVX is a common procedure used to simulate PMO in a small-animal model. DXA scans were used to assess body composition over time to confirm the expected phenotype. Both groups rapidly gained fat mass over with the OVX initially accruing more rapidly before both groups reaching a steady state around 20-25 grams (**Fig 5.1B, top)**. As expected, mice that underwent the OVX procedure had reduced BMD. BMD was significantly lowered at 6-9 months of age but a leveling of the OVX group and a gradual decrease in the SHAM group resulted in groups no longer being significantly different from 10-12 months of age (**Fig 5.1B, bottom)**.

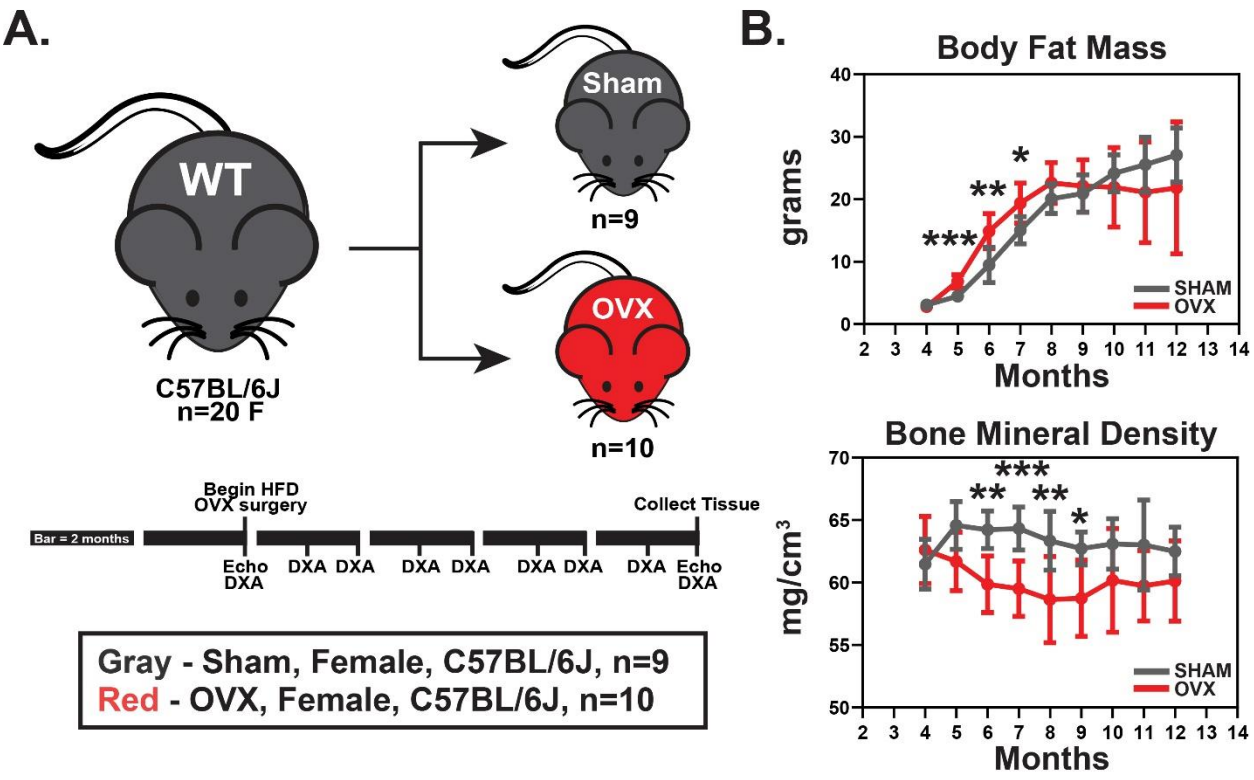

Figure 5.1. The ovariectomy surgical model of post-menopausal osteoporosis, combined with aging and high-cholesterol diet, was evaluated as a potential model for pre-clinical study of aortic valve stenosis. A. At four months of age, 20 female C57BL/6J mice received sham or ovariectomy procedure. They were then aged to 12 months receiving monthly DXA scanning and echocardiography at 4 and 12 months of age. **B.** DXA scans were used to measure body composition. High-cholesterol diet induced rapid fat mass gain in both groups (top) and OVX mice had reduced bone mineral density compared to SHAM mice (bottom) indicating success develop of estrogen-depletion induced osteoporosis. Mean+/-SD, Unpaired Students t-test, *p<0.05, **p<0.01, ***p<0.001, ****p<0.0001

Ovariectomy results in increased left ventricular mass but an inconclusive aortic valve phenotype

Hemodynamics off the AV as well as the structure and function of the LV was tracked over time using echocardiography. OVX mice had a slight increase in PV whereas SHAM remained unchanged (95% CI [-7.209,19.53] vs [3.14, 73.6]; p=0.31 vs p=0.036] (**Fig 5.2, top left**). OVX mice had a significant increase in LV mass while SHAM again remained unchanged (95% CI [-0.86, 43.31] vs [31.29, 75.28]; p=0.058 vs p=0.0004) (**Fig 5.2, top right**). MG across the AV (**Fig 5.2, bottom left**) and the LV emptying ability as measured by the EF (**Fig 5.2, bottom right**) were unchanged in both SHAM and OVX groups (Mean Gradient: 95% CI [-37.1, 51.15] vs [-8.59, 119.8]; p=0.72 vs p=0.082) (Ejection Fraction: 95% CI [-5.93, 40.3] vs [-1.92, 22.96]; p=0.12 vs p=0.09).

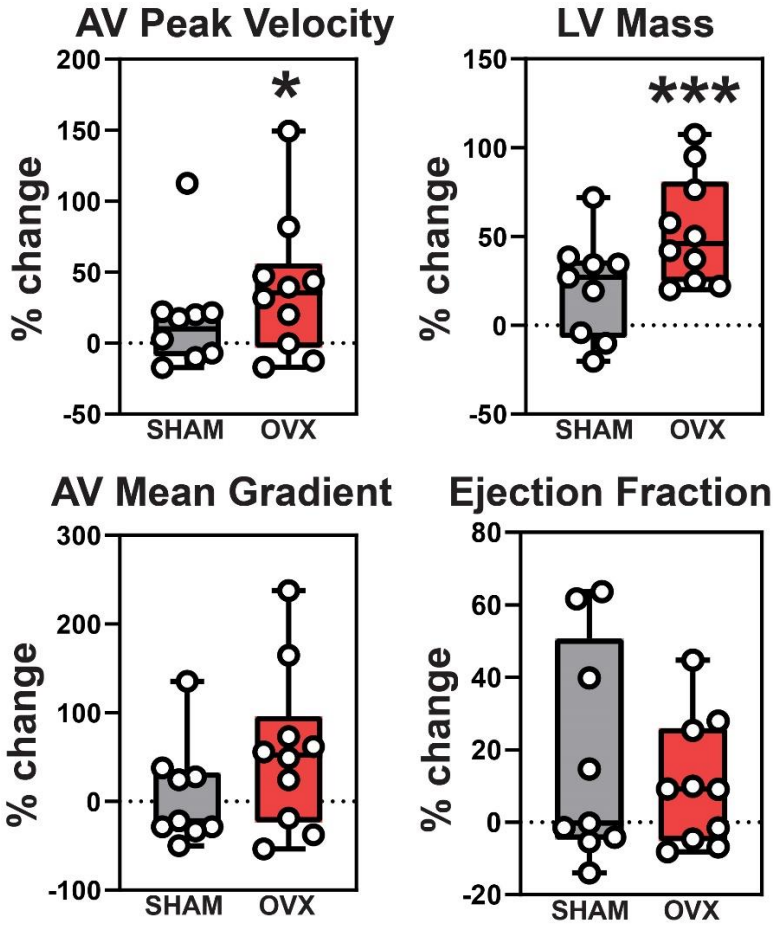

Figure 5.2. Ovariectomy results in increased left ventricular mass and an inconclusive aortic valve stenosis phenotype. M-mode and pulsed wave doppler echocardiography was used to compare aortic valve and left ventricle metrics between 4 and 12 months of age. Peak velocity was significantly increased in the OVX group with no change in the SHAM, although there was one statistical outlier in the SHAM group which was removed from analysis (top left). There was no change in either groups in mean pressure gradient across the aortic valve (bottom left). Left ventricular mass was significantly increased in OVX while unchanged in SHAM (top right) however there was no functional change noted in either group as measured by ejection fraction of the left ventricle (bottom right). Data show mean of percent change with interquartile range denoted. The ROUT method was used to determine statistical outliers which were removed from analysis. The single-sample Students t-test was used to determine if percent change data deviated significantly from 0 (no change). *p<0.05, **p<0.01, ***p<0.001, ****p<0.0001.

Histological analysis shows no change in collagen or aortic valve morphology but increased left ventricular area

LV and AV morphology and collagen composition were measured using MTC stain while AV leaflet calcification was assessed using ARS staining (**Fig 5.3A**). AV thickening (**Fig 5.3B, top left)** was not detected in SHAM nor OVX groups (95% CI [39.06, 53.13] vs [36.97, 52.91]; p=0.81) as well as no significant change in collagen leaflet density (95% CI [16.6, 39.51] vs [27.83, 46.74]; p=0.17) (**Fig 5.3B, top right**). The average area of the LV was increased in OVX mice as expected based on results from echocardiographic measurements (95% CI [17.54, 25.15] vs [23.15, 29.63]; p=0.033) (**Fig 5.3B, bottom left**). There was no evidence of significant fibrosis in the LVs at 12 months in the SHAM or OVX mice (95% CI [0.96, 2.11] vs [1.45, 2.62]; p=0.19) (**Fig 5.3B, bottom right**). ARS calcium staining was absent and the data is not shown.

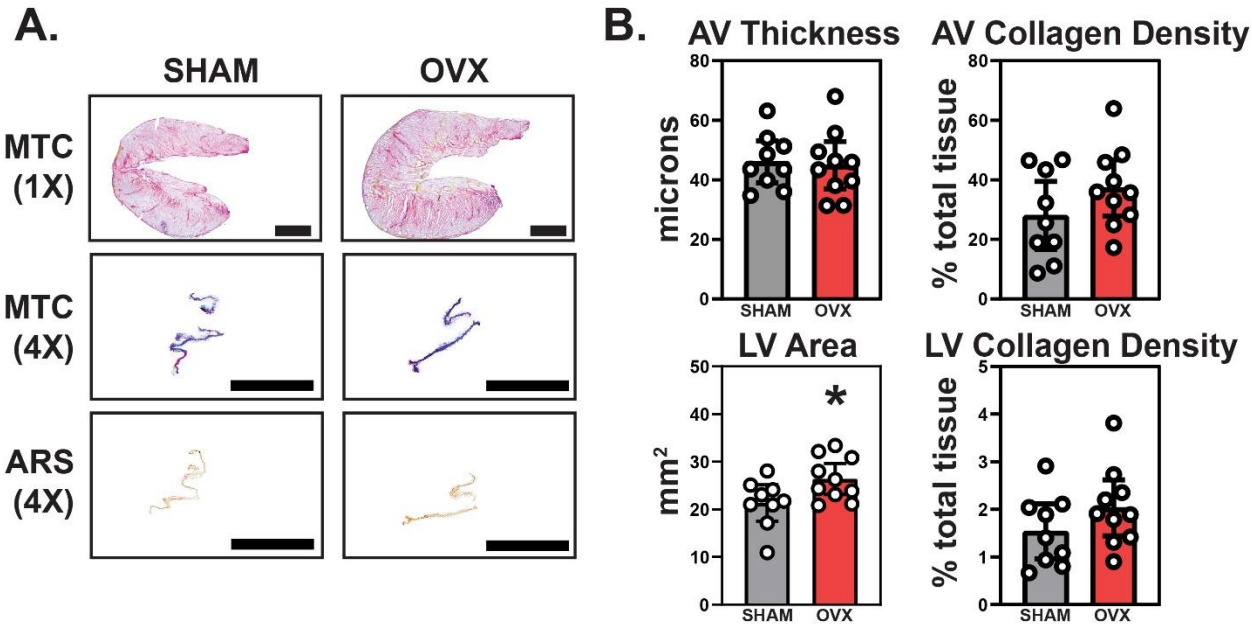

Figure 5.3. Left ventricle hypertrophy was noted in OVX hearts via *ex vivo* analysis, but valves were absent of any significant thickening, collagen alteration, or calcification. A. Masson's Trichrome staining was used to study gross and collagen-specific morphology in the left ventricle (top row) and aortic valve (middle row). Alizarin Red S staining was used to identify potential regions of calcification on the aortic valve leaflets (bottom row). **B.** Measurement of aortic valve fibrosa-ventricularis thickness (top left) and collagen density (top right) showed no difference between groups further proving a significant aortic valve disease phenotype secondary to ovariectomy unlikely. However, the left ventricle area (bottom left) was significantly greater in OVX mice bolstering the left ventricle hypertrophic phenotype noted in echocardiography. There was no significant difference in left ventricular fibrosis (bottom right). **A.** Scale bar magnitudes: 1X=10 mm, 4X=1mm. **B.** Mean+/-95% CI, Unpaired Students t-test, *p<0.05, **p<0.01, ***p<0.001, ****p<0.0001.

Neither dystrophic nor osteogenic markers are elevated in OVX aortic valves

The progression of dystrophic (aSMA) or osteogenic (Runx2) calcification of the AV leaflets was assessed by IF targeting of common protein markers of the disease phenomena (**Fig 5.4A**). aSMA prevalence was unchanged between the two groups (95% CI [40.65, 74.69] vs [53.37, 75.23]; p=0.45) (**Fig 5.4B, left)** along with nuclear expression of Runx2 (95% CI [0, 6.1] vs [0, 2.96]; p=0.44) (**Fig 5.4B, right**).

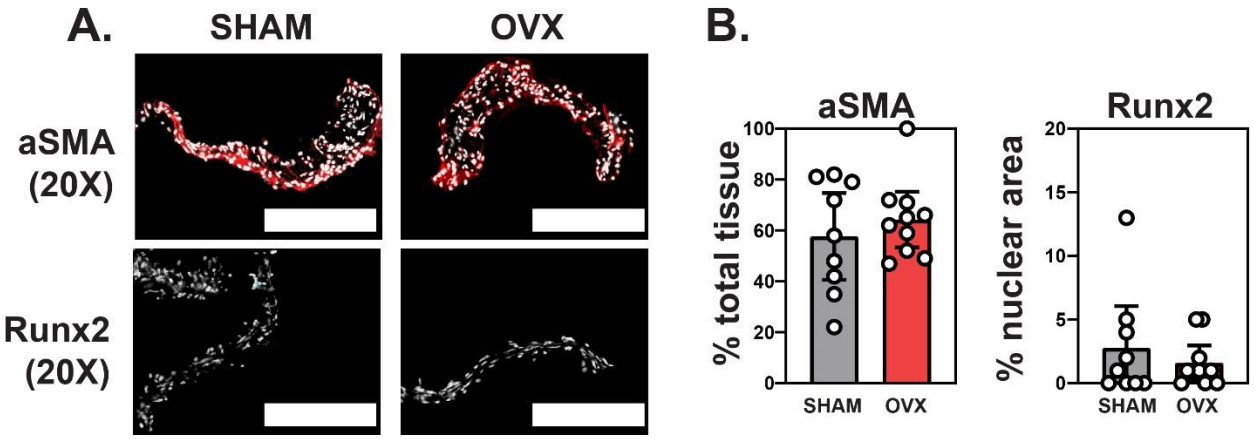

Figure 5.4. Ovariectomy did not induce expression of markers of dystrophic or osteogenic calcification. A. Immunofluorescent staining was used to determine changes in dystrophic/myofibroblast (aSMA, top row) or osteogenic (Runx2, bottom row) between OVX and SHAM groups. **B.** Quantification of stains indicated no change in overall presence of aSMA (left) or nuclear expression of Runx2 (right). **A.** Scale bar magnitudes: 20X=100 microns. **B.** Mean+/-95% CI, Unpaired Students t-test, *p<0.05, **p<0.01, ***p<0.001, ****p<0.0001

Discussion

AVS is an increasingly prevalent CV disease mostly afflicting the very elderly. Females commonly develop AVS but the bulk of pre-clinical research is skewed towards males [8,36]. Additionally, the mechanisms of diagnosing valve disease are not optimized to detect it in female patients. Therefore, there is a great need to develop improved methods of studying the disease in female patients in a pre-clinical setting in order develop a better understanding of the disease as well as potentially engineer new procedures, diagnostic methods, and pharmaceuticals [186–188]. The OVX is a simple and commonly used procedure used to induce the effects of post-menopause, specifically diminished BMD leading to PMO. The effects of the OVX on development of CV disease are not well understood. Female patients in menopause with greater bone loss tend to have worse CV outcomes. Estrogen is known to have a protective effect in many CV diseases including those of the AV, so it stands to reason that mice undergoing the OVX procedure may have development of CV and AV disease faster than SHAM controls [197].

In response to these treatment and knowledge gaps, we aimed to characterize the utility of the OVX procedure combined with high-cholesterol diet and one-year of aging on development of AVS in a mouse model. This could potentially lead to an easily repeatable pre-clinical model of AVS in an understudied patient population. To our knowledge, this is the first study to undertake this specific analysis.

In vivo imaging (echo and DXA) was used to monitor mouse body composition and AV/LV hemodynamics over time. Both groups of mice underwent substantial weight gain in response to the high-cholesterol diet as well as diminished BMD for the majority of the study, indicating a successful recapitulation of the PMO phenotype (**Fig 5.1**). Mice in the OVX group developed a slight increase in PV from baseline but not in MG. There was a marked increase in

LV mass in the OVX group which may indicate early LV hypertrophy, however there was no change in EF which may point to no difference in LV performance at this early disease stage (**Fig 5.2**). A similar analysis was performed in aortic regurgitation in rats however there was no change between OVX and SHAM animals [198]. This may indicate the need for Western diet and aging to produce the phenotype. Myocardial hypertrophy commonly occurs in post-menopausal women at greater rates than male counterparts [199]. The most common methods of inducing myocardial hypertrophy in mice include surgical intervention (transverse aortic constriction, aortic banding) or genetic modifications (collagens, matrix metalloproteinases) [200]. Using OVX and aging may present a more generalized model as well as specifically focus on an understudied patient group at risk for the disease.

In order to better understand the observed *in vivo* phenotype, quantitative histology was performed to characterize AV and LV disease progression (**Fig 5.3**). There was no noted increase in AV thickness or collagen morphology as determined by MTC staining and no evidence of calcium deposition based on ARS staining. Similarly, there was no evidence of widespread LV fibrosis. However, the LV of OVX mice were significantly enlarged which bolstered the increase in LV mass noted from echocardiography. This appears to confirm the lack of significant AVS or fibrocalcific disease development on the AVs of the OVX mice. The C57BL6/J mouse is notoriously resistant to development of hemodynamic alterations although some studies note gross histological disease hallmarks [175,191]. LV hypertrophy is often thought to be a compensatory mechanism to normalize cardiac output as the leaflet orifice becomes smaller and less compliant. Fibrosis typically accompanies hypertrophic tissue during progression to HF. It is possible AVS is occurring via stiffening of the valve leaflet ECM in a way that is not measurable using collagen or calcium stains. It is also possible that other pressure overload is occurring due

to distal causes such as hypertension which is shown to commonly correlate with osteoporosis [201].

To investigate any potential AV phenotype, markers of dystrophic (aSMA) and osteogenic (Runx2) pathways of AV fibrocalcification were assessed (**Fig 5.4**). While aSMA expression was present, there was not any statistical change between SHAM and OVX mice. aSMA is a marker of myofibroblast activation which can lead to fibrosis and dystrophic calcification, the most common type of ectopic calcification found in excised valves [202,203]. Runx2 expression was minimal and there was no trend between groups. Runx2 is a marker of osteogenic transdifferentiation of resident AVICs [204]. These data further suggest that the OVX procedure alone is not adequate to induce AVS absent some other genetic insult.

Limitations

12 months of aging is relatively low and aging to 18 or 24 months may have more accurately mimicked the advanced age patients generally develop AVS. However, we have found that aging past 14 months generally leading to unexpected death and loss of samples when combined with high-cholesterol diet.

Conclusions

AVS is an increasingly prevalent disease and is very understudied in relevant female patient populations. Females commonly develop fibrosis related AVS and standard methods of disease detection are inadequate for female presentation of disease. There are very few small animal models of valve disease that do not rely on genetic manipulation and none that focus on female disease. OVX is a common model used to simulate PMO. Women in menopause with

osteoporosis tend to develop CV disease more often. The focus of this study was to determine the feasibility of using the OVX procedure as a pre-clinical model to study AVS in female patients. Our findings suggest that mice do not develop a strong AV phenotype after OVX, high-cholesterol diet- and 12 months of aging. However there does appear to be a significant increase in LV hypertrophy which may indicate potential utility as a model for LV disease in female mice.

CHAPTER 6

Improving Programming Content Delivery in an Introductory Biomechanics Course Using a Blended Classroom Approach

Adapted from:

Joll II JE, Merryman WD. Improving programming content delivery in an introductory biomechanics course using a blended classroom approach. *ASEE Annu. Conf. Expo. Conf. Proc*. July 2021: 37308 [205].

Introduction

BME2100: Biomechanics is a sophomore-level introductory biomechanics course at Vanderbilt University that focuses on the study of structural and material properties of biological tissues and medical devices. In an effort to integrate coding content into each undergraduate BME course, biomechanics-related MATLAB projects are assigned along with standard homework and exams. In course reviews, this content is often described as the most challenging with students often citing the inefficacy of the traditional, lecture-based content delivery in synthesizing biomechanics and programming content. One potential solution to this instructional challenge is converting the course into a blended format.

As the internet becomes more ubiquitous in modern society, it has also become a more common presence in higher education. One in three students take an online class in their undergraduate career, and most public universities are now offering partially or completely online programs [206]. Blended courses combine online and in-person instruction to leverage the strengths of the two modalities. Research indicates that blended instruction can improve student outcomes more than online or in-person instruction alone when properly deployed [207]. The COVID19 pandemic has accelerated this shift as more college classes are moved to online or blended formats. In 2020, nearly two-thirds of U.S. colleges had shifted to online or hybrid models [208]. With the general inertia of more online learning integration and the pandemic-related necessity, it is important to understand how shifting courses online can affect student learning.

There are very few comprehensive studies focusing specifically on the efficacy of blended-style classes in a biomedical engineering curriculum. Researchers utilizing a blended model in a Medical Terminology course found that students in the blended course performed

better on exams than those in the traditional class [209]. A comprehensive implementation of biomedical engineering e-learning laboratories was implemented at the same university in the biomedical engineering curriculum but there is no formal analysis comparing this blended style to other educational modalities [210]. Biomedical engineering educators have also described creative development of a blended automation course in response to COVID19 lockdowns [211]. While the methodology is interesting, formal comparison to in-person classes is absent and practically infeasible. While not specifically studying biomedical engineering courses, systematic comparison of general engineering courses using in-person and blended classes showed that students in the blended course experienced improved satisfaction with improved attendance, motivation, and collaboration [212].

The aim of this study was to determine if shifting a biomechanics course section to a blended format can improve student outcomes in programming material. Additionally, this study may also provide more generalized information on the efficacy of converting certain biomedical engineering courses to a blended format, particularly to better streamline content that may appear to be incongruent.

Materials and Methods

This study was carried out with the approval of the Vanderbilt University Institutional Review Board (IRB #192229).

Course Restructure

The first eight weeks of the course were restructured into a blended style by moving the programming content from the traditional course into modules on the course learning management software site (Brightspace). This content included: pseudocoding for planning a solution in non-coding language, how to perform operations on vector and matrix variables, common loops (primarily 'for' loops), and basic data visualization like plotting, specifying line type, and generating subplots. These programming modules could be completed in parallel with the biomechanics-focused lecture. The four programming topics (pseudocode, vector/matrix operations, loops, and data visualization) covered in the modules were the same as those covered in the lecture. The traditional (**top row**) and blended (**bottom row**) course structures are summarized in **Table 6.1**.

	WEEK:	1	2	3	4	5	6	7	8
Traditional (FA19)	*MATLAB (lecture)*						• Pseudocode • Vectors • Loops • Data visualization	• **PROJECT**	• *Confidence* • *Competence*
	Biomechanics	• Forces	• Moments	• Equilibrium	• Skeletal joints • **EXAM**	• Linear Kinetics	• Angular kinematics	• Angular kinetics	• Deformation
Blended (SP20)	*MATLAB (online)*	• *Confidence (pre)*	• Pseudocode	• Vectors		• Loops	• Data visualization	• **PROJECT**	• *Confidence (post)* • *Competence* • *Effectiveness*
	Biomechanics	• Forces	• Moments	• Equilibrium	• Skeletal joints • **EXAM**	• Linear Kinetics	• Angular kinematics	• Angular kinetics	• Deformation

Table 6.1. Traditional and blended course structure comparison.

Each module has three components: review materials, a practice problem, and a reflection prompt (**Figure 6.1A**). Each module was designed to be completed in approximately 20 minutes (mirroring the in-class time spent in the original lecture). The modules were graded based on completion and had high completion rates (**Table A.6.1)**. Anecdotally, students tended to complete the module components thoroughly with reasonable effort. The solutions to the practice problems were provided after the students completed the modules.

Along with the modules, an online video was used to describe the biomechanics programming project, which replaced the previous paper-based assignment description (**Figure 6.1B)**. A complete description of each component of the restructured course can be found in the appendix: full module contents can be found in **Figure A.6.1,** assignment text can be found in **Figure A.6.2,** and the full video-based assignment can be found in **Figure A.6.3**.

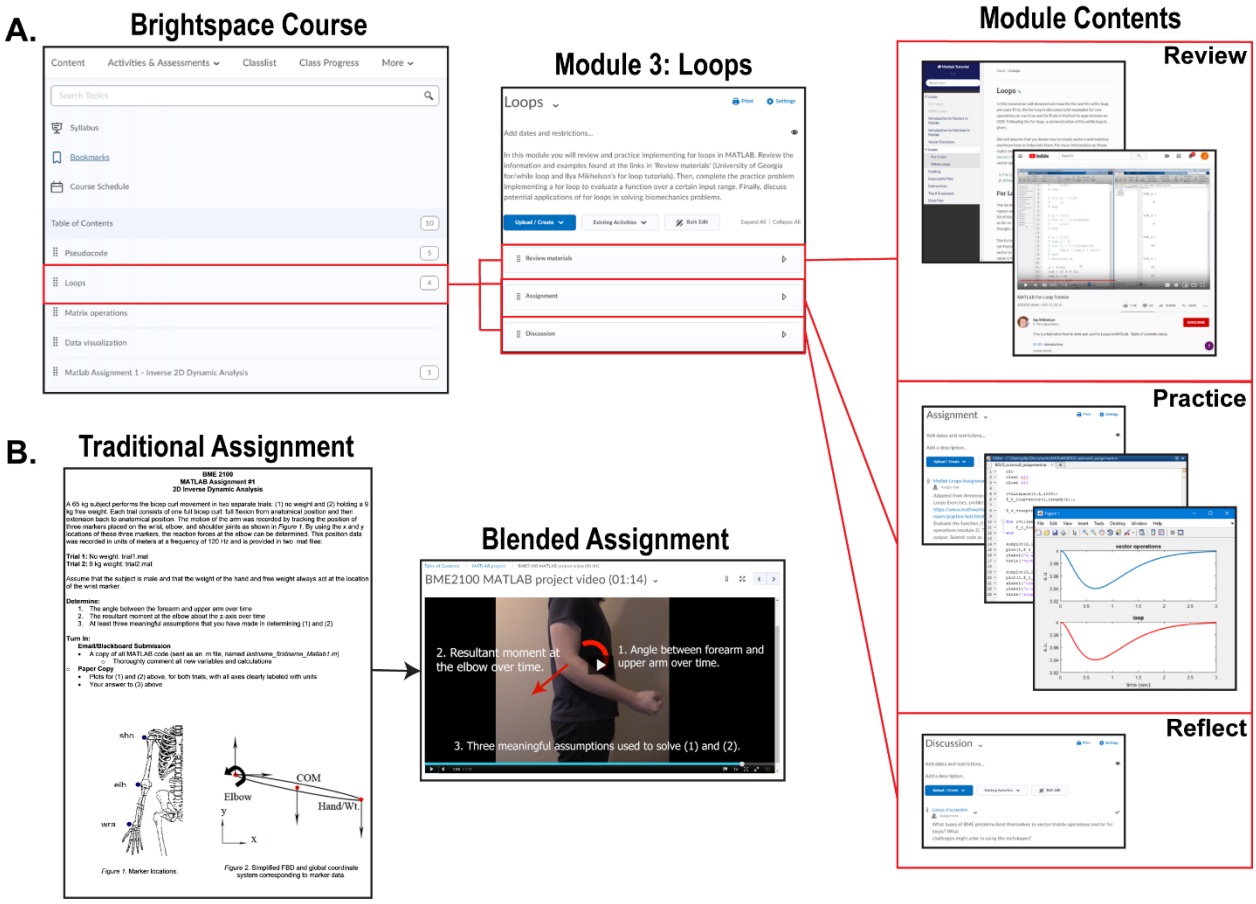

Figure 6.1. A sample of how the online modules were structured (A) and the new video-based project delivery (B). A. Blended course materials were implemented in Brightspace and comprised of review material, practice problems, and a reflection prompt. **B.** The paper-based assignment was converted to a multimedia assignment.

Assessment: Module Effectiveness

A custom survey created by the authors was circulated after completion of the project (Week 8) to assess how students perceived the efficacy of the restructured course. The full text of the survey is found in **Table A.6.2**. Briefly, students were asked to rate their level of agreement with a number of statements such as "MATLAB Project 1 was clearly explained". A 5-point Likert scale was used to record responses with '1' indicating "Strongly Disagree" and '5' indicating "Strongly Agree".

Assessment: MATLAB Coding Confidence

A second custom survey created by the authors was used to assess how students rated their confidence in MATLAB programming. To track student confidence pre- and post-project, the survey was given twice in the blended course (Week 1 and Week 8) and individual responses were tracked over time. The survey was also given to students in the traditional class only at the post-project (Week 8) time point. The survey structure was similar to the effectiveness survey described in the previous section and the full text is located in **Table A.6.3**.

Assessment: MATLAB Coding Ability and characteristics

The coding quality of project submissions was compared between the traditional and blended sections. To perform this assessment, a past teaching assistant familiar with the project who did not teach either of the sections included in the study was asked to grade de-identified assignment submissions from each class. A rubric was used which was adapted from Grading Rubric for Programming Problems by Shelby Kimmel which can be found in **Table A.6.4** [213]**.** This rubric was chosen because it assesses code by metrics other than simple correctness

(program achieving the intended outcome). These additional criteria include readability (code is clean and well-organized), documentation (code is well structured and commented), elegance (code utilizes appropriate methodology which is efficiently applied), and whether the code meets specifications.

The grader was provided with randomly chosen, de-identified project submissions. Each was graded and the scores were returned and reorganized into the appropriate section for analysis.

In order to provide rough measurements of the code characteristics from each class, samples were analyzed for runtime (amount of time taken for code to run to completion without error) and length (non-space character count, including all executable and commented code). Each code was run sequentially three times on the same machine and the runtime averaged while character count was obtained using a standard word processor.

The final assessment strategy is summarized in **Table 6.2.** Module completion statistics and survey response rate data can be found in **Table A.6.1**.

	Pre-project	Post-project
Traditional		*Confidence* *Competence*
Blended	*Confidence*	*Confidence* *Competence* *Effectiveness*

Table 6.2. Data collection strategy.

Data Analysis

Nonparametric statistical tests were used for all comparisons due to non-continuous (ordinal) survey/regrade datasets, unequal variance of datasets, and non-normal distributions in code runtime and length datasets (D'Agostino-Pearson normality test). For paired measurements (blended course confidence surveys), the Wilcoxon matched-pairs signed rank test was used. For non-paired measurements (traditional vs. blended class post-project comparisons) the Mann-Whitney U-test was used. For figures 3-5, the mean and 95% confidence interval are shown for all datasets. For all comparisons, a significance level of $p<0.1$ was used with the following notations: # $p<0.1$, * $p<0.05$, ** $p<0.01$, *** $p<0.001$, and **** $p<0.0001$. Statistical analysis and figure generation was performed in Microsoft Excel, Graphpad Prism, and MATLAB.

Results

Blended course was met with mixed results from students

Efficacy was determined by surveying student perceptions of the blended section (**Figure 6.2, top**). Students had a mixed reception to the blended class with many indicating a neutral response and relatively equal portions expressing positive and negative reception. The video-based assignment and clarity of the project and goals received a neutral to positive response. The effectiveness of the online modules was surveyed (**Figure 6.2, bottom**). Most students found the reflection exercises unhelpful in preparing for the programming project. Review materials had a negative to neutral response while practice problem reception was true neutral. The combined modules received mixed reception with nearly equal amounts of students expressing negative, neutral, and positive reception.

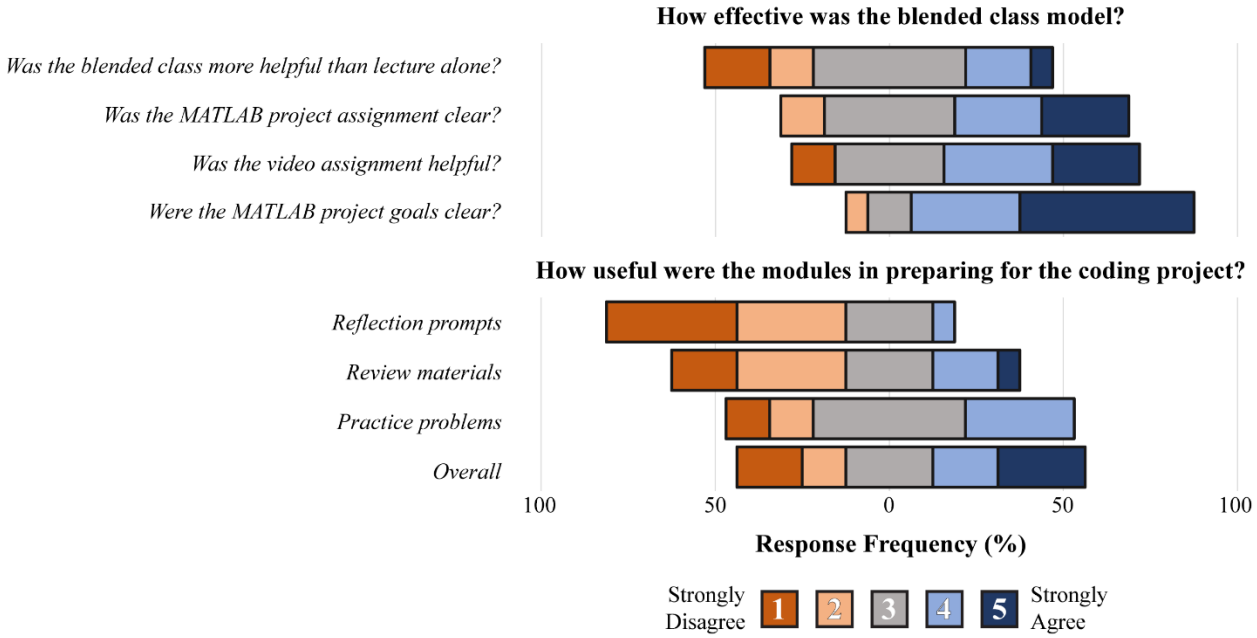

Figure 6.2. Module effectiveness survey results. Students were surveyed on how effective they found aspects of the blended course to be (top) and how useful the module components were (bottom). Students were mixed in their reception of the course but found the video assignment helpful. Students were mixed overall in how helpful they perceived the modules to be with practice being the most helpful and reflection prompts being the least.

Students had significantly improved confidence after completing blended course materials

Students in the blended class completed pre-and post-project programming confidence surveys and individual responses were tracked over time (**Figure 6.3**). Increases in confidence were apparent in MATLAB programming overall as well as each of the individual competencies focused on in the refresher modules and project.

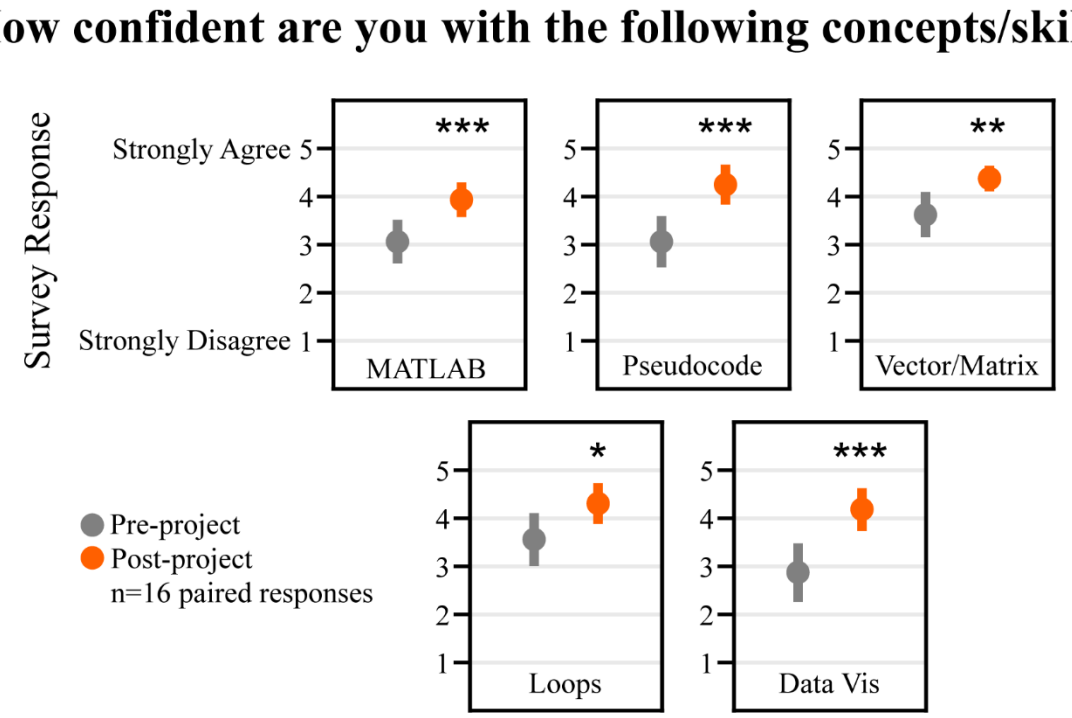

Figure 6.3. Blended course pre- and post-MATLAB project coding comfort. Students in the were significantly more comfortable in all of the queried MATLAB skills after completing the blended modules. Mean+/-95%CI. Mann-Whitney U test. #p<0.1, *p<0.05, **p<0.01, ***p<0.001, ****p<0.0001.

Students in the blended class were significantly more confidence in course material than students in the traditional class

The coding confidence survey results from the traditional and blended classes were compared after project completion (week 8) (**Figure 6.4**). The two groups show unequal variance due to differences in sample size (although response rate was similar as shown in **Table A.6.1)**. In addition, the intentional focusing on improving these areas in the blended class may have produced more homogeneity in post-project responses. While overall confidence using MATLAB was not different between the two classes, confidence in technical skills like vector and matrix operations, loops, and data visualization was significantly higher in the blended class than traditional.

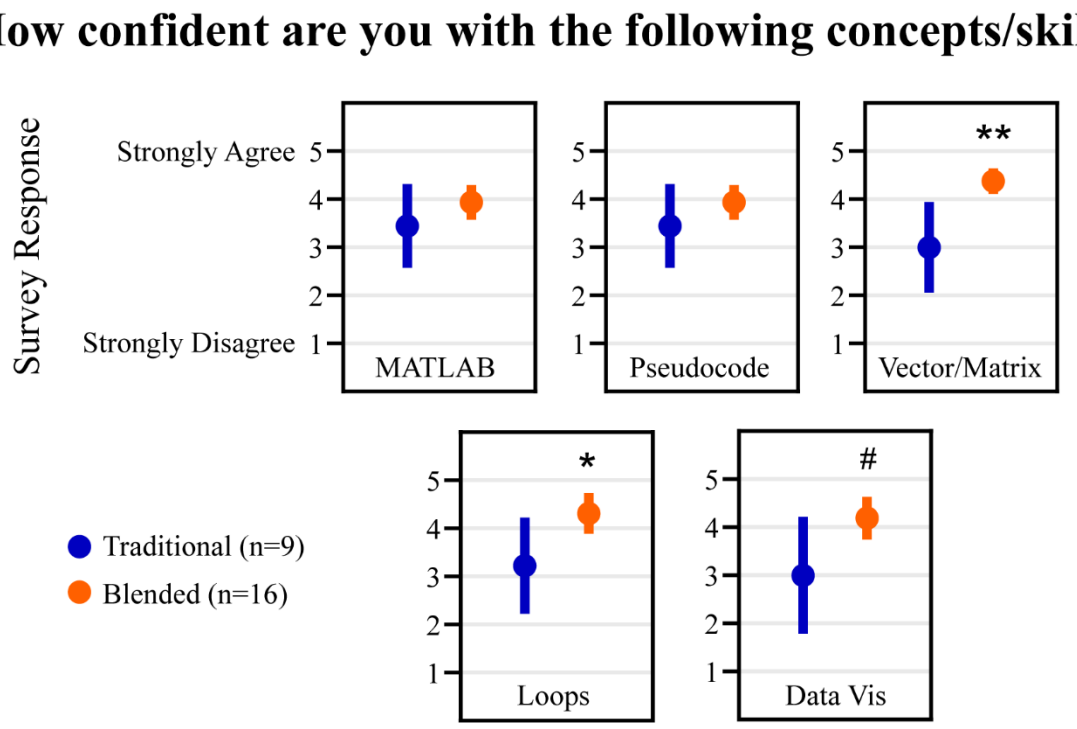

Figure 6.4. Traditional vs. blended course post-MATLAB project coding comfort. Students did not differ in their confidence MATLAB overall or pseudocoding between the traditional and blended courses (top left, top center). Students in the blended course were significantly more confident in using vector/matrix operations, loops, and data visualization compared to traditional course students. Mean+/-95%CI. Mann-Whitney U test. #p<0.1, *p<0.05, **p<0.01, ***p<0.001, ****p<0.0001.

Students in the blended course had shorter and more readable code

A standard rubric was applied by a blinded grader to determine whether there was any difference in coding quality between the two classes (**Figure 6.5A**). Scores were quite similar overall as well as in most subcategories except code readability (code is clean, understandable, and well-organized) where there was a slight improvement in the blended course compared to traditional.

The runtime and length were compared between samples from the traditional and blended course (**Figure 6.5B**). Variance was slightly greater in the traditional course as this class was approximately 2/3 the size of the blended section. While runtimes were nearly identical, samples from the blended class tended to be ~1000 non-space characters shorter, on average.

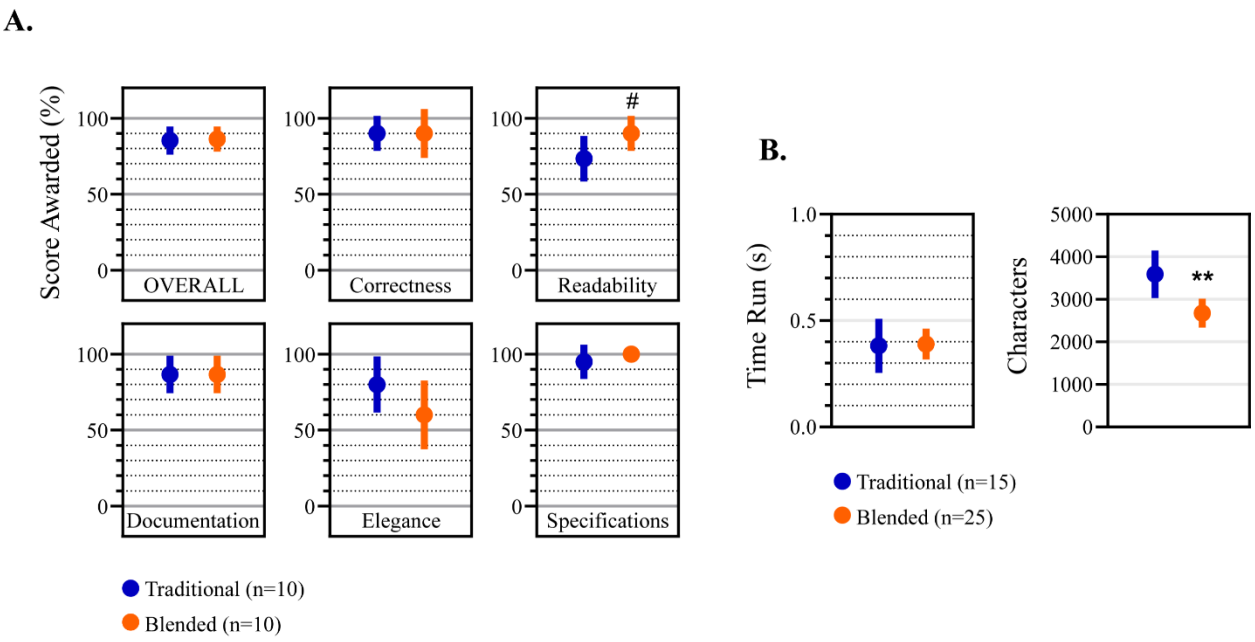

Figure 6.5. Traditional vs. blended course MATLAB project coding quality (A) and characteristics (B). A. There was little difference in scoring between students in the traditional and blended course except for a slight improvement in code readability in the blended course (top right). **B.** There was no difference in code efficiency (left) however students in the blended course tended to have shorter coding samples overall (right). Mean+/-95%CI. Mann Whitney U test. #p<0.1, *p<0.05, **p<0.01, ***p<0.001, ****p<0.0001.

Discussion

Integrating programming projects into biomedical engineering courses can develop skills crucial to careers in industry and academia. This can result in instructional challenges for courses which may not lend themselves to computational projects, such as biomechanics. In the biomechanics course at Vanderbilt University, programming projects are cited in course reviews as the most challenging portion of the course.

Typically, MATLAB content is delivered using a lecture-based method. One of the issues described by students was the inefficacy of this instructional style in seamlessly combining MATLAB and biomechanics content. A blended (combination of in-person and online) course has been shown to improve outcomes for students in certain circumstances. With the COVID19 pandemic, more classes have moved to online or hybrid configurations, and converting computer content into online modules may be an intuitive solution to the instructional problem (**Table 6.1**).

To test this hypothesis, programming content for a section of the biomechanics course was converted into online modules to be completed in parallel with in-person lectures (**Figure 6.1**). Changes in coding confidence were tracked before and after completing the MATLAB content in the blended course along with how students perceived the efficacy of the restructure. Coding confidence and ability were compared after completion of the project in traditional and blended styles (**Table 6.2**).

While project and goal clarity were high in the blended class, reception to the format was mixed (**Figure 6.2**). Students did not find the module components particularly helpful in preparation for the MATLAB project. Reflection prompts had a negative reception which may be due to poor formulation of prompts and reformulating this section may improve reception. Module review materials were collated from online resources. Specific videos made to

seamlessly integrate with course content could improve their usefulness. Practice problems could also be better integrated with course material with more personalized customization.

Despite a lukewarm reception, students experienced increases in coding confidence in the blended section style (**Figure 6.3**). While it is impossible to say whether the modules alone caused this improvement, the MATLAB components of the course seem to help students become more comfortable with coding content. Comparing post-project confidence data from the two structures (traditional vs. blended) indicates that confidence was higher for students in the blended section in technical skills like vector and matrix operations, loops, and data visualization (**Figure 6.4**). This course structure may allow students to learn these important MATLAB skills more effectively in a way that improves their confidence than in the traditional lecture style.

Using the blinded regrade system and a standardized rubric, overall code quality was similar between the two classes with slight improvements in code readability (code is clean, understandable, and well-organized) in the blended class (**Figure 6.5A**). The average code length was much lower in the blended class compared to traditional with no concurrent change in runtime (**Figure 6.5B**). Greater code readability and shorter length (while maintaining overall quality) indicate improved coding skill in blended course participants. While these measurements are subjective, the combination of results from confidence surveys and regrading point to an improvement in instruction after section restructure.

The modules need to be improved in a way that students perceive them as being useful and not just extra busy work to be done for the completion grade. Despite lukewarm reviews, the modules and coding project greatly improved confidence of students in the blended class. These students also had greater end-point confidence in technical programming skills compared to students in the traditional, lecture-only class. Furthermore, increased confidence in technical

skills likely translates to improved application of these tools in such a way that leads to increased code quality. This instructional improvement may begin to address student concerns about the poor integration of biomechanics and coding material in the original course structure.

Limitations and Future Directions

Due to the timing of the BOLD fellowship, study design, and IRB approval, only post-project survey data could be collected in the traditional class. The different timing of delivery of MATLAB coding material between traditional and blended courses may have affected results and future studies should control for this. Only one section (about half the class) was converted to the blended style and future studies should attempt to convert the entire course. Only one class could be studied for each course structure. A relatively small sample completed surveys (n=9 traditional and n=16 blended) but a similar response rate was achieved for each class (50% traditional and 57% blended). Future studies may link survey participation to a grade or extra credit to improve response rate. Surveys were created by the authors and are thus un-validated and should be interpreted as such. Future studies should aim to incorporate validated surveys which are rooted in the conceptual framework of blended learning. Future development of coding competencies should focus on more generalizable concepts such as problem abstraction and code reusability. The solution presented in this article is specific to a certain project and may limit translatability. While the courses were identical, different instructors taught each section which may have changed how biomechanics material was taught. MATLAB-specific content was taught by the authors in both classes to maintain consistency. Future studies should continue to refine the blended structure as well as include more students and classes, controlling for

instructors if possible. Studying other code metrics may also be useful to introduce more objective measures of code quality including comment density, loop density, and efficiency.

Conclusions

While the instruction problem in this study was challenging, blended classes have shown to have positive outcomes for students and moving coding content online is a simple and intuitive solution. While this first attempt at restructuring a portion of the course was not all that well received by students, there were significant improvements in coding confidence compared to the previous class-type. Additionally, students in the blended section tended to submit code with greater readability which suggest improvement in confidence as well as tangible skills. These are positive results as moving content online can allow instructors to focus more on in-person class time covering core concepts of the course. Students can also refresh their programming skill online at their own pace. As courses have been converted to online or hybrid structures in response to the COVID19 pandemic, it is encouraging to see that moving certain content to this format is not only safer and more convenient but can also improve student outcomes. Instructors should retain these online and hybrid teaching strategies that have improved overall instruction quality. Future studies could focus on increasing sample sizes, survey coverage, and inclusion of students from different sections, instructors, and institutions. In addition, further expansion and refinement of surveys, code quality assessment, and code characteristics may provide further insights into how the course structure can result in downstream effects on student attitudes toward coding as well as their skill.

CHAPTER 7

Impact and Future Directions

Dissertation Summary

AV disease is one of the most common CV diseases – a disease set which accounts for the most common cause of death in the U.S.A. AVS itself is a difficult disease to treat in that it does not have any associated drug therapies . The only option is replacement of the diseased valve with a prosthetic replacement. While there are recent advances in the space of interventional valve replacement via TAVR, there is still a need for non-invasive methods of slowing or resolving the disease [41]. This is necessary as AVS is most commonly a disease of the very elderly who often have many comorbidities that add risk to any level of sedation and surgery.

Osteoporosis is associated with reduction of bone mineral content and an increase in risk of fracture and lower quality of life . The pharmaceutical treatment landscape for osteoporosis is much better than AV disease with numerous treatments availability [214]. One of the more recent treatments developed is a mAb-based therapy targeting the protein sclerostin. This sclerostin antibody is extremely effective in halting bone resorption and reducing fracture risk. However, off-target side effects necessitate an investigation into how the drug affects the progression of AV disease [7].

Investigating osteoporosis is impossible without confronting the sex differences aspects which accompany it. One of the most common subsets of osteoporosis patients are elderly women with PMO. Chapter 5 of this dissertation focuses on how AV disease manifests in a PMO model commonly used in skeletal research. The aim for this section was the development of a new model for understanding how AV disease and osteoporosis interact. This includes common mechanisms and potential drug targets to ameliorate the shared effects of these diseases. This includes sclerostin targeting antibodies as well as others such as anti-resorptive drugs. In

addition, female specific CV disease is woefully understudied in pre-clinical research and this section of research aims to help address this.

The final section of new studies focuses on how biomedical engineering material is transmitted in the college classroom. Specifically, the role of technology in a post-COVID19 pandemic landscape is addressed by evaluating the outcomes of traditional lecture courses and hybrid-style classes in delivering coding content. The aim of this section is to make a fundamental contribution to biomedical engineering by providing novel data for the best instruction modalities.

Impact

Sclerostin Studies

The overarching impacts of the first two sections of this dissertation involve the relationship between AVS and skeletal disease and drug treatment. Chapter 4 aims to understand the role of sclerostin in AVS development. Because there had been no direct investigations on sclerostin and the AV, a fundamental approach was utilized by using a germline deletion of the *Sost* gene in mice and conducting a thorough longitudinal study using *in vivo* imaging as well as extensive *ex vivo* analysis using histology, *in vitro* analysis of isolated AVICs, and finally taking a step back and looking at a complete effect of sclerostin deletion on signaling in the aortic root using RNA sequencing.

Perhaps the groundbreaking takeaway from this study was the conclusion that sclerostin deletion results in mice not developing the hallmarks of AVS when compared to WT controls. This is at odds with our initial hypothesis for the study. Results from clinical trials of the sclerostin targeting antibody results in an increase in CV side effects including heart attack and

stroke [7]. Sclerostin acting as a calcification inhibitor logically follows that genetic ablation would increase ectopic calcification often associated with AVS. Studies in the vasculature confirm this protective effect of sclerostin in aortic aneurysm and atherosclerosis [92]. The new data presented seem to indicate the opposite is true, at least regarding the progression AV disease. This adds a confusing, yet interesting, new development in the understanding of sclerostin's role in CV disease.

Ex vivo analysis of the AVs pointed to interesting explanations of the observed *in vivo* phenotype. The applicability of this data is a bit difficult to estimate partially due to the relatively early time point we assess *ex vivo* valve health. AVS typically becomes severe and symptomatic at advanced age (usually 60 and above) [215,216]. Mice are notoriously resistant to valve disease (necessitating genetic modification and high cholesterol diet administration) [217]. The one-year time point is roughly correlative to middle age (40-50) [176]. Therefore, it is not surprising that valve disease is mild for a middle-aged mouse and that there is relatively little evidence of osteogenic calcification. Despite looking at mice at the one-year timepoint, WT mice had mild thickening of AV leaflets compared to sclerostin null mice as well as increased expression of myofibroblast marker αSMA. This is in tandem with little expression of Runx2, an osteogenic marker often indicating a very late disease state. Therefore, it would appear that sclerostin plays a role in early activation of myofibroblasts which can lead to fibrosis and dystrophic calcification.

Sclerostin's role in myofibroblast early activation of AV disease is bolstered by analysis of sclerostin null AVICs isolated from immortalized mice. The Merryman Mechanobiology Laboratory was the first research group to extensively use mouse AVICs (most studies use porcine, human, or ovine cells due to the technical difficulty of establishing cell lines from such

small tissue samples) [53]. This work further emphasizes the utility of using a constant species model and more direct applicability between *in vivo* and *in vitro* studies. Pigs may be a more superior model of human heart function, but they are much less flexible and more expensive to maintain than standard laboratory mice. Further, genetic alteration is impossible which would likely be necessary for reliable development of AVS in a reasonable time frame.

In vitro experimentation revealed that mice lacking the sclerostin gene had less contractile capacity than WT cells. Similarly, treatment with recombinant sclerostin protein caused greater contraction when compared to vehicle control. This further implies that sclerostin has a role in myofibroblast activation and may be a mechanoactive protein.

These interesting revelations about sclerostin's pro-disease role in AVS as well as its involvement in myofibroblast activation had very little precedent in the literature. Sclerostin is a fairly well characterized inhibitor of Wnt signaling by interacting with the LRP surface receptors [99]. The protein has also been shown to indirectly modulate RANKL signaling [111]. However, the observed phenotype ran counter to what might be expected in modulating these pathways in AV disease. To help explain this discordance, RNA sequencing was performed on aortic roots from sclerostin WT and null mice at the endpoint. Around 700 genes were upregulated in NULL mice and 300 upregulated in WT. This indicates that the removal of the inhibitory regulatory protein sclerostin seems to prompt and increase in signaling which may be expected. A number of bioprocesses were shown to be altered between the two groups in biomineralization and cell patterning, among others. Perhaps the most interesting discovery was the upregulation of pan-HOX signaling in the NULL mice. The HOX signaling pathway is fundamental in body patterning during development [218]. However, new research has indicated a role for the pathway in disease, including new discoveries of protective affects in CV disease [178]. A

number of HOX genes were shown to be upregulated in the NULL cells, confirming this as a potential protective mechanism spurred by loss of the sclerostin protein. The primary discoveries from this study are the protective effect of sclerostin ablation on AV disease development as well as the upregulation of HOX-signaling this seems to have. These discoveries could have a major impact on AVS, the side effects of sclerostin drug targeting, and the burgeoning field of HOX signaling in CV disease.

The initial genetic investigation of sclerostin ablation lead to the question of the effects of antibody inhibition of the protein on the development of AVS. The original research plan was to perform OVX on laboratory mice and treat them with antibody in order to see if the protective effects noted in the genetic study translated to the pharmaceuticals. However, the COVID19 pandemic and lack of industry partnership necessitated a scale back and revision of the aim for the second portion of the dissertation. Instead, our research was refocused on a more fundamental question of how preclinical models of PMO interacted with AV disease. This new aim tackled fundamental questions. There is a lack of general translational models of AV disease in the lab. This study would provide knowledge and how a commonly used, easy to perform, and well-characterized surgical model affected valve disease progression in mice. At the same time, AV disease in female patients is woefully understudied and there are no models which focus on the female progression of disease. CV disease is correlated with severity of osteoporosis in female patients, yet treatment and diagnosis are not optimized for this patient subset. Therefore, we hoped to shed light on these blind spots in the second portion of this dissertation.

To do this, the OVX procedure was performed at 4 months combined with aging to one year and high-cholesterol diet. These mice were compared to sham controls. *In vivo* analysis using echocardiography was used to track AV and LV disease progression over time as well as

DXA to monitor body composition. At 12 months the heart was excised and tissue analyzed using histology and immunostaining. Results indicated that ovariectomized mice did not develop significant AV disease at one year, however exhibited potential evidence of LV hypertrophy absent of significant collagen deposition.

The impacts of this research lead to a new model for LV hypertrophy in PMO patients. While there was no evidence of a strong AV phenotype, this model may be useful in understanding diseases of the LV in an understudied patient population. Current models of inducing HF, LV hypertrophy, and LV fibrosis tend to rely on invasive procedures including transaortic constriction or agonistic insults using compounds such as angiotensin [219]. Using such models can result in limited translatability to human cases. This study will result in better translatability as this procedure is minimally invasive and mice recover quickly. Further, aging, and high-cholesterol diet are strong models for CV disease. The strong LV hypertrophy phenotype can be used as a window of therapy for pre-clinical studies of procedures and drug treatments that aim to reduce LV hypertrophy at early stages.

Biomedical Engineering Hybrid Education

Chapter 6 of this dissertation focuses on biomedical engineering education topics. Particularly, the best strategies for integrating technology and the internet into the classroom using a hybrid approach. This involved reformatting a traditional style lecture into a new delivery that utilized in person instruction in tandem with online modules related to the content. Pre- and post-analysis of student comfort in the topics indicated a marked improvement and students in the hybrid class were more comfortable with the material and performed better on assessment that lecture-style alone.

The applicability of this research in a larger context is evident in response to the COVID19 pandemic. During the pandemic, most American universities moved to a hybrid or online delivery system in order to ensure student safety [208]. This shift in modality raised a lot of questions (and continues to raise a lot of questions) regarding the long-term efficacy and effects on shifting college instruction online. The research in chapter 6begins to answer that question and can also begin to provide some data and guidance for instructors aiming to shift content online for safety reasons or to free up class time to cover other material. Results indicate that student learning does not have to be sacrificed when moving content online assuming data is collected and the course design is performed with intention. In addition to the new data generated, the section also provides a template for instructors to gather information in their own classes to make changes.

Future Directions

Sclerostin Studies

There are many potential directions future studies could take that stem from the research performed in this dissertation. The most pressing would be to continue the work in chapters 4 and 5 of this work. As previously explained, the original intention linking the two sections was to assess the effects of the sclerostin neutralizing antibody in the OVX model. This course of study was not pursued for several reasons mainly stemming from the slowing of laboratory research due to persistent lockdowns from the COVID19 pandemic and postposed industry partnerships to use their sclerostin blocking antibody. As vaccines and treatments for COVID19 allow for greater research activity it would be worth attempting to reinvigorate this area of study with

private partnership or attempt to form collaborations at Vanderbilt to formulate our own blocking antibody.

The research gathered in the OVX study indicated that female mice with OVX, one year of aging, and high-cholesterol diet do not develop significant AVS. This is in line with research showing mice are resistant to AV disease without genetic modification and female mice even more so. Therefore, it would first be prudent to define a laboratory model which reliably developed AVS in a reasonable time frame (within one year). Commonly used models include *Notch1* and *Apo* genetic ablation mice [217]. Performing OVX on mice genetically predisposed to the disease may result in a stronger phenotype. Recently wire injuries have been studied as a surgical method of inducing AVS in a reasonable time frame which also may be another option [220]. The data was insignificant in our study at one year but OVX mice were numerically higher and closer to being significant. Aging out to 18 months may provide a stronger phenotype. However, unpublished data from this work indicates that mice quickly begin to perish around 14 months so this increased mortality would need to be accounted for when initially planning the study.

After development of a stronger model of post-menopausal AVS a pharmaceutical study with the sclerostin blocking antibody would be the next best study to understand the role of sclerostin in CAVD. The sclerostin neutralizing antibody would be administered after the OVX procedure when there was a confirmed osteoporotic phenotype as determined by DXA. The data shown in the chapter 5 indicate this happens as early as 1-month post-op. The mice would then be treated for approximately 4-8 weeks with the drug and then allowed to age to one year. Sclerostin antibody is used for approximately one year to achieve skeletal affects in humans and this would approximate that time frame. The mice would then be aged to one year (or longer

depending on system validation experiments). Echocardiography should be performed similar to studies in chapter 4 and 5 as well as DXA analysis to monitor disease progression. Histological analysis should be used to develop a tissue level phenotype. Whole heart histology (as performed in chapter 5) is stronger as you can see the morphology of the LV and AV to account for the entire left heart. RNA sequencing would also be useful as performed in chapter 4 in order to compare to the genetic ablation data set. A mirroring of the upregulation of HOX genes would further confirm that sclerostin signaling and HOX genes are linked in the observed phenotype. If results of the proposed drug experiment mirror those seen in the genetic model, it would make for a very compelling case that sclerostin is a driver of AV disease which should be taken into account when prescribing the drug as well as potentially evaluating it as a therapeutic for individuals suffering both diseases. However, the mounting evidence that sclerostin plays a protective role in other CV diseases must be considered.

HOX Studies

Analysis of the role of HOX genes in the observed phenotype must be further interrogated. It is remarkable that every HOX gene is upregulated in the nulls and the sheer likelihood of this is relatively low which is cause for interest. However, it is impossible to ignore that the data contained in this dissertation is descriptive. The easiest method to begin interrogating the signaling pathway would likely be *in vitro* analysis using the established AVIC lines from the experiment animals. Data from RNAseq is based on the aortic root which may contain heart muscle tissue as aorta. To account for this, we performed qPCR on AVICs which should help narrow down the HOX genes of interest specifically in the AV. These include *HOXA1*, *HOXB2*, and *HOXD3*. *HOXA3* is non-significantly increased as well. Most of the data

on HOX genes and CV disease involves the HOXA subset. Therefore, regulation of HOX genes by sclerostin would be an interesting new experiment. Using the recombinant sclerostin protein used in the contraction assays and next seeing if *HOXA1* or *HOXA3* are similarly modulated at the protein or RNA level. The possibility of indirect regulation must also be considered. Next, the HOX genes should be modulated using siRNA or overexpressed using plasmid transfection. If the HOX genes are protective, reducing their expression should result in the NULL cells reverting to the WT phenotype. Assays such as contraction or calcification may be a good place to begin on these experiments.

In vitro analysis of HOX and sclerostin would be the easiest place to begin for fast and cheap experiments. If the HOX phenotype is mirrored in cells it would be prudent to further establish the link using double mutant animals. Research in this dissertation shows the efficacy of the sclerostin NULL mice in preventing the development of AVS. Similar knockout of the HOX genes of interest (*HOXA1*, *HOXA3*, *HOXB2*, or *HOXD3*) on the sclerostin null background would be fruitful. *HOXA1* and *HOXA3* knockout mice have been well characterized and a good place to start. Removal of the protective HOX genes may result in the NULL mice developing disease similar to the WT controls. Partial return of the phenotype may occur as there is overlap between the functionality of HOX genes and there seems to be upregulation across many subsets. Due to the necessity for the HOX gene activity during development, it may be necessary to use activation based genetic knockout using the Cre-recombinase system in order to remove the gene in adulthood after it has performed its necessary developmental role. The strength of the presented studies is the flexibility. Similar methods of analysis can be used in future studies in a way that creates a rich and broadly applicable dataset where we can probe this novel phenotype. These experiments of the HOX genes should be performed in tandem with future studies on

sclerostin pharmaceutical targeting described in previous paragraphs in order to provide a strong translation pipeline to better understand the utility of the drug in AV diseases and potential side effects it may have in osteoporosis patients.

Ovariectomy Studies

Outside of further investigation of the novel sclerostin phenotype, it is also necessary to follow up on the discoveries from the OVX study in chapter 5. There is very little research on the specific CV effects of the OVX procedure despite its common use in osteoporosis pre-clinical research. It has been shown that osteoporosis bone loss paradoxically correlates with CV calcification and disease and female patients in post menopause have higher rates of diagnosis and worse overall outcomes [194]. The results presented in this dissertation indicate that ovariectomized female mice aged to one year on high-cholesterol diet do not develop significant AVS. However, analysis indicates a potentially strong LV hypertrophy phenotype. The model may be useful as a clinically translatable aged and diet induced LV disease model. Further investigation of the differences in the LV between sham and OVX animals should be interrogated. Omic study of the LV tissue would be enlightening, particularly directly investigating the differences in smooth muscle signaling, differentiation, activation, and fibrosis.

There is room for further histological investigation of the ventricle muscle tissue. Second harmonic imaging has been performed in other studies in our lab to characterize muscle tissue in the LV [164]. *In vitro* experiments of smooth muscle cell lines and cardiac fibroblasts would be useful to probe the differences in signaling and mechanical characterization using assays such as gel contraction or scratch wound healing. There are many generic cell lines and we have shown the ability to generate immortalized cell lines. Because of the large cell sample from the LV

tissue compared to AV, there are also options for using flow cytometry to isolate and interrogate LV cells at the 12 month endpoint (as well as potential intermediate time points) to better understand differences in signaling that arise from the OVX procedure. Because the mouse cohort for the studies in this dissertation were small due to their preliminary nature, all of the tissue was used for analysis and a larger follow up study would be required. Designing a new study with a focus on the LV in mind would be very useful in further clarifying the mechanism of hypertrophy induced from the OVX procedure and how well the observed phenotype will translate to applications in human patients.

Biomedical Engineering Hybrid Education

Finally, there is room for further expansion of the engineering education research outlined in chapter 6 of this dissertation. The study detailed in Chapter 6 compared the effect of transitioning biomechanics programming content from a traditional, lecture-based format to a hybrid format combining in-person and online module instruction. Results indicated that the hybrid approach resulted in improved student confidence in the material as well as their performance on programming projects. The main limitation of the study was the limited sample sizes as the project was performed on a very abbreviated timeline due to the fellowship constraints. Future studies should involve expanding the classes and sample sizes as well as instructors in order to assess how the results translate to a broader educational cohort. Similarly, there is room to further refine the assessment. Surveys were custom written and not formally validated. While the study was approved by the IRB, there are certainly blind spots. Assessment should closely follow established benchmarks of instructional success in engineering. Future assessments should more rigorously engage the field of quantitative classroom assessment.

Additionally, many aspects of the hybrid class drew mediocre response from the students despite improvements in their performance. Reconfiguring the class in order to more engage the students could further strengthen the results seen here. By solidifying this study, it may lead to a large impact in how biomedical engineering undergraduate programs and courses are structured.

Conclusions

In conclusion, there are four primary future paths for this dissertation work. First, a pharmaceutical aspect must be added to improve the translatability of the sclerostin AV disease phenotype. The drug is commonly used in preclinical studies, but first a partner in industry must be brought on board. This project was in the planning steps before the COVID19 pandemic and should now be revisited. Next, the precise mechanism of HOX regulation of sclerostin in AV disease development should be clarified using *in vitro* capabilities and eventually branching into small animal experiments, ideally evaluating *Sost x Hox* double knockout mice. Next, the mechanisms of LV hypertrophy in ovariectomized mice should be further pursued to better understand the observed phenotype. This dissertation lays out a preliminary study that should be expanded and utilize an unbiased analysis to interrogate the mechanisms. Finally, there is room to expand the work done on blended learning in engineering course development. The hybrid course modules and assessment techniques should be reworked to leverage the available validated resources. Next the student population should be expanded to multiple classes as well as more instructors to determine if the redesign is applicable across curriculum or only an artifact of the courses interrogated here. This will hopefully lead to more widespread adoption and intentional structuring of engineering courses in a hybrid fashion to improve student outcomes and free up more class time for high-impact subjects.

BIBLIOGRAPHY

1. Thompson B, Towler DA. Arterial calcification and bone physiology: role of the bone–vascular axis. Nat Rev Endocrinol [Internet]. 2012;8(9):529–43. Available from: https://doi.org/10.1038/nrendo.2012.36

2. Organ JM, Srisuwananukorn A, Price P, Joll JE, Biro KC, Rupert JE, et al. Reduced skeletal muscle function is associated with decreased fiber cross-sectional area in the Cy/+ rat model of progressive kidney disease. Nephrol Dial Transplant. 2016;31(2).

3. Na S, TruongVo T, Jiang F, Joll JE, Guo Y, Utreja A, et al. Dose analysis of photobiomodulation therapy on osteoblast, osteoclast, and osteocyte. J Biomed Opt. 2018;23(7):75008.

4. Rupert JE, Joll JE, Elkhatib WY, Organ JM. Mouse Hind Limb Skeletal Muscle Functional Adaptation in a Simulated Fine Branch Arboreal Habitat. Anat Rec. 2018;301(3).

5. Joll J, Vickery B, Rupert J, Biro K, Wallace J, Byron C, et al. Mechanical effects of fine-wire climbing on the hindlimb skeleton of mice. FASEB J. 2015;29:692–8.

6. Joll J, Rupert JE, Mihajlovich J, Organ JM. Structure and Mechanics of Mammalian Prehensile Tail Vertebrae. Off Vice Chancell Res - IUPUI. 2014;

7. Saag KG, Petersen J, Brandi ML, Karaplis AC, Lorentzon M, Thomas T, et al. Romosozumab or Alendronate for Fracture Prevention in Women with Osteoporosis. N Engl J Med [Internet]. 2017 Sep 11; Available from: http://dx.doi.org/10.1056/NEJMoa1708322

8. Ramirez FD, Motazedian P, Jung RG, Di Santo P, MacDonald Z, Simard T, et al. Sex Bias Is Increasingly Prevalent in Preclinical Cardiovascular Research: Implications for Translational Medicine and Health Equity for Women. Circulation [Internet]. 2017 Feb 7;135(6):625–6. Available from: https://doi.org/10.1161/CIRCULATIONAHA.116.026668

9. Shakeri A, Adanty C. Romosozumab (sclerostin monoclonal antibody) for the treatment of osteoporosis in postmenopausal women: A review. J Popul Ther Clin Pharmacol. 2020;27(1):e25–31.

10. Männer J, Yelbuz TM. Functional morphology of the cardiac jelly in the tubular heart of vertebrate embryos. J Cardiovasc Dev Dis. 2019;6(1):12.

11. Menon V, Lincoln J. The Genetic Regulation of Aortic Valve Development and Calcific Disease. Front Cardiovasc Med [Internet]. 2018 Nov 6;5:162. Available from: https://www.ncbi.nlm.nih.gov/pubmed/30460247

12. Kovacic JC, Dimmeler S, Harvey RP, Finkel T, Aikawa E, Krenning G, et al. Endothelial to mesenchymal transition in cardiovascular disease: JACC state-of-the-art review. J Am Coll Cardiol. 2019;73(2):190–209.

13. Akiyama H, Chaboissier M-C, Behringer RR, Rowitch DH, Schedl A, Epstein JA, et al. Essential role of Sox9 in the pathway that controls formation of cardiac valves and septa.

Proc Natl Acad Sci. 2004;101(17):6502–7.

14. Rosenthal N, Harvey RP. Heart development and regeneration. Vol. 1. Academic Press; 2010.

15. Culver JC, Dickinson ME. The effects of hemodynamic force on embryonic development. Microcirculation. 2010;17(3):164–78.

16. Goddard LM, Duchemin A-L, Ramalingan H, Wu B, Chen M, Bamezai S, et al. Hemodynamic Forces Sculpt Developing Heart Valves through a KLF2-WNT9B Paracrine Signaling Axis. Dev Cell [Internet]. 2017;43(3):274-289.e5. Available from: https://www.sciencedirect.com/science/article/pii/S1534580717307827

17. Rajamannan NM, Evans FJ, Aikawa E, Grande-Allen KJ, Demer LL, Heistad DD, et al. Calcific aortic valve disease: Not simply a degenerative process: A review and agenda for research from the national heart and lung and blood institute aortic stenosis working group. Circulation. 2011;124(16):1783–91.

18. Taylor PM. Biological matrices and bionanotechnology. Philos Trans R Soc B Biol Sci. 2007;362(1484):1313–20.

19. Vesely I. The role of elastin in aortic valve mechanics. J Biomech [Internet]. 1997;31(2):115–23. Available from: https://www.sciencedirect.com/science/article/pii/S002192909700122X

20. Ayoub S, Ferrari G, Gorman RC, Gorman JH, Schoen FJ, Sacks MS. Heart valve biomechanics and underlying mechanobiology. Compr Physiol. 2016;

21. Schoen FJ. Morphology, Clinicopathologic Correlations, and Mechanisms in Heart Valve Health and Disease. Cardiovasc Eng Technol [Internet]. 2018;9(2):126–40. Available from: https://doi.org/10.1007/s13239-016-0277-7

22. Aggarwal A, Pouch AM, Lai E, Lesicko J, Yushkevich PA, Gorman JH, et al. In-vivo heterogeneous functional and residual strains in human aortic valve leaflets. J Biomech. 2016;

23. Bowler MA, Merryman WD. In vitro models of aortic valve calcification: Solidifying a system. Vol. 24, Cardiovascular Pathology. 2015. p. 1–10.

24. Mongkoldhumrongkul N, H. Yacoub M, H. Chester A. Valve Endothelial Cells - Not Just Any Old Endothelial Cells. Curr Vasc Pharmacol. 2016;

25. Bischoff J, Aikawa E. Progenitor cells confer plasticity to cardiac valve endothelium. J Cardiovasc Transl Res. 2011;

26. Markwald RR, Norris RA, Moreno-Rodriguez R, Levine RA. Developmental basis of adult cardiovascular diseases: Valvular heart diseases. In: Annals of the New York Academy of Sciences. 2010.

27. Liu AC, Joag VR, Gotlieb AI. The emerging role of valve interstitial cell phenotypes in regulating heart valve pathobiology. Am J Pathol [Internet]. 2007;171(5):1407–18. Available from:

http://www.pubmedcentral.nih.gov/articlerender.fcgi?artid=2043503&tool=pmcentrez&rendertype=abstract

28. Chester AH, El-Hamamsy I, Butcher JT, Latif N, Bertazzo S, Yacoub MH. The living aortic valve: From molecules to function. Glob Cardiol Sci Pract. 2014;

29. Travers JG, Kamal FA, Robbins J, Yutzey KE, Blaxall BC. Cardiac fibrosis: The fibroblast awakens. Vol. 118, Circulation Research. 2016. p. 1021–40.

30. Schoen FJ. Mechanisms of Function and Disease of Natural and Replacement Heart Valves. Annu Rev Pathol Mech Dis. 2011;

31. Latif N, Sarathchandra P, Chester AH, Yacoub MH. Expression of smoothmuscle cellmarkers and co-activators in calcified aortic valves. Eur Heart J. 2015;

32. Li C, Xu S, Gotlieb AI. The response to valve injury. A paradigm to understand the pathogenesis of heart valve disease. Cardiovascular Pathology. 2011.

33. Christie GW, Barratt-Boyes BG. Age-dependent changes in the radial stretch of human aortic valve leaflets determined by biaxial testing. Ann Thorac Surg. 1995;

34. Stephens EH, de Jonge N, McNeill MP, Durst CA, Grande-Allen KJ. Age-Related Changes in Material Behavior of Porcine Mitral and Aortic Valves and Correlation to Matrix Composition. Tissue Eng Part A. 2009;

35. Elena A, Peter W, Mark F, Karen M, F. PR, Masanori A, et al. Human Semilunar Cardiac Valve Remodeling by Activated Cells From Fetus to Adult. Circulation [Internet]. 2006 Mar 14;113(10):1344–52. Available from: https://doi.org/10.1161/CIRCULATIONAHA.105.591768

36. Virani SS, Alonso A, Aparicio HJ, Benjamin EJ, Bittencourt MS, Callaway CW, et al. Heart Disease and Stroke Statistics—2021 Update. Circulation [Internet]. 2021 Feb 23;143(8):e254–743. Available from: https://doi.org/10.1161/CIR.0000000000000950

37. Lindman BR, Clavel M-A, Mathieu P, Iung B, Lancellotti P, Otto CM, et al. Calcific aortic stenosis. Nat Rev Dis Prim [Internet]. 2016 Mar 3;2:16006. Available from: https://doi.org/10.1038/nrdp.2016.6

38. Mohler ER, Gannon F, Reynolds C, Zimmerman R, Keane MG, Kaplan FS. Bone Formation and Inflammation in Cardiac Valves. Circulation [Internet]. 2001;103(11):1522–8. Available from: http://circ.ahajournals.org/cgi/doi/10.1161/01.CIR.103.11.1522

39. R. CC, A. BM, Caleb SJ, David MW. Targeting Cadherin-11 Prevents Notch1-Mediated Calcific Aortic Valve Disease. Circulation [Internet]. 2017 Jun 13;135(24):2448–50. Available from: https://doi.org/10.1161/CIRCULATIONAHA.117.027771

40. Rashedi N, Otto CM. Aortic Stenosis: Changing Disease Concepts. J Cardiovasc Ultrasound. 2015;

41. Lindman BR, Bonow RO, Otto CM. Current management of calcific aortic stenosis. Circ Res. 2013;113(2):223–37.

42. Rajamannan NM, Evans FJ, Aikawa E, Grande-Allen KJ, Demer LL, Heistad DD, et al. Calcific Aortic Valve Disease: Not Simply a Degenerative Process. Circulation [Internet]. 2011 Oct 17;124(16):1783 LP – 1791. Available from: http://circ.ahajournals.org/content/124/16/1783.abstract

43. He C, Tang H, Mei Z, Li N, Zeng Z, Darko KO, et al. Human interstitial cellular model in therapeutics of heart valve calcification. Amino Acids. 2017;1–17.

44. Liu X, Xu Z. Osteogenesis in calcified aortic valve disease: From histopathological observation towards molecular understanding. Vol. 122, Progress in Biophysics and Molecular Biology. 2016. p. 156–61.

45. Towler DA. Molecular and cellular aspects of calcific aortic valve disease. Circ Res. 2013;113(2).

46. Torre M, Hwang DH, Padera RF, Mitchell RN, Vanderlaan PA. Osseous and chondromatous metaplasia in calcific aortic valve stenosis. Cardiovasc Pathol. 2016;

47. Rajamannan NM, Subramaniam M, Rickard D, Stock SR, Donovan J, Springett M, et al. Human aortic valve calcification is associated with an osteoblast phenotype. Circulation. 2003;107(17):2181–4.

48. Cheek JD, Wirrig EE, Alfieri CM, James JF, Yutzey KE. Differential activation of valvulogenic, chondrogenic, and osteogenic pathways in mouse models of myxomatous and calcific aortic valve disease. J Mol Cell Cardiol. 2012;52(3):689–700.

49. O'Brien KD. Pathogenesis of calcific aortic valve disease: A disease process comes of age (and a good deal more). Vol. 26, Arteriosclerosis, Thrombosis, and Vascular Biology. 2006. p. 1721–8.

50. Kaden JJ, Dempfle C-E, Grobholz R, Fischer CS, Vocke DC, Kılıç R, et al. Inflammatory regulation of extracellular matrix remodeling in calcific aortic valve stenosis. Cardiovasc Pathol [Internet]. 2005;14(2):80–7. Available from: http://www.sciencedirect.com/science/article/pii/S1054880705000062

51. Li C, Xu S, Gotlieb AI. The progression of calcific aortic valve disease through injury, cell dysfunction, and disruptive biologic and physical force feedback loops. Cardiovascular Pathology. 2013.

52. Fisher CI, Chen J, Merryman WD. Calcific nodule morphogenesis by heart valve interstitial cells is strain dependent. Biomech Model Mechanobiol. 2013;12(1):5–17.

53. Chen J, Ryzhova LM, Sewell-Loftin MK, Brown CB, Huppert SS, Baldwin HS, et al. Notch1 mutation leads to valvular calcification through enhanced myofibroblast mechanotransduction. Arterioscler Thromb Vasc Biol. 2015;35(7):1597–605.

54. D. HJ, Joseph C, M.K. S-L, M. RL, I. FC, Ru SY, et al. Cadherin-11 Regulates Cell–Cell Tension Necessary for Calcific Nodule Formation by Valvular Myofibroblasts. Arterioscler Thromb Vasc Biol [Internet]. 2013 Jan 1;33(1):114–20. Available from: https://doi.org/10.1161/ATVBAHA.112.300278

55. Bowler MA, Bersi MR, Ryzhova LM, Jerrell RJ, Parekh A, Merryman WD. Cadherin-11

as a regulator of valve myofibroblast mechanobiology. Am J Physiol Circ Physiol [Internet]. 2018 Oct 25;315(6):H1614–26. Available from: https://doi.org/10.1152/ajpheart.00277.2018

56. Yutzey KE, Demer LL, Body SC, Huggins GS, Towler DA, Giachelli CM, et al. Calcific aortic valve disease: a consensus summary from the Alliance of Investigators on Calcific Aortic Valve Disease. Arterioscler Thromb Vasc Biol. 2014;34(11):2387–93.

57. Lerman DA, Prasad S, Alotti N. Calcific aortic valve disease: Molecular mechanisms and therapeutic approaches. Eur Cardiol Rev . 2015;

58. Mozaffarian D, Benjamin EJ, Go AS, Arnett DK, Blaha MJ, Cushman M, et al. Executive summary: Heart disease and stroke statistics-2016 update: A Report from the American Heart Association. Circulation. 2016.

59. Otto CM, Burwash IG, Legget ME, Munt BI, Fujioka M, Healy NL, et al. Prospective study of asymptomatic valvular aortic stenosis: Clinical, echocardiographic, and exercise predictors of outcome. Circulation. 1997;

60. Nkomo VT, Gardin JM, Skelton TN, Gottdiener JS, Scott CG, Enriquez-Sarano M. Burden of valvular heart diseases: a population-based study. Lancet (London, England). 2006 Sep;368(9540):1005–11.

61. Mack MJ, Leon MB, Smith CR, Miller DC, Moses JW, Tuzcu EM, et al. 5-year outcomes of transcatheter aortic valve replacement or surgical aortic valve replacement for high surgical risk patients with aortic stenosis (PARTNER 1): A randomised controlled trial. Lancet. 2015;

62. Thiago L, Tsuji SR, Nyong J, Puga MES, Gois AFT, Macedo CR, et al. Statins for aortic valve stenosis. Cochrane Database Syst Rev [Internet]. 2016;(9). Available from: https://doi.org//10.1002/14651858.CD009571.pub2

63. Capoulade R, Clavel M-A, Mathieu P, Côté N, Dumesnil JG, Arsenault M, et al. Impact of hypertension and renin–angiotensin system inhibitors in aortic stenosis. Eur J Clin Invest [Internet]. 2013 Dec 1;43(12):1262–72. Available from: https://doi.org/10.1111/eci.12169

64. Kostyunin AE, Yuzhalin AE, Ovcharenko EA, Kutikhin AG. Development of calcific aortic valve disease: Do we know enough for new clinical trials? J Mol Cell Cardiol [Internet]. 2019;132:189–209. Available from: https://www.sciencedirect.com/science/article/pii/S0022282819301014

65. Cowell SJ, Newby DE, Prescott RJ, Bloomfield P, Reid J, Northridge DB, et al. A randomized trial of intensive lipid-lowering therapy in calcific aortic stenosis. N Engl J Med [Internet]. 2005;352(23):2389–97. Available from: http://www.ncbi.nlm.nih.gov/pubmed/15944423%5Cnhttp://www.nejm.org/doi/pdf/10.1056/NEJMoa043876

66. Gomel MA, Lee R, Grande-Allen KJ. Comparing the Role of Mechanical Forces in Vascular and Valvular Calcification Progression [Internet]. Vol. 5, Frontiers in Cardiovascular Medicine. 2019. p. 197. Available from: https://www.frontiersin.org/article/10.3389/fcvm.2018.00197

67. New SEP, Aikawa E. Molecular imaging insights into early inflammatory stages of arterial and aortic valve calcification. Circ Res. 2011;108(11):1381–91.

68. Hanley DA, Adachi JD, Bell A, Brown V. Denosumab: Mechanism of action and clinical outcomes. Int J Clin Pract. 2012;

69. Kaden JJ, Dempfle CE, Kiliç R, Sarikoç A, Hagl S, Lang S, et al. Influence of receptor activator of nuclear factor kappa B on human aortic valve myofibroblasts. Exp Mol Pathol. 2005;

70. Steinmetz M, Skowasch D, Wernert N, Welsch U, Preusse CJ, Welz A, et al. Differential profile of the OPG/RANKL/RANK-system in degenerative aortic native and bioprosthetic valves. J Heart Valve Dis. 2008;

71. Kaden JJ, Bickelhaupt S, Grobholz R, Haase KK, Sarikoc A, Kilic R, et al. Receptor activator of nuclear factor kappaB ligand and osteoprotegerin regulate aortic valve calcification. J Mol Cell Cardiol. 2004 Jan;36(1):57–66.

72. Clark CR, Bowler MA, Snider JC, Merryman WD. Targeting Cadherin-11 Prevents Notch1-Mediated Calcific Aortic Valve Disease. Circulation [Internet]. 2017 Jun 12;135(24):2448 LP – 2450. Available from: http://circ.ahajournals.org/content/135/24/2448.abstract

73. Stewart BF, Siscovick D, Lind BK, Gardin JM, Gottdiener JS, Smith VE, et al. Clinical factors associated with calcific aortic valve disease. J Am Coll Cardiol. 1997;

74. Hjortnaes J, Butcher J, Figueiredo J-L, Riccio M, Kohler RH, Kozloff KM, et al. Arterial and aortic valve calcification inversely correlates with osteoporotic bone remodelling: a role for inflammation. Eur Heart J [Internet]. 2010 Jul 2;31(16):1975–84. Available from: https://doi.org/10.1093/eurheartj/ehq237

75. Lampropoulos CE, Papaioannou I, D'Cruz DP. Osteoporosis - A risk factor for cardiovascular disease? Nature Reviews Rheumatology. 2012.

76. Parhami F, Tintut Y, Beamer WG, Gharavi N, Goodman W, Demer LL. Atherogenic high-fat diet reduces bone mineralization in mice. J Bone Miner Res. 2001;

77. Lerman DA, Prasad S, Alotti N. Denosumab could be a Potential Inhibitor of Valvular Interstitial Cells Calcification in vitro. Int J Cardiovasc Res [Internet]. 2016 Jan 3;5(1):10.4172/2324-8602.1000249. Available from: https://www.ncbi.nlm.nih.gov/pubmed/27468412

78. Pawade TA, Doris MK, Bing R, White AC, Forsyth L, Evans E, et al. Effect of denosumab or alendronic acid on the progression of aortic stenosis: a double-blind randomized controlled trial. Circulation. 2021;143(25):2418–27.

79. Gay A, Towler DA. Wnt signaling in cardiovascular disease: opportunities and challenges. Curr Opin Lipidol [Internet]. 9000;Publish Ah. Available from: http://journals.lww.com/co-lipidology/Fulltext/publishahead/Wnt_signaling_in_cardiovascular_disease__.99479.aspx

80. Rajamannan NM, Subramaniam M, Springett M, Sebo TC, Niekrasz M, McConnell JP, et

al. Atorvastatin inhibits hypercholesterolemia-induced cellular proliferation and bone matrix production in the rabbit aortic valve. Circulation. 2002;105(22):2660–5.

81. Caira FC, Stock SR, Gleason TG, McGee EC, Huang J, Bonow RO, et al. Human Degenerative Valve Disease Is Associated With Up-Regulation of Low-Density Lipoprotein Receptor-Related Protein 5 Receptor-Mediated Bone Formation. J Am Coll Cardiol. 2006;47(8):1707–12.

82. Yin YCY, Jan-Hung C, Ruogang Z, A. SC. Calcification by Valve Interstitial Cells Is Regulated by the Stiffness of the Extracellular Matrix. Arterioscler Thromb Vasc Biol [Internet]. 2009 Jun 1;29(6):936–42. Available from: https://doi.org/10.1161/ATVBAHA.108.182394

83. Mani A, Radhakrishnan J, Wang H, Mani A, Mani MA, Nelson-Williams C, et al. LRP6 mutation in a family with early coronary disease and metabolic risk factors. Science (80-). 2007;

84. Sarzani R, Salvi F, Bordicchia M, Guerra F, Battistoni I, Pagliariccio G, et al. Carotid artery atherosclerosis in hypertensive patients with a functional LDL receptor-related protein 6 gene variant. Nutr Metab Cardiovasc Dis. 2011;

85. Beazley KE, Deasey S, Lima F, Nurminskaya M V. Transglutaminase 2-mediated activation of β-catenin signaling has a critical role in warfarin-induced vascular calcification. Arterioscler Thromb Vasc Biol. 2012;

86. Hamersma H, Gardner J, Beighton P. The natural history of sclerosteosis. Clin Genet [Internet]. 2003 Mar 1;63(3):192–7. Available from: https://doi.org/10.1034/j.1399-0004.2003.00036.x

87. Brandenburg VM, Kramann R, Koos R, Krüger T, Schurgers L, Mühlenbruch G, et al. Relationship between sclerostin and cardiovascular calcification in hemodialysis patients: A cross-sectional study. BMC Nephrol. 2013;

88. Koos R, Brandenburg V, Mahnken AH, Schneider R, Dohmen G, Autschbach R, et al. Sclerostin as a potential novel biomarker for aortic valve calcification: an in-vivo and ex-vivo study. J Hear Valve Dis. 2013;22(0966-8519 (Print)):317–25.

89. Brandenburg VM, D'Haese P, Deck A, Mekahli D, Meijers B, Neven E, et al. From skeletal to cardiovascular disease in 12 steps-the evolution of sclerostin as a major player in CKD-MBD. Pediatr Nephrol [Internet]. 2016 Feb [cited 2016 Oct 7];31(2):195–206. Available from: http://www.ncbi.nlm.nih.gov/pubmed/25735207

90. Zhu D, Mackenzie NCW, Millán JL, Farquharson C, MacRae VE. The Appearance and Modulation of Osteocyte Marker Expression during Calcification of Vascular Smooth Muscle Cells. Zoccali C, editor. PLoS One [Internet]. 2011 May 17;6(5):e19595. Available from: http://www.ncbi.nlm.nih.gov/pmc/articles/PMC3096630/

91. Didangelos A, Yin X, Mandal K, Baumert M, Jahangiri M, Mayr M. Proteomics Characterization of Extracellular Space Components in the Human Aorta. Mol & Cell Proteomics [Internet]. 2010 Sep 1;9(9):2048 LP – 2062. Available from: http://www.mcponline.org/content/9/9/2048.abstract

92. Krishna SM, Seto S-W, Jose RJ, Li J, Morton SK, Biros E, et al. Wnt Signaling Pathway Inhibitor Sclerostin Inhibits Angiotensin II-Induced Aortic Aneurysm and Atherosclerosis. Arterioscler Thromb Vasc Biol. 2016 Dec;

93. Hampson G, Edwards S, Conroy S, Blake GM, Fogelman I, Frost ML. The relationship between inhibitors of the Wnt signalling pathway (Dickkopf-1(DKK1) and sclerostin), bone mineral density, vascular calcification and arterial stiffness in post-menopausal women. Bone. 2013;

94. Brandenburg VM, Kramann R, Koos R, Krüger T, Schurgers L, Mühlenbruch G, et al. Relationship between sclerostin and cardiovascular calcification in hemodialysis patients: a cross-sectional study. BMC Nephrol [Internet]. 2013;14:219. Available from: http://www.pubmedcentral.nih.gov/articlerender.fcgi?artid=3851854&tool=pmcentrez&rendertype=abstract

95. Register TC, Hruska KA, Divers J, Bowden DW, Palmer ND, Carr JJ, et al. Sclerostin is positively associated with bone mineral density in men and women and negatively associated with carotid calcified atherosclerotic plaque in men from the African American-diabetes heart study. J Clin Endocrinol Metab. 2014;

96. Claes KJ, Viaene L, Heye S, Meijers B, D'Haese P, Evenepoel P. Sclerostin: Another vascular calcification inhibitor? J Clin Endocrinol Metab. 2013;

97. Kanbay M, Solak Y, Siriopol D, Aslan G, Afsar B, Yazici D, et al. Sclerostin, cardiovascular disease and mortality: a systematic review and meta-analysis. Int Urol Nephrol [Internet]. 2016;48(12):2029–42. Available from: https://doi.org/10.1007/s11255-016-1387-8

98. van Bezooijen RL, Roelen BAJ, Visser A, van der Wee-Pals L, de Wilt E, Karperien M, et al. Sclerostin Is an Osteocyte-expressed Negative Regulator of Bone Formation, But Not a Classical BMP Antagonist. J Exp Med [Internet]. 2004 Mar 15;199(6):805 LP – 814. Available from: http://jem.rupress.org/content/199/6/805.abstract

99. Delgado-Calle J, Sato AY, Bellido T. Role and mechanism of action of sclerostin in bone. Bone [Internet]. 2017;96:29–37. Available from: http://www.sciencedirect.com/science/article/pii/S8756328216302976

100. Krishnan V, Bryant HU, MacDougald OA. Regulation of bone mass by Wnt signaling. J Clin Invest [Internet]. 2006 May 1;116(5):1202–9. Available from: https://doi.org/10.1172/JCI28551

101. Leupin O, Piters E, Halleux C, Hu S, Kramer I, Morvan F, et al. Bone overgrowth-associated mutations in the LRP4 gene impair sclerostin facilitator function. J Biol Chem. 2011;286(22):19489–500.

102. Fijalkowski I, Geets E, Steenackers E, Van Hoof V, Ramos FJ, Mortier G, et al. A Novel Domain-Specific Mutation in a Sclerosteosis Patient Suggests a Role of LRP4 as an Anchor for Sclerostin in Human Bone. J Bone Miner Res. 2016;

103. Chang M-K, Kramer I, Huber T, Kinzel B, Guth-Gundel S, Leupin O, et al. Disruption of Lrp4 function by genetic deletion or pharmacological blockade increases bone mass and

serum sclerostin levels. Proc Natl Acad Sci U S A [Internet]. 2014;111(48):E5187-95. Available from: http://www.pubmedcentral.nih.gov/articlerender.fcgi?artid=4260537&tool=pmcentrez&rendertype=abstract

104. Johnson ML, Rajamannan N. Diseases of Wnt signaling. Rev Endocr Metab Disord. 2006 Jun;7(1–2):41–9.

105. Holdsworth G, Slocombe P, Doyle C, Sweeney B, Veverka V, Le Riche K, et al. Characterization of the interaction of sclerostin with the low density lipoprotein receptor-related protein (LRP) family of wnt co-receptors. J Biol Chem. 2012;

106. Rubin CT, Lanyon LE. Regulation of bone mass by mechanical strain magnitude. Calcif Tissue Int. 1985;

107. Bonewald LF, Johnson ML. Osteocytes, mechanosensing and Wnt signaling. Vol. 42, Bone. 2008. p. 606–15.

108. Frost HM. Skeletal structural adaptations to mechanical usage (SATMU): 1. Redefining Wolff's Law: The bone modeling problem. Anat Rec. 1990;

109. Robling AG, Niziolek PJ, Baldridge LA, Condon KW, Allen MR, Alam I, et al. Mechanical stimulation of bone in vivo reduces osteocyte expression of Sost/sclerostin. J Biol Chem [Internet]. 2008 Feb 29 [cited 2016 Oct 7];283(9):5866–75. Available from: http://www.ncbi.nlm.nih.gov/pubmed/18089564

110. Robling AG, Niziolek PJ, Baldridge LA, Condon KW, Allen MR, Alam I, et al. Mechanical stimulation of bone in vivo reduces osteocyte expression of Sost/sclerostin. J Biol Chem. 2008;

111. Wijenayaka AR, Kogawa M, Lim HP, Bonewald LF, Findlay DM, Atkins GJ. Sclerostin Stimulates Osteocyte Support of Osteoclast Activity by a RANKL-Dependent Pathway. PLoS One [Internet]. 2011 Oct 4;6(10):e25900. Available from: https://doi.org/10.1371/journal.pone.0025900

112. Lin C, Jiang X, Dai Z, Guo X, Weng T, Wang J, et al. Sclerostin mediates bone response to mechanical unloading through antagonizing Wnt/β-catenin signaling. J Bone Miner Res. 2009;

113. Tu X, Rhee Y, Condon KW, Bivi N, Allen MR, Dwyer D, et al. Sost downregulation and local Wnt signaling are required for the osteogenic response to mechanical loading. Bone. 2012;

114. Suen PK, Qin L. Sclerostin, an emerging therapeutic target for treating osteoporosis and osteoporotic fracture: A general review. Journal of Orthopaedic Translation. 2016.

115. Truswell AS. OSTEOPETROSIS WITH SYNDACTYLY. J Bone Joint Surg Br [Internet]. 1958 May 1;40-B(2):208–18. Available from: https://doi.org/10.1302/0301-620X.40B2.208

116. van Lierop AH, Appelman-Dijkstra NM, Papapoulos SE. Sclerostin deficiency in humans. Bone [Internet]. 2017;96:51–62. Available from:

http://www.sciencedirect.com/science/article/pii/S8756328216303003

117. BEIGHTON P, DURR L, HAMERSMA H. The Clinical Features of Sclerosteosis: A Review of the Manifestations in Twenty-Five Affected Individuals. Ann Intern Med [Internet]. 1976 Apr 1;84(4):393–7. Available from: https://doi.org/10.7326/0003-4819-84-4-393

118. Potgieter JM, Swanepoel DW, Heinze BM, Hofmeyr LM, Burger AAS, Hamersma H. An auditory profile of sclerosteosis. J Laryngol & Otol [Internet]. 2014/03/19. 2014;128(4):336–44. Available from: https://www.cambridge.org/core/article/an-auditory-profile-of-sclerosteosis/55F062183C8DD207C5F7FD1A233BD38F

119. Beighton P, Barnard A, Hamersma H, Wouden A van der. The syndromic status of sclerosteosis and van Buchem disease. Clin Genet [Internet]. 1984 Feb 1;25(2):175–81. Available from: https://doi.org/10.1111/j.1399-0004.1984.tb00481.x

120. Plessis JJ du. Sclerosteosis: neurosurgical experience with 14 cases. J Neurosurg [Internet]. 1993;78(3):388–92. Available from: https://thejns.org/view/journals/j-neurosurg/78/3/article-p388.xml

121. van Lierop AH, Hamdy NAT, Hamersma H, van Bezooijen RL, Power J, Loveridge N, et al. Patients with sclerosteosis and disease carriers: Human models of the effect of sclerostin on bone turnover. J Bone Miner Res [Internet]. 2011 Dec 1;26(12):2804–11. Available from: https://doi.org/10.1002/jbmr.474

122. van Buchem FSP, Hadders HN, Ubbens R. An uncommon familial systemic disease of the skeleton: Hyperostosis corticalis generalisata familiaris. Acta radiol [Internet]. 1955 Aug 1;44(2):109–20. Available from: https://doi.org/10.3109/00016925509170789

123. van Lierop AH, Hamdy NAT, van Egmond ME, Bakker E, Dikkers FG, Papapoulos SE. Van Buchem disease: Clinical, biochemical, and densitometric features of patients and disease carriers. J Bone Miner Res [Internet]. 2013 Apr 1;28(4):848–54. Available from: https://doi.org/10.1002/jbmr.1794

124. van Lierop AHJM, Hamdy NAT, Papapoulos SE. Glucocorticoids are not always deleterious for bone. J Bone Miner Res [Internet]. 2010 Dec 1;25(12):2796–800. Available from: https://doi.org/10.1002/jbmr.151

125. Van Hul W, Balemans W, Van Hul E, Dikkers FG, Obee H, Stokroos RJ, et al. Van Buchem Disease (Hyperostosis Corticalis Generalisata) Maps to Chromosome 17q12-q21. Am J Hum Genet [Internet]. 1998;62(2):391–9. Available from: http://www.sciencedirect.com/science/article/pii/S0002929707635046

126. Balemans W, Van Den Ende J, Freire Paes-Alves A, Dikkers FG, Willems PJ, Vanhoenacker F, et al. Localization of the Gene for Sclerosteosis to the van Buchem Disease–Gene Region on Chromosome 17q12–q21. Am J Hum Genet [Internet]. 1999;64(6):1661–9. Available from: http://www.sciencedirect.com/science/article/pii/S0002929707636684

127. Brunkow ME, Gardner JC, Van Ness J, Paeper BW, Kovacevich BR, Proll S, et al. Bone Dysplasia Sclerosteosis Results from Loss of the SOST Gene Product, a Novel Cystine

Knot–Containing Protein. Am J Hum Genet [Internet]. 2001;68(3):577–89. Available from: http://www.sciencedirect.com/science/article/pii/S0002929707630985

128. Paes-Alves AF, Vickery B, Lacza C, Stratakis C, Foernzler D, Van Hul E, et al. Increased bone density in sclerosteosis is due to the deficiency of a novel secreted protein (SOST). Hum Mol Genet [Internet]. 2001 Mar 1;10(5):537–44. Available from: https://doi.org/10.1093/hmg/10.5.537

129. Staehling-Hampton K, Proll S, Paeper BW, Zhao L, Charmley P, Brown A, et al. A 52-kb deletion in the SOST-MEOX1 intergenic region on 17q12-q21 is associated with van Buchem disease in the Dutch population. Am J Med Genet [Internet]. 2002 Jun 15;110(2):144–52. Available from: https://doi.org/10.1002/ajmg.10401

130. Balemans W, Patel N, Ebeling M, Van Hul E, Wuyts W, Lacza C, et al. Identification of a 52 kb deletion downstream of the SOST gene in patients with van Buchem disease. J Med Genet [Internet]. 2002 Feb 1;39(2):91 LP – 97. Available from: http://jmg.bmj.com/content/39/2/91.abstract

131. Loots GG, Kneissel M, Keller H, Baptist M, Chang J, Collette NM, et al. Genomic deletion of a long-range bone enhancer misregulates sclerostin in Van Buchem disease. Genome Res. 2005;15(7):928–35.

132. Li X, Ominsky MS, Niu QT, Sun N, Daugherty B, D'Agostin D, et al. Targeted deletion of the sclerostin gene in mice results in increased bone formation and bone strength. J Bone Miner Res. 2008;

133. Sebastian A, Loots GG. Genetics of Sost/SOST in sclerosteosis and van Buchem disease animal models. Metabolism [Internet]. 2018;80:38–47. Available from: http://www.sciencedirect.com/science/article/pii/S0026049517302792

134. Tian X, Jee WSS, Li X, Paszty C, Ke HZ. Sclerostin antibody increases bone mass by stimulating bone formation and inhibiting bone resorption in a hindlimb-immobilization rat model. Bone. 2011;

135. Spatz JM, Ellman R, Cloutier AM, Louis L, Van Vliet M, Suva LJ, et al. Sclerostin antibody inhibits skeletal deterioration due to reduced mechanical loading. J Bone Miner Res. 2013;

136. Ji M, Yu Q. Primary osteoporosis in postmenopausal women. Maturitas. 2015;

137. Li X, Ominsky MS, Warmington KS, Morony S, Gong J, Cao J, et al. Sclerostin antibody treatment increases bone formation, bone mass, and bone strength in a rat model of postmenopausal osteoporosis. J Bone Miner Res. 2009;

138. Demontiero O, Vidal C, Duque G. Aging and bone loss: New insights for the clinician. Therapeutic Advances in Musculoskeletal Disease. 2012.

139. Russow G, Jahn D, Appelt J, Märdian S, Tsitsilonis S, Keller J. Anabolic Therapies in Osteoporosis and Bone Regeneration. Int J Mol Sci [Internet]. 2018 Dec 26;20(1):83. Available from: https://www.ncbi.nlm.nih.gov/pubmed/30587780

140. Li X, Warmington KS, Niu QT, Asuncion FJ, Barrero M, Grisanti M, et al. Inhibition of

sclerostin by monoclonal antibody increases bone formation, bone mass, and bone strength in aged male rats. J Bone Miner Res. 2010;

141. Tian XY, Setterberg RB, Li X, Paszty C, Ke HZ, Jee WSS. Treatment with a sclerostin antibody increases cancellous bone formation and bone mass regardless of marrow composition in adult female rats. Bone. 2010;

142. Agholme F, Li X, Isaksson H, Ke HZ, Aspenberg P. Sclerostin antibody treatment enhances metaphyseal bone healing in rats. J Bone Miner Res. 2010;

143. Suen PK, He YX, Chow DHK, Huang L, Li C, Ke HZ, et al. Sclerostin monoclonal antibody enhanced bone fracture healing in an open osteotomy model in rats. J Orthop Res. 2014;

144. McDonald MM, Morse A, Mikulec K, Peacock L, Yu N, Baldock PA, et al. Inhibition of sclerostin by systemic treatment with sclerostin antibody enhances healing of proximal tibial defects in ovariectomized rats. J Orthop Res. 2012;

145. Ominsky MS, Li C, Li X, Tan HL, Lee E, Barrero M, et al. Inhibition of sclerostin by monoclonal antibody enhances bone healing and improves bone density and strength of nonfractured bones. J Bone Miner Res. 2011;

146. Ominsky MS, Vlasseros F, Jolette J, Smith SY, Stouch B, Doellgast G, et al. Two doses of sclerostin antibody in cynomolgus monkeys increases bone formation, bone mineral density, and bone strength. J Bone Miner Res. 2010;

147. Padhi D, Jang G, Stouch B, Fang L, Posvar E. Single-dose, placebo-controlled, randomized study of AMG 785, a sclerostin monoclonal antibody. J Bone Miner Res. 2011;

148. Padhi D, Allison M, Kivitz AJ, Gutierrez MJ, Stouch B, Wang C, et al. Multiple doses of sclerostin antibody romosozumab in healthy men and postmenopausal women with low bone mass: A randomized, double-blind, placebo-controlled study. J Clin Pharmacol. 2014;

149. Drake MT, Clarke BL, Khosla S. Bisphosphonates: Mechanism of action and role in clinical practice. Mayo Clinic Proceedings. 2008.

150. McClung MR, Grauer A, Boonen S, Bolognese MA, Brown JP, Diez-Perez A, et al. Romosozumab in Postmenopausal Women with Low Bone Mineral Density. N Engl J Med [Internet]. 2014 Jan 1;370(5):412–20. Available from: https://doi.org/10.1056/NEJMoa1305224

151. Cosman F, Crittenden DB, Adachi JD, Binkley N, Czerwinski E, Ferrari S, et al. Romosozumab Treatment in Postmenopausal Women with Osteoporosis. N Engl J Med. 2016;

152. Langdahl BL, Libanati C, Crittenden DB, Bolognese MA, Brown JP, Daizadeh NS, et al. Romosozumab (sclerostin monoclonal antibody) versus teriparatide in postmenopausal women with osteoporosis transitioning from oral bisphosphonate therapy: a randomised, open-label, phase 3 trial. Lancet. 2017;

153. Mullard A. Calls grow to tap the gold mine of human genetic knockouts. Nat Rev Drug Discov. 2017;

154. Compton JT, Lee FY. A review of osteocyte function and the emerging importance of sclerostin. J Bone Joint Surg Am [Internet]. 2014 Oct 1;96(19):1659–68. Available from: https://pubmed.ncbi.nlm.nih.gov/25274791

155. Beighton P. Sclerosteosis. J Med Genet [Internet]. 1988 Mar;25(3):200–3. Available from: https://pubmed.ncbi.nlm.nih.gov/3351908

156. Li X, Zhang Y, Kang H, Liu W, Liu P, Zhang J, et al. Sclerostin Binds to LRP5/6 and Antagonizes Canonical Wnt Signaling *. J Biol Chem [Internet]. 2005 May 20;280(20):19883–7. Available from: https://doi.org/10.1074/jbc.M413274200

157. Ellies DL, Viviano B, McCarthy J, Rey J-P, Itasaki N, Saunders S, et al. Bone Density Ligand, Sclerostin, Directly Interacts With LRP5 but Not LRP5G171V to Modulate Wnt Activity. J Bone Miner Res [Internet]. 2006 Nov 1;21(11):1738–49. Available from: https://doi.org/10.1359/jbmr.060810

158. Lewiecki EM, Dinavahi R V, Lazaretti-Castro M, Ebeling PR, Adachi JD, Miyauchi A, et al. One Year of Romosozumab Followed by Two Years of Denosumab Maintains Fracture Risk Reductions: Results of the FRAME Extension Study. J Bone Miner Res [Internet]. 2019 Mar 1;34(3):419–28. Available from: https://doi.org/10.1002/jbmr.3622

159. Lewiecki EM, Blicharski T, Goemaere S, Lippuner K, Meisner PD, Miller PD, et al. A Phase III Randomized Placebo-Controlled Trial to Evaluate Efficacy and Safety of Romosozumab in Men With Osteoporosis. J Clin Endocrinol Metab [Internet]. 2018 Sep 1;103(9):3183–93. Available from: https://doi.org/10.1210/jc.2017-02163

160. Dutta P, Lincoln J. Calcific Aortic Valve Disease: a Developmental Biology Perspective. Curr Cardiol Rep [Internet]. 2018;20(4):21. Available from: https://doi.org/10.1007/s11886-018-0968-9

161. Economides AN, Frendewey D, Yang P, Dominguez MG, Dore AT, Lobov IB, et al. Conditionals by inversion provide a universal method for the generation of conditional alleles. Proc Natl Acad Sci [Internet]. 2013 Aug 20;110(34):E3179 LP-E3188. Available from: http://www.pnas.org/content/110/34/E3179.abstract

162. Ferruzzi J, Di Achille P, Tellides G, Humphrey JD. Combining in vivo and in vitro biomechanical data reveals key roles of perivascular tethering in central artery function. PLoS One [Internet]. 2018 Sep 7;13(9):e0201379. Available from: https://doi.org/10.1371/journal.pone.0201379

163. Bersi MR, Khosravi R, Wujciak AJ, Harrison DG, Humphrey JD. Differential cell-matrix mechanoadaptations and inflammation drive regional propensities to aortic fibrosis, aneurysm or dissection in hypertension. J R Soc Interface [Internet]. 2017 Nov 30;14(136):20170327. Available from: https://doi.org/10.1098/rsif.2017.0327

164. Snider JC, Riley LA, Mallory NT, Bersi MR, Umbarkar P, Gautam R, et al. Targeting 5-HT2B Receptor Signaling Prevents Border Zone Expansion and Improves Microstructural Remodeling After Myocardial Infarction. Circulation [Internet]. 2021 Mar

30;143(13):1317–30. Available from: https://doi.org/10.1161/CIRCULATIONAHA.120.051517

165. Joll II JE, Clark CR, Peters CS, Raddatz MA, Bersi MR, Merryman WD. Genetic ablation of serotonin receptor 2B improves aortic valve hemodynamics of Notch1 heterozygous mice in a high-cholesterol diet model. PLoS One [Internet]. 2020 Nov 25;15(11):e0238407. Available from: https://doi.org/10.1371/journal.pone.0238407

166. Wienert S, Heim D, Saeger K, Stenzinger A, Beil M, Hufnagl P, et al. Detection and Segmentation of Cell Nuclei in Virtual Microscopy Images: A Minimum-Model Approach. Sci Rep [Internet]. 2012;2(1):503. Available from: https://doi.org/10.1038/srep00503

167. Lindman BR, Merryman WD. Unloading the Stenotic Path to Identifying Medical Therapy for Calcific Aortic Valve Disease. Circulation [Internet]. 2021 Apr 13;143(15):1455–7. Available from: https://doi.org/10.1161/CIRCULATIONAHA.120.052531

168. Wright NC, Looker AC, Saag KG, Curtis JR, Delzell ES, Randall S, et al. The Recent Prevalence of Osteoporosis and Low Bone Mass in the United States Based on Bone Mineral Density at the Femoral Neck or Lumbar Spine. J Bone Miner Res [Internet]. 2014 Nov 1;29(11):2520–6. Available from: https://doi.org/10.1002/jbmr.2269

169. Teng GG, Warriner A, Curtis JR, Saag KG. Improving quality of care in osteoporosis: Opportunities and challenges. Curr Rheumatol Rep [Internet]. 2008;10(2):123. Available from: https://doi.org/10.1007/s11926-008-0022-9

170. Qaseem A, Forciea MA, McLean RM, Denberg TD. Treatment of Low Bone Density or Osteoporosis to Prevent Fractures in Men and Women: A Clinical Practice Guideline Update From the American College of Physicians. Ann Intern Med [Internet]. 2017 May 9;166(11):818–39. Available from: https://www.acpjournals.org/doi/abs/10.7326/M15-1361

171. Tu KN, Lie JD, Wan CKV, Cameron M, Austel AG, Nguyen JK, et al. Osteoporosis: A Review of Treatment Options. P T [Internet]. 2018 Feb;43(2):92–104. Available from: https://www.ncbi.nlm.nih.gov/pubmed/29386866

172. van Bezooijen RL, DeRuiter MC, Vilain N, Monteiro RM, Visser A, van der Wee-Pals L, et al. SOST expression is restricted to the great arteries during embryonic and neonatal cardiovascular development. Dev Dyn [Internet]. 2007 Feb 1;236(2):606–12. Available from: https://doi.org/10.1002/dvdy.21054

173. Otto CM, Kuusisto J, Reichenbach DD, Gown AM, O'Brien KD. Characterization of the early lesion of "degenerative" valvular aortic stenosis. Histological and immunohistochemical studies. Circulation [Internet]. 1994;90(2):844–53. Available from: http://circ.ahajournals.org/cgi/doi/10.1161/01.CIR.90.2.844

174. Lee SH, Choi J-H. Involvement of inflammatory responses in the early development of calcific aortic valve disease: lessons from statin therapy. Animal Cells Syst (Seoul) [Internet]. 2018 Sep 28;22(6):390–9. Available from: https://www.ncbi.nlm.nih.gov/pubmed/30533261

175. Marie-Claude D, Elise R, Yves D, Jacques C, Marie A. A High Fat/High Carbohydrate Diet Induces Aortic Valve Disease in C57BL/6J Mice. J Am Coll Cardiol [Internet]. 2006 Feb 21;47(4):850–5. Available from: https://doi.org/10.1016/j.jacc.2005.09.049

176. Dutta S, Sengupta P. Men and mice: Relating their ages. Life Sci [Internet]. 2016;152:244–8. Available from: https://www.sciencedirect.com/science/article/pii/S0024320515300527

177. Krumlauf R. Hox genes in vertebrate development. Cell [Internet]. 1994;78(2):191–201. Available from: https://www.sciencedirect.com/science/article/pii/0092867494902909

178. Roux M, Zaffran S. Hox Genes in Cardiovascular Development and Diseases. Vol. 4, Journal of Developmental Biology . 2016.

179. Makki N, Capecchi MR. Cardiovascular defects in a mouse model of HOXA1 syndrome. Hum Mol Genet [Internet]. 2012 Jan 1;21(1):26–31. Available from: https://doi.org/10.1093/hmg/ddr434

180. Tischfield MA, Bosley TM, Salih MAM, Alorainy IA, Sener EC, Nester MJ, et al. Homozygous HOXA1 mutations disrupt human brainstem, inner ear, cardiovascular and cognitive development. Nat Genet [Internet]. 2005;37(10):1035–7. Available from: https://doi.org/10.1038/ng1636

181. Chisaka O, Capecchi MR. Regionally restricted developmental defects resulting from targeted disruption of the mouse homeobox gene hox-1.5. Nature [Internet]. 1991;350(6318):473–9. Available from: https://doi.org/10.1038/350473a0

182. Murphy S, Kochanek K, Xu J, Arias E. Mortality in the United States, 2020. Natl Cent Heal Stat [Internet]. 2021;427. Available from: https://www.cdc.gov/nchs/data/databriefs/db427.pdf

183. Danielsen R, Aspelund T, Harris TB, Gudnason V. The prevalence of aortic stenosis in the elderly in Iceland and predictions for the coming decades: the AGES-Reykjavík study. Int J Cardiol [Internet]. 2014/08/15. 2014 Oct 20;176(3):916–22. Available from: https://pubmed.ncbi.nlm.nih.gov/25171970

184. Makkar RR, Thourani VH, Mack MJ, Kodali SK, Kapadia S, Webb JG, et al. Five-Year Outcomes of Transcatheter or Surgical Aortic-Valve Replacement. N Engl J Med [Internet]. 2020 Jan 29;382(9):799–809. Available from: https://doi.org/10.1056/NEJMoa1910555

185. Donato M, Ferri N, Lupo MG, Faggin E, Rattazzi M. Current Evidence and Future Perspectives on Pharmacological Treatment of Calcific Aortic Valve Stenosis. Vol. 21, International Journal of Molecular Sciences . 2020.

186. Goliasch G, Lang IM. Impact of sex on the management and outcome of aortic stenosis patients: a female aortic valve stenosis paradox, and a call for personalized treatments? Eur Heart J [Internet]. 2021 Jul 15;42(27):2692–4. Available from: https://pubmed.ncbi.nlm.nih.gov/34128046

187. Bienjonetti-Boudreau D, Fleury M-A, Voisine M, Paquin A, Chouinard I, Tailleur M, et al. Impact of sex on the management and outcome of aortic stenosis patients. Eur Heart J

[Internet]. 2021 Jul 14;42(27):2683–91. Available from: https://doi.org/10.1093/eurheartj/ehab242

188. Raddatz MA, Gonzales HM, Farber-Eger E, Wells QS, Lindman BR, Merryman WD. Characterisation of aortic stenosis severity: a retrospective analysis of echocardiography reports in a clinical laboratory. Open Hear [Internet]. 2020 Aug 1;7(2):e001331. Available from: http://openheart.bmj.com/content/7/2/e001331.abstract

189. Aggarwal SR, Clavel M-A, Messika-Zeitoun D, Cueff C, Malouf J, Araoz PA, et al. Sex Differences in Aortic Valve Calcification Measured by Multidetector Computed Tomography in Aortic Stenosis. Circ Cardiovasc Imaging [Internet]. 2013 Jan 1;6(1):40–7. Available from: https://doi.org/10.1161/CIRCIMAGING.112.980052

190. Louis S, Nancy C, François D, Patrick M, Christian C, Sylvain T, et al. Sex-Related Discordance Between Aortic Valve Calcification and Hemodynamic Severity of Aortic Stenosis. Circ Res [Internet]. 2017 Feb 17;120(4):681–91. Available from: https://doi.org/10.1161/CIRCRESAHA.116.309306

191. Miller JD, Weiss RM, Heistad DD, Towler DA. Calcific Aortic Valve Stenosis: Methods, Models, and Mechanisms. Circ Res [Internet]. 2011 May 27;108(11):1392–412. Available from: https://doi.org/10.1161/CIRCRESAHA.110.234138

192. Garg V, Muth AN, Ransom JF, Schluterman MK, Barnes R, King IN, et al. Mutations in NOTCH1 cause aortic valve disease. Nature. 2005;437(7056):270–4.

193. Komori T. Animal models for osteoporosis. Eur J Pharmacol [Internet]. 2015;759:287–94. Available from: https://www.sciencedirect.com/science/article/pii/S0014299915002435

194. Tankó LB, Christiansen C, Cox DA, Geiger MJ, McNabb MA, Cummings SR. Relationship Between Osteoporosis and Cardiovascular Disease in Postmenopausal Women. J Bone Miner Res [Internet]. 2005 Nov 1;20(11):1912–20. Available from: https://doi.org/10.1359/JBMR.050711

195. Rivera CM, Grossardt BR, Rhodes DJ, Brown Jr RD, Roger VL, Melton 3rd LJ, et al. Increased cardiovascular mortality after early bilateral oophorectomy. Menopause [Internet]. 2009;16(1):15–23. Available from: https://pubmed.ncbi.nlm.nih.gov/19034050

196. Schroer AK, Bersi MR, Clark CR, Zhang Q, Sanders LH, Hatzopoulos AK, et al. Cadherin-11 blockade reduces inflammation-driven fibrotic remodeling and improves outcomes after myocardial infarction. JCI Insight [Internet]. 2019 Sep 19;4(18). Available from: https://doi.org/10.1172/jci.insight.131545

197. Baker L, Meldrum KK, Wang M, Sankula R, Vanam R, Raiesdana A, et al. The role of estrogen in cardiovascular disease. J Surg Res [Internet]. 2003;115(2):325–44. Available from: https://www.sciencedirect.com/science/article/pii/S0022480403002154

198. Drolet M-C, Lachance D, Plante E, Roussel E, Couet J, Arsenault M. Gender-related differences in left ventricular remodeling in chronic severe aortic valve regurgitation in rats. J Heart Valve Dis. 2006;

199. Dannenberg AL, Levy D, Garrison RJ. Impact of age on echocardiographic left ventricular mass in a healthy population (the Framingham study). Am J Cardiol [Internet].

1989;64(16):1066–8. Available from: https://www.sciencedirect.com/science/article/pii/0002914989908163

200. Rai V, Sharma P, Agrawal S, Agrawal DK. Relevance of mouse models of cardiac fibrosis and hypertrophy in cardiac research. Mol Cell Biochem. 2016;424(1–2):123–45.

201. Pérez-Castrillon JL, Justo I, Sanz-Cantalapiedra A, Pueyo C, Hernandez G, Dueñas A. Effect of the antihypertensive treatment on the bone mineral density and osteoporotic fracture. Curr Hypertens Rev. 2005;1(1):61–6.

202. Walker GA, Masters KS, Shah DN, Anseth KS, Leinwand LA. Valvular myofibroblast activation by transforming growth factor-β: Implications for pathological extracellular matrix remodeling in heart valve disease. Circ Res. 2004;95(3):253–60.

203. R. ME, Francis G, Carol R, Robert Z, G. KM, S. KF. Bone Formation and Inflammation in Cardiac Valves. Circulation [Internet]. 2001 Mar 20;103(11):1522–8. Available from: https://doi.org/10.1161/01.CIR.103.11.1522

204. Miller JD, Weiss RM, Serrano KM, Castaneda LE, Brooks RM, Zimmerman K, et al. Evidence for active regulation of pro-osteogenic signaling in advanced aortic valve disease. Arterioscler Thromb Vasc Biol. 2010;30(12):2482–6.

205. Joll JE, Merryman WD. Improving programming content delivery in an introductory biomechanics course using a blended classroom approach. In: 2021 ASEE Virtual Annual Conference Content Access. 2021.

206. Allen IE, Seaman J. Changing course: Ten years of tracking online education in the United States. ERIC; 2013.

207. Means B, Toyama Y, Murphy R, Bakia M, Jones K. Evaluation of evidence-based practices in online learning: A meta-analysis and review of online learning studies. 2009;

208. Elias J, Troop D, Wescott D. Here's Our List of Colleges' Reopening Models. The Chronicle of Higher Education [Internet]. 2020 Oct; Available from: https://www.chronicle.com/article/Here-s-a-List-of-Colleges-/248626?&bc_nonce=fllmqr7wyydsu3uowtdo1m&cid=reg_wall_signup

209. Kožuško J, Dietrich H, Abdel-Haq A, Weichelt C, Hebestadt S, Kuß J, et al. Benefits of Blended Learning in Biomedical Engineering. 2013;58(SI-1-Track-R). Available from: https://doi.org/10.1515/bmt-2013-4414

210. Kozusko J, Abdel-Haq A, Kuß J, Morgenstern U, Bartels A. Enhanced laboratory exercises for biomedical engineering courses. In: International Conference on Education and e-Learning Innovations. 2012. p. 1–6.

211. Ożadowicz A. Modified Blended Learning in Engineering Higher Education during the COVID-19 Lockdown—Building Automation Courses Case Study. Vol. 10, Education Sciences . 2020.

212. Martínez-Caro E, Campuzano-Bolarín F. Factors affecting students' satisfaction in engineering disciplines: traditional vs. blended approaches. Eur J Eng Educ [Internet]. 2011 Oct 1;36(5):473–83. Available from: https://doi.org/10.1080/03043797.2011.619647

213. Kimmel S. Grading Rubric for Programming Problems [Internet]. ShelbyKimmel.com. Available from: http://shelbykimmel.com/Documents/Teaching/Templates/ProgramGrading.pdf

214. Lin JT, Lane JM. Osteoporosis: A Review. Clin Orthop Relat Res [Internet]. 2004;425. Available from: https://journals.lww.com/clinorthop/Fulltext/2004/08000/Osteoporosis__A_Review.17.aspx

215. Ross Jr J, Braunwald E. Aortic stenosis. Circulation. 1968;38(1s5):V–61.

216. Braunwald E. Aortic Stenosis. Circulation [Internet]. 2018 May 15;137(20):2099–100. Available from: https://doi.org/10.1161/CIRCULATIONAHA.118.033408

217. Sider KL, Blaser MC, Simmons CA. Animal Models of Calcific Aortic Valve Disease. Aikawa E, editor. Int J Inflam [Internet]. 2011;2011:364310. Available from: https://doi.org/10.4061/2011/364310

218. Yu M, Zhan J, Zhang H. HOX family transcription factors: related signaling pathways and post-translational modifications in cancer. Cell Signal. 2020;66:109469.

219. Hasenfuss G. Animal models of human cardiovascular disease, heart failure and hypertrophy. Cardiovasc Res [Internet]. 1998 Jul 1;39(1):60–76. Available from: https://doi.org/10.1016/S0008-6363(98)00110-2

220. Niepmann ST, Steffen E, Zietzer A, Adam M, Nordsiek J, Gyamfi-Poku I, et al. Graded murine wire-induced aortic valve stenosis model mimics human functional and morphological disease phenotype. Clin Res Cardiol [Internet]. 2019; Available from: https://doi.org/10.1007/s00392-019-01413-1

APPENDIX

Tables

Target	Forward primer	Reverse primer
Gapdh	atgacaatgaatacggctacag	tctcttgctcagtgtccttg
Hoxa1	ccaccagggttatgctggg	cgtggagaggggataaggagtta
Hoxa3	tcagcgatctacggtggcta	gaggcaaaggtggttcaccc
Hoxa7	tatgtgaacgcgctttttagca	gggggctgttgacattgtataa
Hoxb2	gcctacaccaacacgcaact	cggcacaggtacttattgaagtg
Hoxd3	atactacgagaacccaggactc	caggtctcatacagctaccattg

Table A.4.1. Primer sequences used for RT-qPCR analysis.

			Peak Velocity (cm/s)			Mean Gradient (mmHg)			Ejection Fraction (%)			Left Ventricle Mass (mg)		
			Months of age			Months of age			Months of age			Months of age		
ID	Sex	Genotype	4	9	12	4	9	12	4	9	12	4	9	12
3175 - 3635	M	WT	192.96	207.54	163.42	3.47	3.54	2.09	41.32	43.97	46.47	118.23	125.10	127.11
3176 - 3637 - 8398	M	WT	188.98	318.83	484.59	3.70	11.02	24.35	59.70	61.45	42.40	103.97	166.63	219.84
3177	M	WT	190.88	147.21	206.62	3.32	1.72	3.53	45.58	45.42	46.02	101.65	116.88	147.21
3181 - 9573	M	WT	191.99	115.54	122.13	3.86	1.08	1.25	53.55	51.59	37.47	101.30	110.17	109.97
3178 - 3636	F	WT	98.61	120.45	105.38	0.90	2.22	1.58	42.52	46.19	50.98	81.53	116.62	141.12
3130	F	WT	89.36	102.92	151.66	0.87	0.87	3.23	55.65	57.62	52.75	82.13	84.54	61.09
3131 - 9024	F	WT	144.13	100.50	148.39	2.85	0.82	1.98	51.04	55.71	64.24	88.02	102.83	90.41
3132 - 0293	F	WT	114.26	130.51	183.43	1.96	1.59	2.97	46.48	59.17	68.48	97.42	96.79	88.46
3168	F	WT	209.07	258.52	318.17	3.40	5.75	13.98	53.34	48.02	55.96	108.22	124.57	169.09
5984	F	WT	155.37	183.75	138.45	2.39	3.18	2.77	51.66	48.03	55.75	88.89	96.07	135.35
5970 - 8295	F	WT	182.18	101.46	185.06	3.82	0.91	4.95	48.33	23.39	52.83	76.12	119.56	123.72
3187	M	WT	158.94	138.95	191.34	1.99	1.69	5.12	44.18	54.56	45.81	110.78	115.30	141.61
3144 - 8689	M	WT	138.73	155.07	163.77	2.03	3.32	2.16	42.78	36.80	36.09	105.08	114.32	132.76
3188	F	WT	131.82	132.34	120.22	1.70	1.28	2.13	40.16	55.43	46.71	80.44	82.53	75.36
3148	F	WT	195.13	288.24	162.43	3.53	11.70	3.66	43.21	51.40	37.62	116.15	139.45	142.82
3146	F	WT	176.08	174.26	123.97	3.30	2.90	2.22	38.85	43.28	44.46	101.25	110.77	90.72
3145	F	WT	119.46	113.98	99.40	1.52	1.09	0.84	48.33	60.94	47.65	90.69	108.25	95.34
3153 - 9029	M	WT	144.61	175.52	186.15	2.11	2.32	4.97	39.33	50.08	41.69	106.80	112.79	115.40
3152	M	WT	139.41	208.41	213.81	1.64	3.80	3.96	42.09	45.95	39.60	90.25	117.45	105.31

3172 - 9030	M	WT	111.40	148.47	120.92	0.96	1.89	2.15	46.97	61.15	47.82	117.04	103.89	101.33
7720	M	WT	139.36	134.97	156.03	1.58	2.50	3.26	38.62	60.06	51.86	97.41	100.54	120.12
7724	M	WT	81.66	175.24	218.91	0.74	2.47	3.74	54.46	54.73	42.94	98.55	166.18	117.56
7723	M	WT	98.77	162.56	161.14	1.47	2.33	3.80	50.93	51.98	52.86	90.23	101.41	119.22
7721	M	WT	147.04	160.62	161.51	1.94	2.13	3.45	45.83	51.39	54.28	79.45	91.64	103.66
3689	M	WT	71.49	139.85	199.10	0.42	1.45	5.56	51.30	40.89	49.57	120.90	137.27	138.12
3684 - 9572 - 0292	F	WT	107.86	135.76	135.96	1.08	1.55	1.63	45.42	61.67	51.07	69.42	90.46	83.12
3668	F	WT	102.32	156.42	102.96	1.06	2.33	1.52	38.93	58.48	45.03	78.84	91.52	111.09
3666	F	WT	130.53	165.38	184.73	1.73	2.63	3.13	44.98	37.18	40.20	64.94	102.14	119.74
3665	F	WT	111.83	90.94	200.95	1.31	0.76	2.89	36.08	52.26	47.28	74.41	103.37	104.64
5995	M	NULL	102.58	115.16	129.83	0.93	0.89	1.33	43.44	56.74	45.16	78.97	107.44	118.43
5780	M	NULL	203.91	171.60	163.16	3.53	2.23	3.92	47.13	55.72	46.41	115.34	123.45	152.71
5783 - 3113	M	NULL	203.04	167.21	80.21	4.00	2.38	0.43	50.29	51.35	65.48	122.33	119.41	90.98
5785	M	NULL	93.23	100.72	129.65	0.82	0.75	1.38	43.16	41.52	51.21	96.71	146.98	128.01
5786 - 3166 - 3600 - 8871	M	NULL	148.38	137.39	135.69	1.98	1.42	1.37	39.48	36.37	42.28	93.88	115.59	121.01
5784	F	NULL	132.06	125.91	106.23	1.92	1.42	0.86	42.68	41.20	39.29	100.50	104.92	123.93
5790 - 3601 - 8861	F	NULL	142.39	81.60	106.71	1.79	0.57	0.89	47.22	56.05	40.14	82.24	110.48	82.39
5182	F	NULL	134.49	144.74	125.17	1.60	1.81	1.20	42.46	51.79	50.30	113.90	131.90	67.99
5183	F	NULL	96.57	108.22	97.70	0.79	0.99	0.75	42.53	42.76	52.76	82.32	98.03	90.14
5007	M	NULL	145.56	97.38	186.08	2.10	0.67	2.88	53.10	30.63	63.13	121.74	146.72	163.16
5011	M	NULL	131.94	186.39	180.10	1.96	3.12	2.92	51.67	28.00	51.50	122.98	167.26	129.62
5998	M	NULL	143.93	139.26	135.38	1.76	2.78	2.63	38.19	36.70	33.47	82.96	109.60	120.33
5989	M	NULL	143.55	124.16	141.32	1.94	1.16	1.49	36.94	35.00	31.54	96.69	123.90	132.02

5981	F	NULL	89.55	87.31	102.22	1.14	0.66	0.82	40.19	37.31	64.66	81.42	104.98	108.59
5983	F	NULL	116.13	109.47	99.22	1.36	1.01	1.46	45.18	43.47	56.10	68.58	95.42	112.56
3123	F	NULL	116.20	101.08	156.73	1.54	0.91	2.30	50.93	59.16	79.76	92.21	108.62	108.97
7098 - 9074	F	NULL	48.89	79.11	137.67	0.23	0.90	1.55	36.26	54.89	46.67	91.49	85.80	86.37
7589 - 9036	F	NULL	74.15	131.18	139.83	0.54	2.54	2.78	43.70	51.33	51.93	92.43	97.03	106.52

Table A.4.2. Raw echo data separated by genotype and sex.

Component	Assignment	Reflection
Module 1. Pseudocode	28/28 (100%)	28/28 (100%)
Module 2. Matrix and Vector Operations	27/28 (96%)	26/28 (93%)
Module 3. Loops	27/28 (96%)	26/28 (93%)
Module 4. Data Visualization	28/28 (100%)	28/28 (100%)
Final Project	28/28 (100%)	

Course	Survey Response Rate
FA19 (Traditional)	9/18 (50%)
SP20 (Blended)	16/28 (57%)

Table A.6.1. Module completion statistics and survey response rate

Module Effectiveness Survey

On a scale from 1 to 5, indicate your level of agreement with the following statements regarding the usefulness of the Matlab review modules.

DISCLAIMER: Participation in this survey is voluntary and will have no impact on course grades. All responses will be confidential. This survey is part of a study to assess a blended learning approach to Matlab programming instruction in a biomechanics course. The data collected from this survey will be shared with the academic community through conference presentations and publication. Participation in this survey indicates agreement for your de-identified responses to be used in this manner.

Question	Response				
1. Please enter your unique identification code (messaged to you in Brightspace).	*Free response*				
2. Matlab assignment 1 (angular kinematics) was clearly explained.	1 (strongly disagree)	2	3	4	5 (strongly agree)
3. The goals (outputs) for the project were clearly stated.	1 (strongly disagree)	2	3	4	5 (strongly agree)
4. The Matlab review modules prepared me for the angular kinematics project.	1 (strongly disagree)	2	3	4	5 (strongly agree)
5. Online review modules were more helpful than in-class instruction alone.	1 (strongly disagree)	2	3	4	5 (strongly agree)
6. The linked review materials were useful in preparing for the project.	1 (strongly disagree)	2	3	4	5 (strongly agree)
7. Mini-assignment problems were useful in preparing for the project.	1 (strongly disagree)	2	3	4	5 (strongly agree)
8. Reflective prompts were useful in preparing the assignment.	1 (strongly disagree)	2	3	4	5 (strongly agree)
9. The project description video helped me understand the angular kinematics problem.	1 (strongly disagree)	2	3	4	5 (strongly agree)
10. Which component of instruction was MOST helpful in preparing for Matlab project 1 - angular kinematics?	In-class instruction	Linked review materials	Coding mini-assignment problems	Reflective prompts	Other
11. Which component of instruction was LEAST helpful in preparing for Matlab project 1 - angular kinematics?	In-class instruction	Linked review materials	Coding mini-assignment problems	Reflective prompts	Other
12. Please elaborate on which component you find most and least helpful.	*Free response*				

Table A.6.2. Blended course module effectiveness survey

MATLAB Coding Confidence Survey					
On a scale from 1 to 5, indicate your level of agreement with the following statements regarding your confidence and comfort implementing various MATLAB coding techniques. DISCLAIMER: Participation in this survey is voluntary and will have no impact on course grades. All responses will be confidential. This survey is part of a study to assess a blended learning approach to Matlab programming instruction in a biomechanics course. The data collected from this survey will be shared with the academic community through conference presentations and publication. Participation in this survey indicates agreement for your de-identified responses to be used in this manner.					
Question	**Response**				
1. Please enter your unique identification code (messaged to you in Brightspace).	*Free response*				
2. I am comfortable using Matlab to solve science and engineering problems.	1 (strongly disagree)	2	3	4	5 (strongly agree)
3. I am confident pseudocoding solutions to physical problems.	1 (strongly disagree)	2	3	4	5 (strongly agree)
4. I am comfortable performing matrix operations in Matlab.	1 (strongly disagree)	2	3	4	5 (strongly agree)
5. I am comfortable using loops to solve problems in Matlab.	1 (strongly disagree)	2	3	4	5 (strongly agree)
6. I am comfortable plotting and visualizing data in Matlab.	1 (strongly disagree)	2	3	4	5 (strongly agree)
7. Please expand on what areas you are MOST confident when approaching problems with Matlab.	*Free response*				
8. Please expand on what areas you are LEAST confident when approaching problems with Matlab.	*Free response*				

Table A.6.3. MATLAB coding confidence survey

Figures

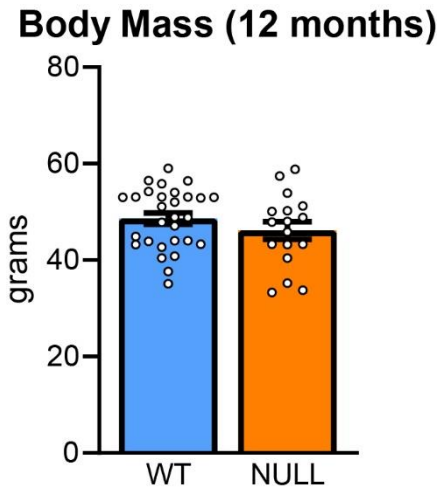

Figure A.4.1. 12-month whole body mass of experimental mice.

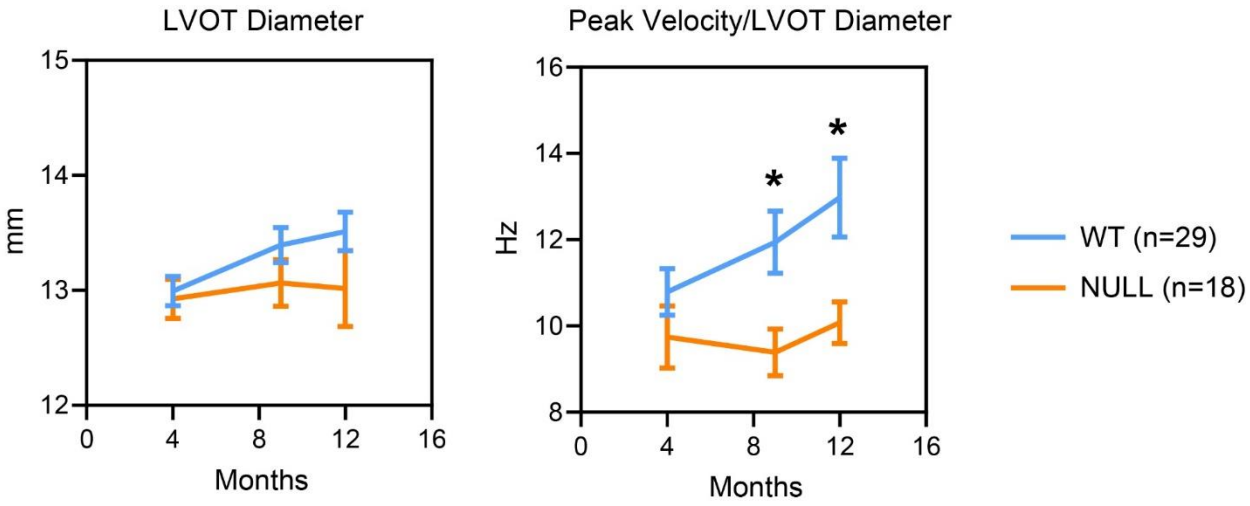

Figure A.4.2. Peak velocity normalized to left ventricular outflow tract diameter.

Module 1: Pseudocode

Review resources

Codecademy: What is Pseudocode And How Do You Use It? (VIDEO)

Cornell University CS341: Pseudocode

University of North Florida COP2221: Pseudocode Examples

Practice problem

Write pseudocode for a program that reads in a data file containing length information of the two legs of 10 different right triangles. Solve the hypotenuse for each right triangle, store data in new variable and display the hypotenuse of each triangle to the user. *Remember to keep the pseudocode general (avoid hardcoding/declarations), use comments, CAPITALIZE actual MATLAB commands (loops, etc.).*

Reflection

How might pseudocoding principles be useful in solving BME problems? At what stages might it be most (and least) helpful?

Module 2: Vector and Matrix Operations

Review resources

Cyclismo (University of Georgia): Introduction to Vectors in MATLAB

Cyclismo (University of Georgia): Introduction to Matrices in MATLAB

Cyclismo (University of Georgia): Vector Functions

Practice problem

Adapted from Mathworks MATLAB and Simulink Training Practice Test, Problem 2.

Download data file 'viewdata.mat'. This is a 19x3 matrix where each row contains three data points for 19 different videos. Column 1 contains length of each video in minutes, column 2 contains total views for each video, column 3 contains total amount of time viewers watched the video in minutes. Determine the percentage viewed for each of the 19 videos using matrix/vector functions. Percentage viewed = (Minutes watched / views) / (Video length). Plot relationship between percentage viewed and

total video length using the ‘scatter’ command. Does there appear to be a relationship between video length and percentage viewed in this data? (no need for any analysis beyond graph). Submit code as .m file.

Reflection

What types of BME problems may involve vector/matrix operations? What challenges might these cause in coding solutions?

Module 3: Loops

Review resources

Cyclismo (University of Georgia): Loops

Ilya Mikhelson: MATLAB For Loop Tutorial (VIDEO)

Practice problem

Adapted from Armstrong State University Engineering Studies MATLAB Marina – For Loops Exercises, problems 9 and 10.

Evaluate the function from $0 \leq t \leq 3$ seconds. First, use vector/matrix operations (module 2). Then use a for loop. Use the ‘plot’ command to ensure identical output. Submit code as .m file.

Reflection

What types of BME problems lend themselves to vector/matrix operations and/or for loops? What challenges might arise in using the techniques?

Module 4: Data Visualization

Review resources

Mathworks Documentation: plot

Mathworks Documentation: figure

Mathworks Documentation: subplot

RobertTalbertPhD: Basic data plotting in MATLAB (VIDEO)

Practice problem

From the previous module, evaluate the function from $0 \leq t \leq 3$ seconds using either vector/matrix operations or a for loop. Replicate the following figure using subplot and MATLAB commands to modify the output. Submit code as .m file.

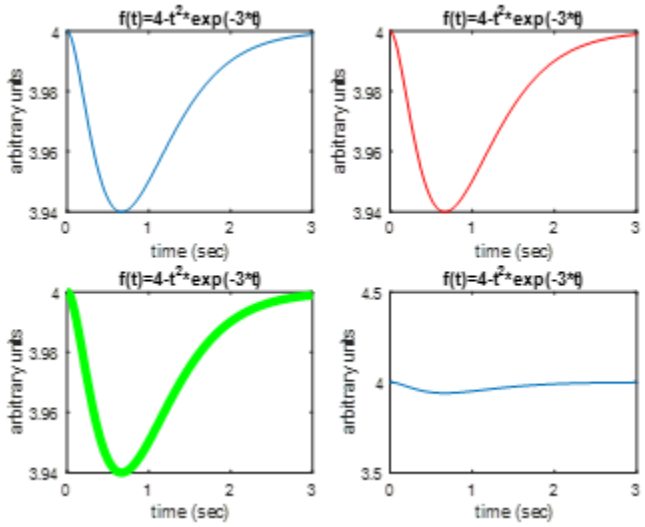

1. Default
2. Red line
3. Green line, line width of 5 points
4. Default, x-axis limits from 3.5-4.5

Reflection

How would you display this type of data for maximum impact and clarity? What are some of the other graphing options in MATLAB (scatter was used in module 2) and what types of data lend themselves to those types of visualization?

Figure A.6.1. Blended course module contents

BME2100

MATLAB Assignment #1

2D Inverse Dynamic Analysis

A 65 kg subject performs the bicep curl movement in two separate trials: (1) no weight and (2) holding a 9 kg free weight. Each trial consists of one full bicep curl: full flexion from anatomical position and then extension back to anatomical position. The motion of the arm was recorded by tracking the position of three markers placed on the wrist, elbow, and shoulder joints as shown in Figure 1. By using the x and y locations of these three markers, the reaction forces at the elbow can be determined. This position data was recorded in units of meters at a frequency of 120 Hz and is provided in two .mat files:

Trial 1: No weight: trial1.mat

Trial 2: 9 kg weight: trial2.mat

Assume that the subject is male and that the weight of the hand and free weight always act at the location of the wrist marker.

Determine:

1. The angle between the forearm and upper arm over time
2. The resultant moment at the elbow about the z-axis over time
3. At least three meaningful assumptions that you have made in determining (1) and (2)

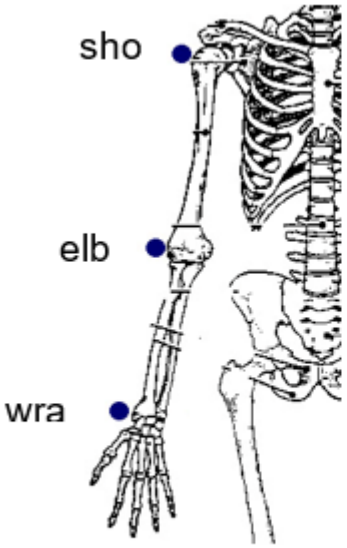

Figure 1. Marker locations.

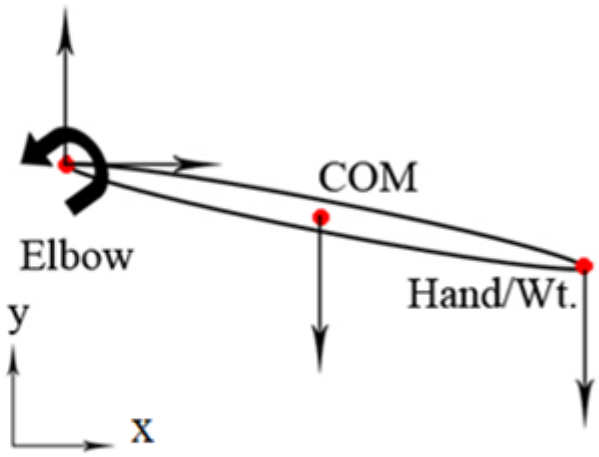

Figure 2. Simplified FBD and global coordinate system corresponding to marker data.

Figure A.6.2. Traditional course assignment.

https://youtu.be/SqvWWapIaPw

Figure A.6.3. Blended course assignment video link

This rubric is adapted from Grading Rubric for Programming Problems by Shelby Kimmel.

Coding goals for assignment:

Assignment specific

1. Resolve elbow angle over time for both trials.
2. Resolve elbow moment over time for both trials.

General coding skills

3. Output clearly labeled plots for each trial with clearly labeled axes.
4. Thoroughly comment all new variables and calculations.
5. Code must be written as script – not command line.
6. Save and manipulate data in vector/matrix format.
7. Use for loops for iterative calculations (differentiating position data, moment calculation over time, etc.)

Program Correctness	*15 points*	*10 points*	*5 points*	*0 points*
Score:	Program always works correctly and meets specifications	Minor details of the program specification are violated, program functions incorrectly in some areas.	Significant details of specification are violated, or the program often exhibits incorrect behavior.	Program does not compile, or errors occur rendering program non-functional.
Readability	*6 points*	*4 points*	*2 points*	*0 points*
Score:	Code is clean, understandable, well-organized	Minor issues such as inconsistent indentation, variable naming, general organization.	At least one major issue that makes it difficult to read.	Several major issues that make it difficult to read.
Documentation	*3 points*	*2 points*	*1 points*	*0 points*
Score:	Code is well commented.	One or two places could benefit from comments, or the code is overly commented.	Major lack of comments make it difficult to understand code.	No comments.
Code elegance		*4 points*	*2 points*	*0 points*
Score:		Code appropriately uses for loops and methods for repeated code.	Code uses a poorly chosen approach in at least one place.	Many instances where could could have used easier/faster/better approach.
Assignment specifications		*2 points*	*1 points*	*0 points*
Score:		Assignment meets specifications.	Minor specifications are violated.	Significant specifications ignored or violated.
TOTAL (of 30)				
Score:				

Figure A.6.4. MATLAB coding ability rubric